THE INFLUENCE OF DIFFUSION PROCESSES ON THE STRESS-CORROSION OF E-GLASS /POLYESTER COMPOSITES.

Thesis submitted in accordance with the requirements of the University of Liverpool for the degree of Doctor in Philosophy by Brian David Caddock.

October, 1987.

For Lilian

ACKNOWLEDGEMENTS

Particular thanks are due to Professor D.Hull, for arranging for the work to be funded, for supervising the project prior to his move from Liverpool to Cambridge, and for continuing advice and guidance. Grateful thanks are also accorded to Dr. K.E.Evans, who took over the supervision of the project, for his keen interest and for many helpful suggestions and discussions. Some of the radioactive tracer measurements were carried out at Manchester Polytechnic, and thanks are due to Dr.J.M.Marshall for generously providing radioisotope laboratory facilities and advice. Finally, the friendship, help and encouragement received from my many colleagues in the Department of Materials Science and Engineering at Liverpool University is gratefully acknowledged.

CONTENTS

ABSTRACT

A radioactive tracer method has been used to show that hydrochloric acid does not diffuse into polyester resins to a sufficient extent to weaken the fibres in an E-glass/polyester/ composite. Water, however, diffuses freely into these polymers to yield saturation concentrations in the range 1-3.5%wt.. In order to relate the polymer diffusion measurements to fibre weakening, it was necessary to identify the features of the complex relationship between acid concentration and fibre stress that promote fibre fracture. To study this, strength profiles of glass fibre bundles exposed to aqueous hydrochloric acid have been mapped. Tests were carried out under both ageing and static fatigue conditions to yield data covering a wide range of applied loads and failure times. A mechanism has been advanced which accounts for the weakening of the E-glass fibres by the acid. This features the progressive removal of the calcium and aluminium fluxing agents from the glass surface by the leaching action of the acid. The weakening is held to be due to the loss in ionic bonding between these elements and the non-bridging oxygen atoms in the glass network. The rate of attack is diffusion-limited, and only extends relatively slowly into the sub-surface layers of the glass. In a stressed fibre, however, the weakened surface layer is susceptible to cracking. This crack formation exposes fresh surface to the leaching action of the acid, causing further weakening. The high stress intensity at a crack tip favours the further cracking of this newly weakened material. The cracks therefore extend and eventually result in fibre fracture.

The surface attack is similar to that in which sodium is leached from soda-lime glass by water. This type of leaching is known to conform with a diffusion model which features a concentration-

dependent diffusion coefficient. The mechanism requires that the demineralisation occurs in a very thin zone at the glass surface. A TEM technique for using EDX analysis to examine calcium profiles across fibre cross-sections was developed and used to confirm that this also occurs with E-glass fibres that have been leached with hydrochloric acid. Diffusion-controlled surface attack of this type is typical of other materials that exhibit stress-corrosion cracking.

INTRODUCTION

Stress corrosion cracking in polymer composites made from E-glass arises because the glass fibres used for reinforcement are susceptible to weakening on exposure to aqueous solutions of mineral acids. However, the polymer matrix in the composite generally forms a barrier, preventing the acid from penetrating further than the surface layer of the material. For this reason E-glass filaments have successfully been used for resin reinforcement in a wide variety of industrial applications in which the material is exposed to an aqueous acidic environment. Experience with storage tanks, pipework and reaction vessels suggests that problems are only likely when there is a particular combination of circumstances. These involve the bringing together of high stress levels, optimum acid concentrations and defects in the composite such as sharp surface cracks or poor fibre bonding. At the site of a stress corrosion crack the local stress must be sufficiently high to cause fibres weakened by acid attack to break in a sequential manner. Acid of sufficient strength to promote weakening must then gain access to newly exposed fibres at the crack tip, thereby creating the conditions for crack propagation and eventual fracture. The local stress level is a very powerful driving force for stress corrosion crack propagation. This is so firstly because the stress intensification at the tip of a growing crack increases with crack length. Secondly, the weakening of the stressed fibres by the acid is considerably enhanced as the stress level increases.

Stress corrosion cracking with E-glass composites is therefore a specific, rather than a general problem. In developing guidelines for defining the conditions under which it can occur, a comprehensive understanding of the micromechanisms which contribute to the phenome-

non is required. Previous research work on this topic has identified the main features of the problem, but some uncertainties remain. It has not been definitely established how the acid reaches the fibres, which are embedded in an inert but brittle resin matrix. Once the acid has reached the fibres, the very pronounced effect of stress on the rate of fibre weakening has not been fully explained. These are the aspects of the problem that have been addressed in the present work. Stress corrosion cracks nucleate and propagate in E-glass polyester composites by processes that often include a long incubation period. In the case of industrial equipment this may occupy several years. Laboratory tests are usually designed to generate the cracking more quickly, and have the general objective of providing a means for predicting the long term performance of the material. The crack propagation process is seen as one in which crack growth accelerates with time, slowly at first, but eventually very rapidly, leading to fracture. Typically, the crack propagation rate during the slow growth stage of the process is in the range 10^{-6}-10^{-10}m.sec^{-1}. This measured rate is important in that it sets the timescale for events occurring at the crack tip during propagation.

As long as the polymer matrix forms an effective barrier, preventing the acid from reaching the fibres, progressive corrosion will be inhibited. This appears to be the situation in the majority of applications of grp for industrial tanks and pipework where the material gives satisfactory service. Stress corrosion problems can only occur if this barrier fails to protect the fibres from the acid. The two possible ways in which this can arise are as a consequence of a diffusion process, or by the presence or formation of microcracks in the matrix through which the acid can percolate. The presence of a high stress field at the crack tip could influence either of these proc-

esses, by opening up the polymer network to increase the diffusion rate, or by promoting matrix cracking. It is thought, however, that the most important effect of the stress field is concerned with the weakening and fracture of the glass fibres, since these are substantially stronger and stiffer than the polymer. Indeed, it is probable that the stress-enhanced weakening of the fibres is the key process that determines the rate of stress corrosion crack propagation in a polyester composite. This stress effect on fibre weakening can account for the very wide regime of loads over which stress corrosion effects have been observed. Cracking is not confined to situations in which the composite is subjected to a high overall load in an aggressive environment. Problems also occur at modest loads, which are well within the design capability of the original material. This is because cracks can propagate as a consequence of stress intensification at defects in the component. These may be present in the original article, or may arise as a result of physical damage or chemical degradation of the composite. The existence of high local stresses due to the presence of stress concentrators in the grp structure greatly increases the risk of stress corrosion cracking, especially if the material is exposed to an aqueous mineral acid of concentration near to 1.0 molar. It is evident that by preventing the acid from reaching the fibres stress-corrosion problems would be eliminated.

In the present work the combined effects of applied stress and acid concentration on fibre weakening have been quantified. A mechanism for the weakening of the glass has been advanced which accounts for the synergistic effect of stress and acid concentration. Measurements have been made of the solubility and diffusivity of aqueous hydrochloric acid in a range of polyester resins. These measurements have been made both with stressed and unstressed polymer specimens.

Before setting specific objectives for the work, a literature survey was carried out. This is presented in Chapter 1. The experimental work that followed is described in detail in Chapters 2-4. The interpretation of the experimental results is also discussed in Chapters 2-4, in an attempt to make each Chapter self-contained. In Chapter 5 the discussion is more concerned with the wider implications of the results obtained and with the development of the final conclusions of the work.

CHAPTER 1. LITERATURE SURVEY

The project work to be described in this Thesis is concerned with the stress-corrosion of composite materials made from polyester resins reinforced with E-glass. This topic is of importance industrially, and the elucidation of the mechanisms by which composite fracture occurs is interesting scientifically. Current understanding of these mechanisms indicates that diffusion processes, both in the glass fibres and in the polymer matrix, may be important in determining the rate of crack propagation in this type of composite. A study of diffusion effects in the resin was therefore undertaken as one of the initial objectives of the present work. In order to evaluate the results of acid and moisture diffusion in the polymer on the strength of the composite, it was necessary to identify the combinations of environment acidity and applied stress that would encourage fibre fracture. This, in turn, stimulated interest in fibre weakening effects and mechanisms. The experimental work described in Chapters 2-4 is therefore concerned with the weakening of E-glass filaments by aqueous hydrochloric acid and with the measurement of acid and moisture diffusion rates in a range of polyester resins.

A critical discussion of the results obtained requires an understanding of the current state of knowledge in these areas. A survey has therefore been made of published work that is relevant to the chosen project area. This is presented below as a general survey. More detailed discussion of some of the quoted references is reserved for the following Chapters, where the detail is more appropriate to the context of the developing argument.

1-1 The incidence and nature of stress-corrosion cracking in glass-reinforced plastic (grp).

Composite materials, made from polyester resins reinforced with E-glass fibres, have found wide application in the construction of storage tanks, chemical plant and pipework. These materials are light, strong, and stiff and it is relatively easy to fabricate them into complex shapes. Because they are not subject to electrolytic corrosion, they have excellent resistance to atmospheric deterioration. The well-known resistance of bulk glass and polyester resins to corrosion by aqueous acids suggests that a glass/polymer composite would be well suited for applications involving the storage and handling of such media. In general this is so. In the majority of cases in which this type of material has been used for tank or plant construction it has performed in a satisfactory manner.

Experience has shown, however, that in certain circumstances, E-glass/polyester composites become prone to corrosion problems. The problem arises when the material is stressed whilst immersed in an aqueous acid environment. In a few instances the catastrophic failure of large tanks has occurred[1,55,58]. In these cases the cause of failure can usually be attributed to the combined influenced of high local stresses and high acid concentrations. The risk of failure can be minimised by good design, both of the composite itself and of the structure in question. In developing reliable guidelines for design it is essential to have a comprehensive understanding of the nature of the problem. For this reason the topic has attracted much research attention.

It has been established that the principal cause of stress corrosion in grp is the weakening of the glass fibres by the acid[10,17,19,20]. Griffith[16] showed how the strength of fine glass monofilaments exceeded that of ordinary glass by a large margin. Glass is an inherently strong material, but it is readily weakened by the presence of the innumerable flaws or microcracks that exist on the surfaces of common glass objects. These are not present to the same extent in drawn glass fibres and make it possible to produce filaments with strengths close to the cohesive strength of the material[17]. It is the high strength of these drawn fibres, together with their high modulus that makes them attractive as reinforcement elements in polymer composites.

Charles[36], however, showed that in the presence of an aqueous acid, glass surfaces are subject to corrosive attack. With normal glass objects this is of no consequence, because the attack is confined to a surface that is already flawed. The depth of surface that is attacked is negligible compared with the thickness of the glass. This is not the case with glass fibres, which typically have a diameter of 10-20 X 10^{-6}m.. With pristine fibres the slightest amount of surface attack is likely to encourage surface flaw nucleation or growth, thereby restoring the "weak" characteristics of ordinary glass. The extent of this weakening is easily demonstrated by immersing unstressed E-glass fibres in acid solutions for a period, prior to measuring their tensile strength . For example, Chandler and Jones[55] have recorded a 70% strength loss after a 1 week exposure to 2M hydrochloric acid. Even more dramatic is the effect of exposing stressed E-glass fibres to aqueous acid. Scrimshaw[35] examined E-glass fibres immersed in M sulphuric acid at two different stress levels, corresponding to one sixth and one thirtieth of the dry failure load.

He found a decrease in the time to fracture by a factor of 200 for fibres stressed at the higher load. It follows from this that an E-glass/polyester composite exposed to an aqueous acid will only retain its mechanical strength if the polymer is able to form an effective barrier to the acid. Preventing the acid from reaching the fibres in this way eliminates the cause of the corrosion. In service, this barrier can be breached only by mechanical cracking of the polymer, or by the diffusion of the acid through the uncracked polymer.

1-2 Stress-corrosion measurements in E-glass/polyester composites.

The large effect of stress on the rate of corrosion of E-glass fibres in acid solution is reflected by a similar effect in composites reinforced with these fibres. The situation is somewhat more complicated, because there is an additional effect of the applied stress with a composite, compared with that with bare fibres. This involves the promotion of either matrix cracking or enhanced acid diffusion by the stress, creating a pathway through the polymer network that enables the acid to reach the fibres. In assessments of the severity of the problem a wide variety of test methods and composite systems have been studied, and the main features of the grp stress corrosion problem are well established. A useful review has been provided by Hogg and Hull[1].

Pure water is capable of inducing stress corrosion in E-glass composites. Aveston et al[69] have used stress rupture rigs to measure the strength retention of strands of E-glass, held at constant load in a water environment. They compared these with similar strands that had been impregnated with epoxy and polyester resins. They found a progressive reduction in strand strength with time. The load required

for fracture at an exposure time of ten weeks was only about 50% of the dry fracture load. Impregnating the strands with resin to give an estimated thickness of 100 X 10^{-6}m. did not provide much protection for the fibres. Although the initial strength of an impregnated strand was higher, exposure to water under load reduced the strength back to that of the bare strand in about 17 hours. Aveston[6] attributes these results to the diffusion of water through the resin layer protecting the fibres. The timescale for the saturation of the resin with water was consistent with the thickness of the layer and the diffusion coefficients for water in polyester and epoxy resins[69]. In contrast to this, exposing bare or impregnated strands to water for ten weeks in an unstressed condition gave hardly any strength reduction. These data are in accord with the much earlier work of Metcalfe and Schmitz[21] on the stress corrosion of E-glass fibres tested in water vapour at 40% and 100% relative humidity. Acid solutions are significantly more aggressive than water to E-glass fibres. Aveston and SIllwood[6] tested cross-ply E-glass/polyester composite specimens under stress in 0.5M sulphuric acid. Tests were carried out with both static and fatigue loading, with various specimen geometries. Times to failure at various loads were measured and the composites were found to suffer a serious reduction in strength, to about one tenth of the initial value, after exposure under load for about one year. An important finding from this work was that the same result was obtained, irrespective of whether the applied load was static or fatigue. Presoaking the specimens prior to applying the load had virtually no effect on the subsequent performance of the composite.

Using a very different type of specimen, Noble, Harris and Owen[11] studied the stress-corrosion of grp pultruded rods, made from E-glass and epoxy resin. These rods had a very high glass content, by virtue

of the pultrusion process, and were protected by only a very thin layer of resin on the outer rod surface. They were found to be very susceptible to stress-corrosion cracking when tested in aqueous hydrochloric acid, under both bending and tensile loading. Results were obtained for for acid concentrations in the range 0.0001M-5M. However, the results for the dilute acid may not be significantly different from that in water, which was not, apparently, included in the test schedule.

Because of their practical importance in industrial applications, filament wound pipes have been widely used to assess the stress-corrosion resistance of E-glass composites. Barker[9] studied the effect of water and 2.8M sulphuric acid on three layer, angle-ply, filament wound pipes subjected to a constant diametric strain. The pipes were made from polyester resin reinforced with E-glass. Exposure to water led to reductions in elastic modulus to around 60% of the initial value after exposure times of about two years, which was about time required for the specimens to become saturated with water. Applied strains in the range 0-1% did not have much effect on the rate of modulus loss. A much stronger effect was seen with the 2.8M sulphuric acid. For rings immersed in acid and strained to 1%, modulus variations could not be recorded, due to the catastrophic cracking that occurred during the first few days of testing. The fracture surfaces had the flat, smooth appearance that is characteristic of grp stress-corrosion failure. Similar attack of the pipes occurred at lower strains, but required longer times for the cracks to grow. Little or no cracking was seen at strains below 0.15% for times up to 500 days.

Extensive test data are also available[61,62] that have been obtained using ASTM methods[60]. These methods were specifically developed for

measuring the ability of pipes to withstand attack by aqueous liquids. In these tests pipe sections are subjected to diametric compression in a ring compression rig. This puts the inside surface of the pipe into tension and subjects it to the effect of the environment, which is contained inside the pipe. Pipe performance is assessed by the time required for the pipe to leak through the wall, or to develop visible microcracks. The ASTM methods were designed to be carried out at constant displacement, but Hogg[40,61,63,64] extended his measurements to include constant load tests. The constant load situation is the more severe condition and defines the stress-corrosion characteristics of the material. In the constant displacement test, the load slowly decays, as a consequence of the creep that occurs as the cracks propagate. The measurements are therefore indicative of the strain corrosion behaviour of the grp. Collins[62] based his work entirely on strain corrosion measurements. Hogg[63] monitored continuously the increase in specimen displacement during the constant load tests. This provided a more quantitative measure of the progress of the corrosion. From the results obtained, Hogg and Hull[1] concluded that the basic features of stress and strain corrosion were the same. The difference between the phenomena is essentially one of degree, with stress-corrosion being more severe than strain-corrosion.

In another type of test, coupon specimens have been used by many workers to obtain results characteristic of bend, fatigue, or tensile loading[12,31,40,51,55,56]. In the same way that constant load and constant displacement can be featured in static tests, the same distinction can be made in fatigue tests. With some grp systems a very long time is required before stress-corrosion cracks appear. It is often the case that some form of stress concentrator is needed before the attack is initiated[3]. By using starter cracks, however, fatigue

tests can usually be designed to give failure within a reasonable period.

A convenient performance criterion in a fatigue test is the time required for the specimen to develop a specified damage level. In constant load static tests a time to failure is similarly recorded. This similarity, and the generally similar nature of the crack propagation process has led to the description of constant load creep rupture tests as static fatigue tests[36,65].

1-3 Crack growth measurements.

More recently interest has been high in the direct measurement of stress-corrosion crack growth rates[6,31], and in the application of fracture mechanics to the measured data[15]. Evans[37] has shown how the dynamics of stress-corrosion with brittle materials can be described uniquely by V,K_I curves, where V is the crack velocity and K_I is the mode I (opening) stress intensity at the crack tip. Price[15] measured crack growth rates for aligned, long fibre E-glass composites, loaded to a constant stress intensity in 0.6M hydrochloric acid. The stress intensity was kept constant by using specially profiled compact tension specimens. The general pattern of the results obtained were consistent with those of Wiederhorn[8], Aveston and Sillwood[6], and Hogg[63]. The experimental data show that the crack velocity is related to the crack tip stress intensity by a simple power law of the form first suggested by Paris[53]:

$$V = \alpha K_I^{\,n} \qquad (1\text{-}1)$$

Similar conformity with this equation has been reported by Lhymn and Schultz[72]. The value of n is readily obtained from a log log plot of V against K_I. For a range of aligned composites made from E-glass with

five different polyester resins, Price found the value of n to be about 5.

The eventual failure of a grp specimen by stress corrosion is usually preceded by a process in which cracks nucleate and grow, initially at a very slow rate. Chandler and Jones[55] have reported that at low stress this period of slow growth may occupy a number of years. If the cracks are sharp the crack tip stress intensity increases with crack length and a sudden acceleration in growth rate can occur, leading to catastrophic failure[6,11,55,56,57]. At low stress the incubation period may be infinite, and under these conditions no stress-corrosion will occur. This is believed to be the case in the majority of industrial situations, where E-glass composites are being successfully used to contain aqueous solutions. In these circumstances stress corrosion will only be a problem if a stress raiser, such as a notch, crack, or other discontinuity is present in the material[66].

In identifying stress corrosion as the source of failure in a fractured grp specimen, the most striking feature of this type of attack is the very smooth, planar fracture surfaces. This is particularly the case with cracks that have developed slowly, at low stress[15]. In contrast the dry fracture of grp at high stress in an air environment generally produces a highly branched, irregular fracture surface, with a "brushy" appearance. This is associated with the failure under load of the fibre/matrix interface, which leads to extensive fibre pullout on fracture. The fracture surfaces with specimens that have been exposed to an acid environment at intermediate loads, show a gradual transition from the planar to the highly irregular structure. These general features have been observed on fracture

surfaces from failed industrial equipment[67] and in the results obtained from a wide range of laboratory tests[6,9,11,31,40,63,68]

1-4 Matrix cracking in E-glass polyester composites.

Matrix cracking is an important feature in stress-corrosion situations, because it is one of the two ways in which the acid environment can gain access to the fibres. Microcracking can occur as a result of residual thermal strains in the material after postcuring[40], or as a consequence of applying an external strain[51], or following fibre failure during slow crack propagation[75]. Barker[9] observed that with 3-ply, filament-wound, E-glass/polyester pipes, the application of diametric compression to a strain in the range 0.5-1.0% created microdamage in the resin, in the inner and outer hoop-wound layers. The damage consisted of cracks that developed in the direction of the fibres. Subsequent immersion of a strained pipe in 2.8M sulphuric acid led to the growth of further cracks, in a direction perpendicular to the fibres. These secondary cracks were sharp, and propagated through the reinforcement fibres to cause eventual fracture. Jones[9] extended this work by using flat coupon specimens of the same 3-ply, filament-wound, E-glass/polyester system. He noticed the appearance of aluminium and calcium ions in the acid environment during tensile tests and identified this as the cause of the failure of the reinforcement. Bare E-glass fibres immersed in the acid developed a core-sheath structure in which the sheath was depleted in calcium and aluminium. This severely weakened the fibres. In these experiments it was also noted that severe transverse microcracks developed in the internal laminate ply, after exposure to the acid at strains well below that at which they would have developed in air. Further work by Jones, Rock and Bailey[56] on coupon specimens and on single E-glass fibres,exposed

to M sulphuric acid, showed that, at initial applied strains greater than 0.15%, severe matrix cracking occurs. In this situation the resin does not protect the fibres, which fracture at the same time as bare fibres. At lower applied strains, with partially immersed specimens, matrix cracking developed in the unexposed part of the coupons, and led to fracture at that location. It was thought that the matrix cracking in this case was due to the pressure exerted by salts, leached from the glass filaments, crystallising within the resin. This effect also occurs when coupons are partially immersed in the acid at zero load. Aveston and Sillwood[6] also noted that with cross-ply E-glass composites, loaded in tension in 0.5M sulphuric acid, stress-corrosion fracture involved brittle fracture.

Carswell and Roberts[51] examined the effect of fatigue loading on chopped strand mat laminates made from E-glass with ICI 'Atlac' bis-phenol resin. They confirmed Aveston's contention that there is a great similarity between environmental fatigue and stress rupture data. Their fatigue data showed that environmental fatigue fracture occurred at endurances greater than the number of cycles needed to initiate resin cracking. It was significantly greater than that needed to initiate fibre debonding. They concluded that the primary process leading to rupture is the formation of microcracks in the resin, caused by the mechanically applied alternating stress. These resin cracks originate within the body of the laminate, from previously debonded sites, and allow the environment to reach the exposed glass fibres. The resulting environmental stress-corrosion crack propagation then occurs more rapidly than further resin cracking.

The leaching of calcium and aluminium from E-glass, noted by Jones et al[9], was also described by Friederich+[55] and by Lhymn and

Schultz[72]. Working with a thermoplastic resin (PET) reinforced with E-glass, Friederich found evidence of a stress intensity limit, K_{ISCC}, below which crack propagation would not occur. The level of of this was dependent on the acidity of the environment. The composite specimens used were made from short fibre material, and were compact tension specimens subjected to deadweight loading in stress rupture tests. Lhymn and Schultz[31,72] carried this work forward. Their results suggested that far field effects created some fibre fracture and resin microcracking well ahead of the crack tip. The joining up of resin microcracks along the weak path created by this damage, and the weakening of the fibres by acid leaching, preceded the passage of the main crack. The main crack is planar by virtue of the angular dependence of the stress field.

Another contributor to matrix cracking is the presence of residual thermal strains in a post-cured laminate. Thermal strains in long-fibre laminates arise as a consequence of the anisotropic nature of the individual plies in these materials. The thermal expansion coefficients are therefore highly directional. Postcuring of polyesters is usually carried out at temperatures in the region of 80-100°C. Subsequent cooling to room temperature leads to unequal shrinkage, and the development of thermal strains. The magnitude of these thermal strains has been measured by Bailey et al[68], who have shown that tensile thermal strains can reduce the applied strain at which transverse matrix cracking and matrix debonding occurs. In this work it was noted that the measured thermal strains in polyester/E-glass were greater than those found with epoxy/E-glass systems. Later work by Mulheron, Jones and Bailey[46] showed that the presence of residual moisture in postcured polyester resins was responsible for this effect. Dissolved water in polyesters increases the thermal expansion

coefficient. It follows that greater thermal strains develop in polyester laminates in which the postcure has not completely removed the water. In a later paper,Jones Mulheron and Bailey[45] have suggested that a well-cured, fully dried polyester laminate will generate lower thermal strains when cooled to room temperature. Furthermore, the transverse swelling that occurs when the dry composite subsequently takes up water[77] serves to negate the thermal strain and may even produce a strain-free laminate[45,49].

Simple swelling of the resin, due to moisture uptake, will lead to internal strain in a composite, if the fibres constrain the resin expansion. Menges and Lutterbeck[77] have examined this swelling and have reported that, for UP resins, the strain associated with the uptake of 1.5% of water is approximately 0.35%. This is sufficient to promote transverse cracking in grp lamimae with glass volume fractions in the range 0.4-0.7.

Ashbee and Wyatt[78] have discussed various ways in which micromechanical breakdown of the resin matrix and the fibre/resin interface can occur as a result of moisture uptake. The total amount of water that polyesters will take up is in the range 1%-4%$_{wt.}$ at room temperature[32,77]. The rate of uptake is diffusion controlled,however, and is very slow. The saturation of a 1mm. thick layer of resin with water requires many months[80]. However the non-uniform distribution of water in a composite that has not become saturated can be an important factor in creating high internal stresses in the material. For example, Ashbee and Wyatt[78] have identified the development of osmotic pressure as a source of disc-cracking in wet polymers and polymer composites. With the composites, water diffusing to a fibre surface leaches salts from the glass. This leads to the accumulation of solution at voids

along the fibre/matrix interface. The resin acts as a semi-permeable membrane, and water continues to diffuse into these voids until the pressure that develops cracks the surrounding resin. Quite large cracks can propagate by this mechanism.

A prerequisite for osmosis is that water soluble material must be present in the composite, that can be dissolved out by the diffusing water to create local pockets of solution. Ghotra and Pritchard[81] have reviewed the possible sources of these water-soluble materials. Inorganic salts can be either leached from the fibres, or can be present as particulate impurities in the resin. Equally important sources of soluble material are many of the organic substances, such as glycols, that are present in polyester resins. Epoxy resins are much less likely to contain water-soluble organic material, in line with their better resistance to disc cracking. The presence of water-soluble organic material in composite blisters has been confirmed by analysing the blister fluid by gas-liquid chromatography[82].

Walter and Ashbee[83] calculated the critical osmotic pressure needed to initiate disc cracks in a resin. They deduced that the critical condition was:

$$p = (3E\gamma/b)^{\frac{1}{2}}$$

where p = osmotic pressure, E = Young's modulus, γ = specific surface energy and b = crack tip radius. This equation gives too high a value for p if the normal values of E and γ are substituted. The osmosis mechanism is only tenable if the operative value of E is much lower than that of the dry resin. Barker[9], inter alia, has shown how E is reduced by the presence of dissolved water in the resin, but the reduction is not sufficient to justify the cracking mechanism. A more likely explanation concerns the viscoelastic nature of the resin.

Modulus measurements are typically made in tensile test machines, with cross-head speeds of around 2 $mm.min^{-1}$. Compared with this, the rate of strain that develops as a result of osmotic pressure is very slow, since it is diffusion-limited. The viscoelastic resin would be expected to show a much reduced modulus at such low strain rates , because of creep. If this is the case then the osmotic pressure required to nucleate cracks with a tip radius of 10×10^{-6}m. could be generated with dilute solutions of organic or inorganic material in voids in the resin.

It can be seen from the above discussion that there are a variety of mechanisms that can assist in the development of matrix cracks, by complementing the effects of an externally applied stress. This can lead to cracking at very low applied loads. The resulting ingress of the undiluted acid to the fibres is a powerful incentive for fibre weakening and fracture. At higher applied stresses the risk of matrix cracking is increased, particularly if the composite contains defects, which act as stress raisers. The applied stress becomes more dominant as the stress level increases. Criteria have been formulated for predicting the onset of transverse cracking in unidirectional laminae. This was discussed by Aveston[73] and McCartney[85]. Aveston developed a semi-empirical equation for estimating the applied stress required to propagate a pre-existing crack across the entire cross-section of a unidirectional lamina. McCartney has recognised the shortcomings of this treatment and has developed a more fundamental prediction system. The McCartney treatment takes into account the statistical variation in fibre strength that is implicit in the Rosen "weakest link" model[43] for describing fibre failure. The key feature of the argument is that there is a limiting applied stress, below which matrix cracking can not occur. McCartney uses a graphical method to summarise his

approach, which enables this stress level to be predicted. For applied stresses below this level matrix ceacking will not occur, unless one or more of the supplementary internal stress-raising mechanisms becomes operative. In the absence of this the only way the acid can reach the fibres is by diffusion through the resin.

1-5 Moisture and acid diffusion in polyester resins.

A very widely quoted mechanism for the initiation of stress-corrosion cracks in E-glass composites is the diffusion of acid through the resin barrier at the surface of a stressed specimen, to reach fibres close to the surface[11,51,72,74,84]. It has also been suggested that acid diffusion can be rate-determining during slow crack propagation in a composite, where the applied stress is too low to cause microcracking[11,15]. No direct evidence, however, has been advanced to show whether or not mineral acids , such as sulphuric or hydrochloric acid, are capable of dissolving in and diffusing through polyester resins. Regester[74], in an early study, attempted to use X-ray fluorescence to monitor chlorine uptake from aqueous hydrochloric acid solution into resin specimens. A critical examination of the results obtained shows that the sensivity of the measurement method was too low to be able to detect the very small chlorine uptake associated with the diffusion of the molar acid used. Regester concluded that HCl diffusion is minimal in polyester resins, but this conclusion is subject to the limitation imposed by the method sensitivity. He also fitted some specimens with electrodes that were embedded below the surface of the resin. The objective of this latter experiment was to see if a voltage developed within the specimen as a consequence of the preferential diffusion of hydrogen or hydroxonium ions into the resin. No such voltage was observed, and Regester con-

cluded that selective diffusion did not occur. This agrees with the general principle that electrical neutrality is observed in reactions involving the movement of ions.

It is well established that water diffuses through this type of resin and resin composite. In these systems moisture uptake has been widely studied, and a lot of data is available, providing solubilities and diffusion coefficients for water in a wide range of resins. Typical values are in the range 0.5% - 4.0% for the solubilities. At room temperature the diffusion coefficients are of the order of 10^{-8} - 10^{-10} $cm^2 sec^{-1}$. In polyester and epoxy thermoset resins it is generally found that the diffusion of water conforms with the classical laws of diffusion formulated by Fick[86]. This implies that the diffusion process occurs by random molecular movement of the diffusant through the polymer network. Further evidence of this is that moisture uptake appears to be equally effective from the liquid or vapour phases[80].

In a specimen that has not become saturated with the diffusant, the driving force for diffusion is the existence of a concentration gradient within the specimen. Fick showed that the rate of moisture uptake at a station situated at a distance x from the exposed surface of the specimen is given by :

$$\partial C/\partial t = D\ \partial^2 C/\partial x^2 \qquad (1\text{-}1)$$

where D is the diffusion coefficient and $\partial C/\partial x$ is the concentration gradient. A variety of methods have been used to measure diffusion coefficients for water in resins, of which the so-called weight gain method has been the most widely reported. In this method the uptake of water as a function of time is determined, usually by weighing. For a given specimen geometry a closed solution to the diffusion equation 1-1 can usually be found[23,93,94], which allows the uptake data

to be interpreted in terms of a solubility and a diffusion coefficient. A disadvantage with this method is the long time required to achieve saturation with water for the specimen thickness needed to give measurable weight gains in a reasonable time. It is also possible to leach soluble material from the resin, such that the observed weight gain is, in fact a net gain, or even a loss, making interpretation difficult. In a different approach, use can be made of the fact that, in the initial part of the diffusion curve, the uptake is proportional to $(Dt)^{\frac{1}{2}}$. A plot of uptake against $\sqrt{t}$ for the early stages of the diffusion is thus linear, with a slope of $\sqrt{D}$ This method avoids the problem of the long time needed to saturate the specimens, but it is very sensitive to the leaching problem mentioned above.

Marshall[87] has commented on these problems, and has introduced an alternative mrthod of measurement, involving the use of a radioactive tracer. The method has been used to study the diffusion of water in a resilient bisphenol A epoxy vinyl ester resin(Derakane 411-45). Composite samples made from this resin and short E-glass fibres were also examined. Tritiated water was used to follow the diffusion into thick sheets of the polymer. After exposure to the radioactive diffusant, the concentration gradient in the resin was determined by machining off successive layers from the plate, and measuring the tritium content of each layer. This was made possible by the high sensitivity of the radioactive counting method employed, i.e. liquid scintillation counting. A significant practical problem was the risk of loss of diffusant by evaporation during the machining process. This was minimised by freezing the sample in liquid nitrogen and by flooding the machined surface with liquid nitrogen during the cutting operation. The results suggested that in this polymer the diffusion was, in fact, non-Fickian, but the departure from ideal behaviour does not

appear to be very large. The results were interpreted by assigning Fickian diffusion coefficients, which were in the range 1.4×10^{-7} - $0.8 \times 10^{-8} cm^2 sec^{-1}$, for temperatures of 50°C and 20°C respectively. THe effect on water diffusion of applying a surface stress of 70MPa. was measured by exposing coupon specimens to tritiated water in a three point bend rig. A small effect was noted, with slightly increased diffusion in the surface under tensile stress. No effect was seen for the lower surface of the specimen, which is under compresion in three-point bend. A much greater effect was seen when the tensile surface was damaged by overstressing, after which it was subsequently exposed to the tritiated water. These results suggest that surface cracking has a significant effect on surface uptake of diffusant, but that stress without cracking has only a minor influence on diffusion rate in the polymer. The very small effect of stress on water uptake in polymers was measured by Marom et al[88,89]. They interpreted data for water uptake in polyester resins in terms of the increase in the free volume of the polymer caused by the stress. The very small measured increase in water uptake with stress agreed well with their calculated increase in free volume.

In subsequent work Marshall[90] compared the diffusivity of water and 2M HCl into the same resin, using tritium to label both solutions. No significant difference in diffusion behaviour was noted. It should be noted that this experiment does not trace acid diffusion specifically since the tritium concentration in the polymer is dominated by the diffusion of the water. This point is discussed further in Chapter 5. Apart from Regester's early experiments and Marshall's work with tritium-labelled hydrochloric acid, little work appears to have been done on the measurement of the diffusivity of this material in thermoset resins. This is not, perhaps, surprising because there is

a severe sensitivity problem to be overcome. A molar solution of HCl contains $3.65\%_{wt.}$ HCl. A resin capable of dissolving say 3% of this aqueous acid would only contain at the most 0.1% HCl. Small samples that will saturate in a reasonable time will only contain very small amounts of the acid, and present a difficult analytical problem. Regester's attempt to use X-ray fluorescence to measure chlorine uptake was hindered by the basic insensitivity of the method. Attempts to use scanning electron microscopy in the EDX mode are limited by the same problem.

Radioactive tracer methods hold out the most promise for solving the sensivity problem, and a suitable tracer isotope, ^{36}Cl, is available for experimental use. This isotope has been used to study the diffusion of hydrochloric acid in rubber[91], but no reference was found to work involving measurements with polyester resins. The provision of solubility and diffusion data, by means of ^{36}Cl tracer experiments, was an important initial objective in the present work.

1-6 Fibre weakening mechanisms.

Proctor[5] has surveyed the strength loss of bare glass fibres of different composition in various corrosive environments, and has related this to the long-term behaviour of fibre-reinforced composites. Pristine E-glass fibres, as manufactured on an industrial scale, have a maximum strength of around 3500MPa.. The fibres are very sensitive to abrasion damage, which introduces surface flaws. Because of this, the handling associated with sizing, stranding and coiling of the final product, causes the strength to fall to 1500 - 2000MPa.. Sizing is very effective in minimising further abrasion damage when strands are used to make a composite. However, further strength losses of the

fibres result from exposure to corrosive media, such as aqueous acids. Proctor identified two different regimes of corrosive attack which lead to fibre weakening. These are (a) ageing, where the strength loss is measured after the removal of the unstressed fibre from the corrosive medium, and (b) exposure under stress to the corrosive agent. Condition (b) is much more severe than condition (a) and is capable of causing fibres to break at loads well below the dry failure load. It is also capable of causing weakening at lower acid concentrations than is possible by ageing. Cockram[34] and Scrimshaw[35] have shown that the strength loss due to ageing in acid solutions is critically dependent on the concentration of the acid. There is a sharp maximum in the strength loss in the region 1M - 10M for both hydrochloric and sulphuric acids. Collins[62] also noted this effect.

1-7 Glass structure.

Any explanation of the weakening of E-glass must take into account the structure of the material. The most widely accepted model of the structure of silicate glasses is the random network model of Zachariasen[24]. This features the fundamental unit of a silicon-oxygen tetrahedron, in which a central silicon atom is surrounded by four oxygen atoms. A continuous, but irregular 3-dimensional network is built up from these tetrahedra, joined corner to corner via a common oxygen atom. Other oxides in the formulation produce metal cations, which fit into interstices in the structure, and cause a number of broken linkages in the network. The bonds holding the 3-dimensional structure together are very strong, so that plastic deformation is extremely limited and only occurs at very high stresses[1,2]. Glasses are thus very brittle materials[5]. The structural aspects of fibre

weakening are discussed in more detail in Chapter 3. Two dimensional representations of silicate glass structures are shown in Figure 3-1.

1-8 Fibre ageing.

Bare E-glass fibres that are subject to weakening by the ageing process develop the characteristic core-sheath structure identified by Baird-Smith and Jones[9], Metcalfe, Schmitz and Gulden[10], and Bledski et al[12]. An early study of the effect of this structure on E-glass strength was made by Metcalfe and Schmitz[19]. They noted that on prolonged exposure to either hydrochloric or sulphuric acid in the concentration range 0.5M - 1.0M spontaneous cracking of E-glass fibres occurred. This led to the hypothesis that an ion-exchange process took place at the glass surface that involved the replacement of sodium ions in the glass with hydrogen ions from the acid. The positively charged cations in the glass network (see figure 3-1) are relatively mobile, and can readily be substituted in this way. Metcalfe and Schmitz attributed the spontaneous cracking of the aged fibres to a surface contraction, associated with the replacement of sodium by hydrogen ions in the structure. The ion-exchange process that occurs at the fibre surface can be represented by:

$$Si\ O^{-}Na^{+} + H^{+} \longrightarrow Si\ OH + Na^{+}$$

The reaction product is essentially a layer of silicic acid that forms on the glass surface, and this has a lower molecular volume than the original glass. The resultant shrinkage creates tensile stresses in the surface , balanced by a compressive stress in the core of the fibre. With bare fibres the shrinkage stress was adjudged to be capable of producing the spontaneous cracking that develops on prolonged exposure to the acid. With composite materials the shrinkage stress, associated with a fibre that has been exposed to the acid at the tip

of a stress-corrosion crack, supplements any externally applied stress. This leads to the preferential failure of the exposed fibre, and results in progressive stress-corrosion crack propagation.

This mechanism has been widely quoted as the primary cause of fibre weakening during E-glass stress-corrosion. At high applied stresses, the extent of the surface shrinkage needed to nucleate flaws that will propagate through the fibres, is conjectured to be less than that needed to develop a visible core-sheath structure in the fibres.

An obvious weakness in this argument is that E-glass contains very little sodium, and that the principal cation in the glass structure is calcium. Despite this, it is still reasonable to assume that the replacement of calcium by hydrogen ions will lead to a reduction in molecular volume and that shrinkage will occur. More recently Bledski et al[12] have made a detailed study of core-sheath growth in E-glass fibres. Different patterns of spontaneous cracking were observed, featuring regular spiral cracks and irregular axial and radial cracks of the type shown in **Figure 2-13.** In these experiments it was found that the cracks only developed when the fibres were removed from the aqueous acid environment and were dried , prior to examination in a microscope. Fibres that are kept wet do not crack in this way. Bledski suggested that the shrinkage stresses that cause the cracking were associated with the gel-like, water-saturated siliceous layer that forms when the glass is fully demineralised by the acid. The shrinkage required to develop the surface tensile stress that causes the cracking only occurs when this layer dehydrates on drying. With dried fibres spiral cracks form when the sheath has a thickness of about one third of the fibre diameter. The spiral is a consequence of the balance between hoop and axial shrinkage stresses. When the

sheath is thicker than this the cracking pattern is of the irregular form.

Bledski followed this work with an explanation of the strength loss associated with fibre ageing. He found that the loss in strength could be accounted for by assigning the load bearing capacity of the aged fibre entirely to the strength of the residual core. Initial attempts to correlate aged fibre strength with core cross-sectional area were not successful, because the predicted strength was lower than the observed strength. It was later found that E-glass fibres are **heterogeneous**, in the sense that the surface layers are weaker than the core. Bledski associated this with the manufacturing process, which ensures that the outer layers of the fibres cool more quickly than the core. The outer layers are therefore less dense, and have a more open structure, causing them to be weaker than the core. This was confirmed by making fibres under different cooling conditions. Although these had the same overall composition and size distributions, their physical properties were strongly dependent on the method of preparation. It was shown that there were significant density variations across the fibre diameters. When this ~~anisotropy~~ **heterogeneity** was taken into account, a good correlation was obtained between aged fibre strength and residual core area.

1-9 Fibre demineralisation.

Bledski's work on E-glass fibre ageing was carried out with hydrochloric and sulphuric acids at 80°C. He examined the rate of growth of the sheath and found that the growth slowed markedly with time. This suggests that the rate of demineralisation is diffusion limited, with the hydrated sheath forming a barrier through which acid

and metal ions must diffuse to maintain the attack at the core-sheath interface.

The leaching of calcium ions from E-glass by aqueous acids has many similarities with the leaching of sodium from soda-lime glass by water. This latter system has been studied fairly intensively, since there are very sensitive methods available to measure sodium and hydrogen concentration profiles near the surface of flat glass plates. Flat specimens subjected to aqueous leaching at 90°C. - 100°C. start to develop a core-sheath structure of the type seen when E-glass is attacked by acids. However, the hydrated silicic acid layer that forms on the soda-lime glass surface is readily dissolved or dispersed in the water environment. A visible sheath is not, therefore, formed. This contrasts with the E-glass situation, where the hydrated sheath is insoluble in the acid and a clearly visible boundary between the core and the sheath develops.

Both systems are characteristic of diffusion-controlled reaction at an interface. Crank[23] has shown how the discontinuity at the core-sheath boundary can be represented by the use of a concentration-dependent diffusion coefficient in the diffusion equation:

$$\partial C/\partial t = \partial/\partial x(D\partial C/\partial x) \qquad (1\text{-}2)$$

In physical terms, the growth of the sheath can be visualised as a surface phenomenon, with very little subsurface penetration of the acid into the unreacted glass. Only when the surface is extensively demineralised does hydration of the resulting silicic acid layer enable the attacking acid to penetrate to the subsurface. The attack then continues at a very thin zone at the interface between the developing sheath and the glass core. This mechanism implies that the sheath will

not grow until the demineralisation of the surface is virtually complete. It is likely that this is the reason why fibre ageing with E-glass is limited to situations where the fibres are exposed to relatively concentrated acid solutions. Core-sheath formation has not been reported at concentrations lower than 0.1M. For soda-lime glasses Doremus and his associates[27,28,29], and in an independent treatment Smets and Tholen[25,26], have shown how the development of a sodium-depleted layer can be modelled. In reality, the system is complex, with the reaction rate at the interface dependent on the rate of diffusion of metal ions, hydroxonium ions* and water molecules through the hydrated surface layer. However, by assigning an effective diffusion coefficient, D', to the movement of the boundary, it is possible to show that a steep concentration gradient will exist at the core-sheath boundary. The key feature of D' that creates the steep gradient at the boundary, is its dependence on the concentration of hydroxonium ions at the core-sheath interface. This, in turn, depends on the extent of demineralisation at this interface. An important consequence of this is that the demineralisation occurs only at the interface and not within the body of the unreacted glass. Elementary chemical kinetics predicts that the rate of demineralisation will be dependent on the acid concentration. Since the development of the sheath will not proceed until the surface is fully demineralised, it follows that the core-sheath structure is unlikely to be observed with the more dilute acid solutions. This is in accordance with the reported incidence of this phenomenon.

---

* In English texts the solvated hydrogen ion, H_3O^+, is generally referred to as the hydroxonium ion. American nomenclature designates this ion as the hydronium ion. The English nomenclature is preferred in the present work.

1-10 Static fatigue failure of fibres.

From what has been discussed above it can be seen that fibre weakening by ageing can be satisfactorily correlated with the development of the core-sheath structure. The situation with respect to the static fatigue failure of glass fibres is less clear. Stress-enhanced fibre fracture is usually assumed to stem from the growth of existing surface flaws in the fibres, or from the nucleation and growth of new flaws[1]. Metcalfe and Schmitz[19] attributed the weakening of the fibres in the presence of a stress to the same ion-exchange mechanism that is involved in the ageing process. In this case they suggested that the shrinkage stress will be created at the surface of a fibre freshly exposed to acid at the tip of a propagating crack. When this is supplemented by the applied stress at the fibre surface, which is intensified by the presence of the crack, the conditions favour the growth of flaws in this part of the fibre. Rapid flaw growth occurs and the fibre breaks, exposing the next fibre to the weakening effect of the acid. This concept of an internally generated surface stress, developing as a result of glass demineralisation, is the most widely quoted explanation of the stress-enhanced weakening of E-glass fibres.

The statistics of fibre failure have an important bearing on static fatigue failure, because it is generally accepted that industrially produced fibres exhibit a flaw distribution. It is the number and severity of these flaws that governs the initial fibre strength. Metcalfe and Schmitz[21] showed that the flaw distribution in a fibre population leads to a distribution in fibre strength. This strength distribution was shown experimentally to conform with the Weibull distribution[41], and this has since been confirmed by others[18,84]. The equation describing this distribution is:

$$N = N_0 \exp (- (\sigma/\sigma_0)^m) \qquad (1\text{-}3)$$

In this equation the two Weibull parameters are the shape parameter, m, which characterises the width of the distribution, and the scale parameter, σ_0,which defines the upper limit of the distribution. Implicit in the definition of σ_0 is the length of the fibres,l. Metcalfe and Schmitz[17] showed that, in fact, the flaw distribution was multimodal, with at least two types of flaw in filaments separated from E-glass strand. There are small flaws with a small length separation (called C-type flaws) and larger flaws with a bigger length separation. One consequence of this is a significant decrease in the mean strength of the fresh fibres as the gauge length is increased. This is important in the composite stress-corrosion situation, because the length of fibre exposed to the corrosive environment at the tip of a growing crack is very short.

An alternative hypothesis for the stress-enhanced weakening of fibres during fatigue and creep rupture tests on composites was advanced by Lhymn and Schultz[31,72]. This does not require the presence of pre-existing flaws in the length of fibre exposed to the acid at the crack tip. They suggested that the contribution of the acid environment was to initiate pitting in the exposed fibre surface. This amounts to the nucleation of a new flaw site, which is subject to stress intensification because of its shape. This leads to rapid flaw growth and eventual fibre fracture. The attack features the demineralisation of the glass at the crack tip to produce a weak layer which is easily fractured. Preferential cracking along a planar path is due to the planar nature of the intensified stress field.

1-11 Statement of project objectives.

In the light of the above survey, it was considered that a useful contribution could be made to the understanding of the mechanism of E-glass/polyester stress corrosion by measuring the extent to which the resins are permeable to aqueous hydrochloric acid. In assesing the likely resistance of polymer composites to acidic stress corrosion, it was also considered necessary to identify what combinations of environment acidity and applied stress would cause the fibres to fracture. A natural continuation of this work was then to consider whether or not the extent of acid diffusion can create a sufficiently aggressive environment to weaken the glass fibres in a composite. It was noted that no complete explanation of the synergism between applied stress and environment acidity, in relation to the failure of fibres under a tensile load, has so far been advanced. It was therefore of high interest to see if the results from the diffusion measurements and the assessment of fibre failure characteristics could throw some light on the underlying stress-corrosion mechanism. The research project described in this thesis was therefore structured around the following general objectives:

1. To develop and use a method for measuring the diffusivity and solubility of aqueous hydrochloric acid in a range of polyester resins.
2. To develop and use a method for assessing the extent to which glass fibres are weakened by the simultaneous effect of an applied stress and an aggressive environment.
3. To compare the weakening that occurs when fibres are exposed to an aggressive environment in the presence and absence of an applied load.
4. To use the above data to examine critically the proposition that acid can diffuse through the resin in a composite to a sufficient extent

to initiate and sustain the progressive failure of the reinforcing fibres.

5.To consider the basic mechanism of fibre weakening and to see if an explanation can be found for the very strong activating effect that applied stress has on the failure rate of the fibres.

The experimental programme carried out during the pursuit of these objectives is described in detail in Chapters 2,3 and 4. The results are discussed in Chapter 5, which also contains the final conclusions reached in the work.

CHAPTER 2. WEAKENING OF GLASS FIBRES BY ACID.

In a non-corrosive environment, the principal constraint to the propagation of cracks in a high volume fraction glass fibre/polyester composite is the ability of the fibre reinforcement to withstand much higher tensile loads than the polymer matrix. An important additional factor is the resistance to fracture along the fibre/matrix interface at the tip of the propagating crack. The high modulus of the fibres limits the extension of the composite under load. Provided that the fibre/matrix interface remains intact the polymer matrix is not fully strained and only bears a small proportion of the applied load. In a stress corrosion situation the glass fibres are weakened on exposure to a corrosive agent, to the extent that they fail at loads significantly lower than their normal failure strength.

The polymer matrix normally presents an effective barrier that protects the glass fibres from the aggressive medium when the composite is immersed in an aqueous solution of a mineral acid. Stress corrosion crack propagation is believed to occur as a consequence of the acid solution bridging the resin webs that separate the fibres in the composite. This process occurs predominantly at the tip of a growing crack where stress intensification is considerable and where either diffusion or matrix cracking provide the transport mechanism whereby the acid gains access to the fibres[1].

Fibre weakening and failure is thus a process that occurs sequentially at the tip of a growing crack and evidence is available to show that the fibres fail in a stepwise manner, with a discrete waiting period between individual fibre breakages[2]. It seems reasonable to suppose that this waiting period is associated with the time required

for the acid to reach the fibre surface and to promote the weakening that eventually causes the fibre to break under the action of the local load.

In earlier work[3,15] measurements had been made of stress corrosion crack propagation rates in a series of composite materials made from E-glass roving. Four different resins of varying fracture toughness were used to prepare composite specimens and a technique was developed to enable crack propagation rates to be measured at constant stress intensity. These data can be used to estimate the waiting times for individual fibre fracture events at given stress levels.

In seeking to relate these waiting times to physical mechanisms, it is important to separate the two contributory factors. These are (a) the time taken for the acid to bridge the resin webs separating the fibres in the composite, and (b) the time needed for the acid to weaken the fibres. In different circumstances either of these processes could be rate-determining.

Fibre fracture at the crack tip leads to a very rapid, local release of strain energy, especially at high loads. If this is sufficient to promote crack formation in the resin, extending to the next fibre, a pathway for the transport of the acid to a fresh fibre surface will be established. If the acid can percolate rapidly through this pathway, the time needed to transport acid to the fibre surface will not contribute significantly to the waiting time. Conversely, if the transport of the acid to the fibre is diffusion-limited, this would delay the fibre weakening process to an extent that could control the overall crack propagation rate.

Diffusion-limited acid transport would also result if the matrix cracks were too fine to permit normal capillary flow. It would certainly be featured if molecular diffusion through the bulk resin was the principal mode of acid transport. This latter possibility is explored in detail in the work described in Chapter 4.

The other factor that determines the waiting time between fibre fracture events is that indicated in (a) above. Once the acid has gained access to a fibre a definite time will be required for the acid to weaken the fibre until it breaks. This time will depend on both the the acid concentration and the local stress at the fibre surface. A proper understanding of this factor requires firstly that a method of measuring fibre weakening is available. Secondly it requires the acquisition of data showing how this weakening responds to changes in acid concentration and applied stress levels. The acquisition of such data is one of the main objectives of the work described in this Chapter.

An experimental programme was therefore carried out to define the boundaries of the stress - acid concentration - failure time field within which fibre breakage would occur. In this programme it was envisaged that experiments covering a wide range of conditions would be required. Because of this it was recognised that the multiple replication necessary to obtain statistically significant results from tensile tests on single fibres would be a very lengthy operation. An alternative was to examine the possibility of using strands of roving for the tests, since each of these strands contains about 4000 separate fibres. Proctor[5] has discussed the influence of water and dilute acids on the strength of strands and data on the long term effects of these

agents on E-glass strands has been published by Aveston and Sillwood[6].

In the present work the main area of interest is that in which the mean fibre failure time is between 1 - 20 minutes, since this is the order of the typical time between individual fibre fracture events during stress corrosion crack propagation at low stress intensities[2]. The experimental methods used in this programme are described below.

2-1 Bundle tests with E-glass roving.

Tests on single strands of glass filaments are normally described as bundle tests and this nomenclature will be used in what follows. In all tensile tests it is important to ensure that the load is concentrated in the gauge length rather than in the grips. With glass fibre bundles a further difficulty is the ease with which fibres can be weakened by mechanical damage, leading to fibre fracture in the grips. A solution to this problem is to make the roving into a composite at the strand ends. These ends then become stronger than the central glass strand and when the bundle is subjected to a tensile test fibre fracture occurs within the gauge length. This principle is featured in the bundle test method, used routinely by Pilkington Ltd. to monitor strand strength during production[7]. Their method of specimen preparation has been adapted for use in the present work.

The technique for holding and forming the specimens is shown in Figure 2-1. The strand was aligned on a former made from 1mm. card. The strand ends were treated with a low viscosity epoxy resin (Epikote 815) which would cure at room temperature. A small paint brush was used to ensure good wetting out of the glass. After the first layer

FIGURE 2-1. PREPARATION OF TENSILE SPECIMENS FROM E-GLASS ROVING.

1. 3mm. card marked up with 20mm. X 10mm. holes punched out, to define gauge length between 30mm. X 20mm. end tabs.

2. Strand aligned on card, tensioned with adhesive tape. Epikote resin applied to end tabs. Top tabs of 30 mm. X 20mm. card placed in position. Resin allowed to set.

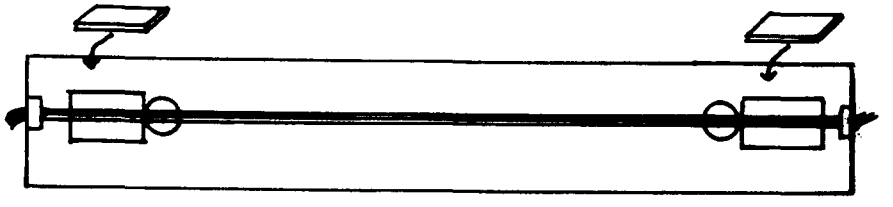

3. After resin has set, specimen trimmed to yield final tensile specimen:

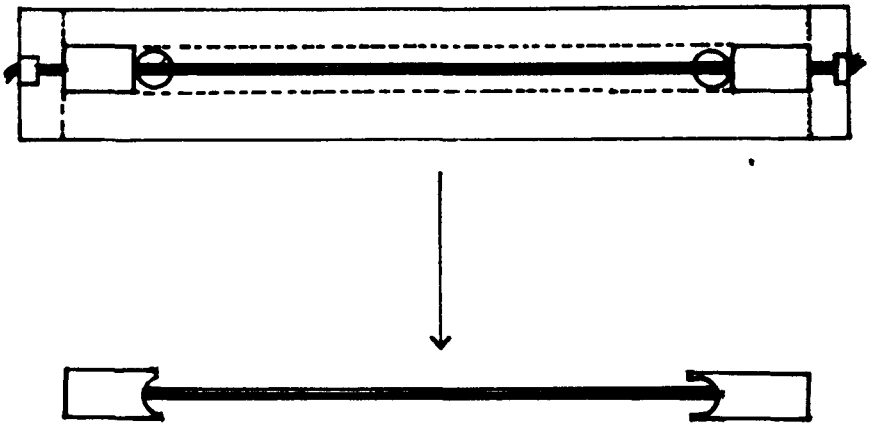

of resin had gelled a further layer of fresh resin was added. A card tab was placed on top of each strand end to sandwich the strand between the two pieces of card. When the resin had set the card ends were trimmed to size and the specimen was gripped at both ends in the tensile test machine. The central part of the former was removed by cutting, as shown in Fig. 2-1, and the specimen was then ready for testing.

Proctor[5] has discussed the difference between specimen ageing and continuous exposure to the environment during testing. The essential feature of ageing is that it involves the exposure of the unstressed strand to the environment. In the ageing tests the simple specimen preparation method described above was used. The protective size on the filaments was removed by immersing the gauge length successively in acetone, deionised water, and again in acetone. This was done to ensure that the environment had unrestricted access to the filament surface. The fibres were allowed to dry in air and were then immersed in the test solution for the prescribed exposure time. Figure 2-2 shows how a simple jig, made from two blocks of wood, enabled the strand to be exposed to a test solution. The end tabs were clamped between the blocks and held in place with an elastic band. The rod through the blocks supported the assembly in the solution and facilitated handling the specimen. After exposure the specimens were removed and washed again with deionised water and acetone. The aged specimens were dried in air and were then ready for tensile testing in an Instron 1185 test machine. With care it was possible to conduct the exposure and mount the specimen in the machine without mechanically damaging the fibre bundle. The extent of weakening was assessed by comparing the mechanical properties with those of the fresh strand.

FIGURE 2-2. ARRANGEMENT FOR EXPOSING BUNDLES TO TEST SOLUTIONS.

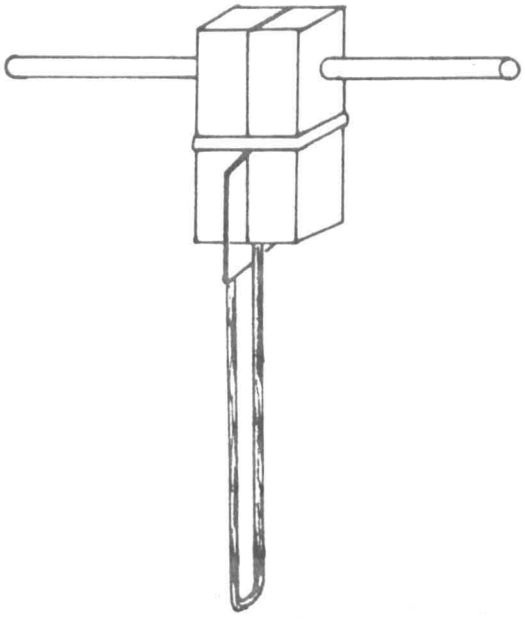

1. JIG FOR HOLDING TENSILE SPECIMENS.

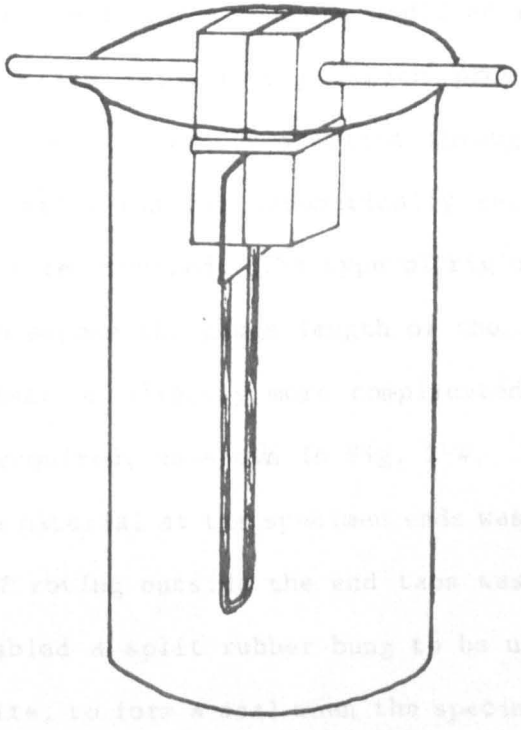

2. JIG IN POSITION, READY FOR ADDITION OF ACID.

Attempts to age specimens by exposure under a static load were frustrated by bundle breakage before the ageing had been completed. This occurred at relatively short exposure times, even with loads below half of the failure load of that of the fresh strand. Typically, the fresh strand would break at a deadweight loading of about 120Kg.. The same roving would support a load of 50Kg. indefinitely, but when immersed in hydrochloric acid of concentrations between 0.01M and 1.0M bundle fracture occurred within 15 minutes.

A different approach was therefore required in order to evaluate fibre weakening during continuous exposure under load. The objective in this part of the work was to determine the mean fibre failure times for various combinations of load and acid concentration. In these tests this could best be achieved by measuring directly the time for the bundle to break under the combined influence of the load and the environment. The test was therefore modified so that it could be carried out in a creep rupture rig, which provided the means for loading the fibres to the required extent through a 10:1 lever arm. The rig also had provision for automatically recording the time at which bundle fracture occurred. The type of rig used is shown in Fig. 2-3. In order to expose the gauge length of the loaded roving to the aqueous environment a slightly more complicated method of specimen preparation was required, as shown in Fig. 2-4. In this case the region of composite material at the specimen ends was extended, such that a short length of roving outside the end tabs was treated with epoxy resin. This enabled a split rubber bung to be used to sandwich this length of composite, to form a seal when the specimen was inserted into a length of glass tubing. The faces of the split bung were coated with silicone rubber sealant before assembly. This arrangement provided

FIGURE 2-3. CREEP RUPTURE RIG, WITH STRESSED E-GLASS STRAND IN ENCLOSURE CONTAINING AQUEOUS ACID.

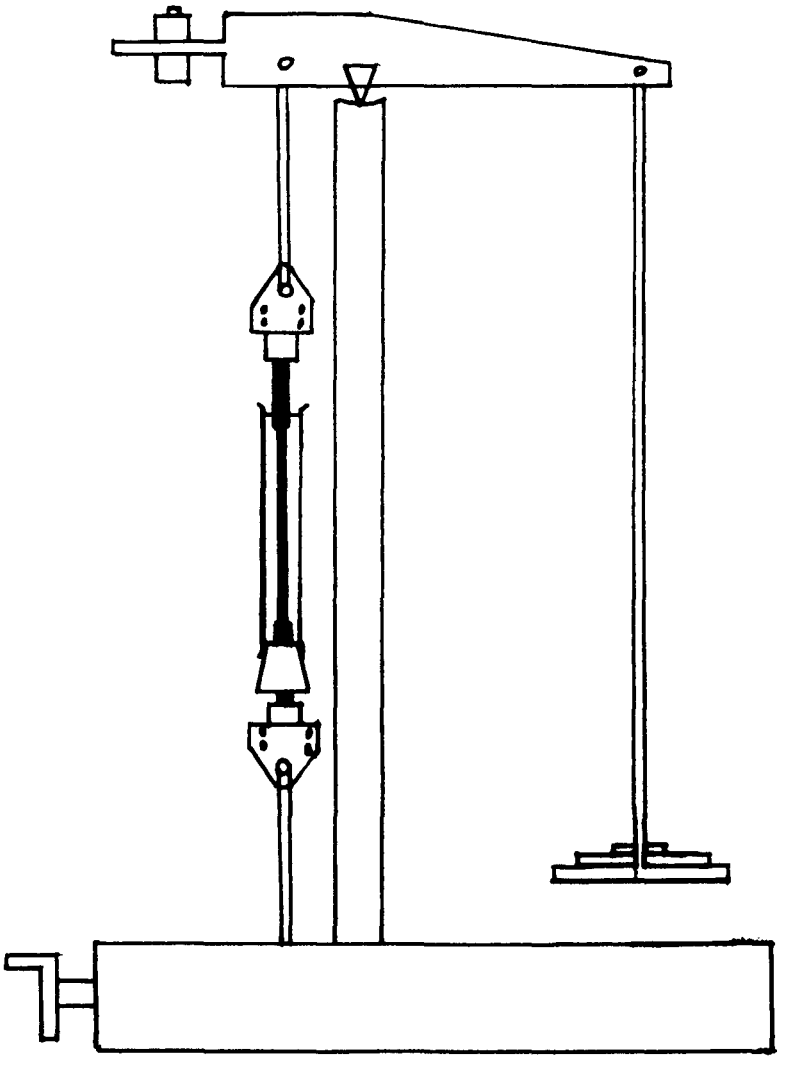

FIGURE 2-4. PREPARATION OF TENSILE SPECIMENS FOR CONTINUOUS EXPOSURE TESTS.

1. 3mm. card marked up with elongated holes to define gauge length:

2. Strand specimen prepared as in Figure 3-1, with Epikote treatment extended to limit of elongated holes to yield:

3. Split bung affixed to Epikote region of one of the end tabs, using silicone rubber sealant to make a liquid-tight joint:

4. Other end tab pulled through glass sleeve until bung locates to form enclosure:

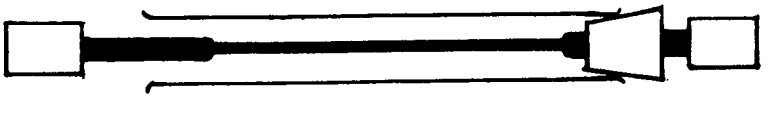

5. In vertical position enclosure holds liquid, as shown in Figure 3-3.

an enclosure within which the gauge length could be continuously exposed to an aqueous solution whilst under load.

This type of test is similar to conventional fatigue tests, apart from the fact that the applied load is static, rather than cyclic. In both tests the time to failure under load is the critical measure of the performance of the material. Tests featuring continous exposure under static loads have been called "static fatigue tests" by Wiederhorn[8], and this nomenclature will be used in the present work.

2-2 Experiments with aged bundles.

Tests using the bundle ageing method were carried out to explore the effects of exposure time and acid concentration on bundle strength. The results obtained are shown in Tables 2-1,2-2, and 2-3. The tensile tests were carried out with an Instron 1185 machine in the usual way. To assess the effects of exposure time and acid concentration on strand strength, a convenient measure is the maximum load the bundle will withstand under the test conditions. These are the loads listed in Tables 2-1 - 2-3.

TABLE 2-1 EQUEROVE 2347 BUNDLE TESTS WITH 4 HOUR EXPOSURE TIME.

SPECIMEN NUMBER	PRETREATMENT AND EXPOSURE MEDIUM	GAUGE LENGTH mm.	MAXIMUM LOAD,N
9	As-found; water	76	1070
10	As-found; water	75	1230
11	As-found; air	70	1130
12	As-found; air	70	1120
13	Desized; water	76	1200
14	Desized; water	84	1220
15	Desized; M HCL	70	695
16	Desized; M HCL	75	670

All these tests were conducted on dried bundles, at a constant strain rate, with a crosshead speed of 0.5 mm./min.. A more detailed analysis

TABLE 2-2 EQUEROVE 2347 BUNDLE AGEING TESTS. EFFECT OF ACID CONCENTRATION AT EXPOSURE TIME OF 16 HOURS.

SPECIMEN NUMBER	ACID STRENGTH	GAUGE LENGTH mm.	MAXIMUM LOAD,N
28	0	71	1120
29	0	84	1080
17	0.2M	65	938
18	0.2M	72	970
19	0.4M	67	879
20	0.4M	78	865
21	0.6M	70	738
22	0.6M	70	738
24	0.8M	70	470
25	0.8M	70	420
26	1.0M	70	431
27	1.0M	70	424

Note: All specimens except 28 and 29 were desized with acetone prior to exposure to acid. All specimens except 28 and 29 were washed with water and dried with acetone before the tensile test.
of the stress - strain curves obtained during these and similar tests will be discussed later.

Examination of the results shows that prolonged exposure to molar hydrochloric acid led to very severe reductions in bundle strength. The reduction was critically dependent on the exposure time. Thus,a reduction by a factor of two in bundle strength was observed at an exposure time of about four hours. However,it was noted that only very slight reductions in bundle strength resulted from short exposures to the acid solution. During stress corrosion crack propagation in a composite the time available for fibre weakening to occur by exposure to the acid solution is typically in the range 5-20 minutes. The data in Table 2-3 show that such exposure times do not cause unstressed fibres to be weakened to a significant extent.

In these ageing tests the reduction in bundle strength was also found to depend strongly on the concentration of the aqueous acid used for the exposure. From the results in Table 2-1 it can be seen that

TABLE 2-3 EQUEROVE 2347 BUNDLE AGEING TESTS. TESTS WITH DEIONISED WATER AND HCL AT SHORT EXPOSURE TIMES.

SPECIMEN NUMBER	EXPOSURE TIME MINUTES	EXPOSURE MEDIUM	GAUGE LENGTH mm.	MAXIMUM LOAD,N
31	5	MHCL	90	1120
33	10	MHCL	90	1050
34	15	MHCL	90	1210
36	20	MHCL	90	960
38	5	WATER	90	950
83	10	WATER	90	1250
84	15	WATER	90	1000

at a concentration of 0.1M and below very little weakening of the unstressed fibres had occurred,even after an exposure time of 16 hours.

2-3 Core -sheath structures in aged fibres.

It is well known that the long term exposure of unstressed E-glass fibres to mineral acids, at concentrations of around 1.0M, results in the selective removal of calcium and aluminium from the surface of the glass[9,10,12]. This demineralisation process has a very marked effect on the mechanical strength of the glass. E-glass fibres exposed to acid solutions for periods in excess of 8 hours develop a characteristic core-sheath morphology. This is shown in Figure 2-5 which is an SEM photograph of cross-sections of some of the fibres from specimen 26. Bledski et al[12] have shown that the demineralised siliceous sheath is much weaker than the E-glass core and have made a detailed study of the strength reduction of fibres exhibiting the core-sheath structure. Their results show that the reduction in tensile strength is well correlated with the reduction in area of the load-bearing core of the acid treated fibre. In their analysis they noted that the winding speed and the rate of fibre cooling during manufacture influence the density of the glass across the fibre section. This makes the centre of the filament section intrinsically stronger than the surface layers. This effect is probably responsible for the effect

FIGURE 2-5. SEM MICROGRAPH OF FIBRE CROSS-SECTIONS, SHOWING CORE-SHEATH STRUCTURE.

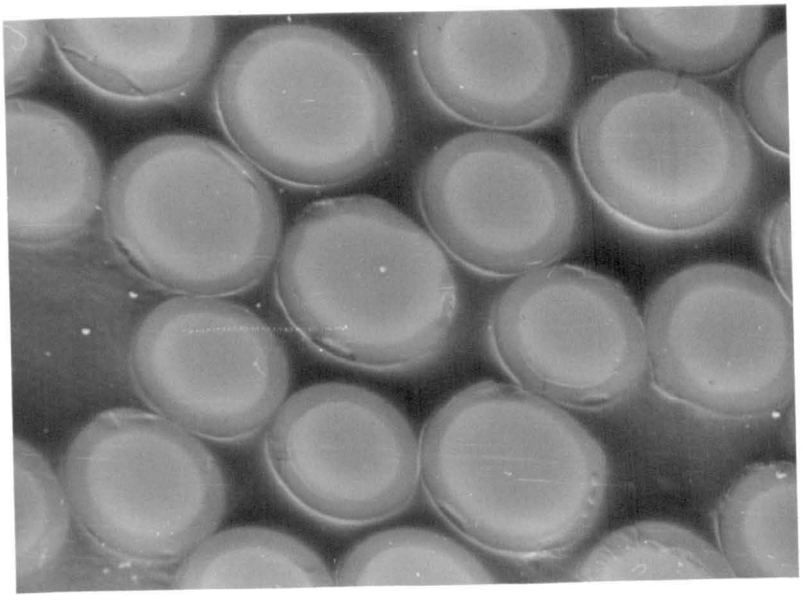

FIGURE 2-6. SEM MICROGRAPH OF FIBRE CROSS-SECTIONS OF ORIGINAL FIBRES.

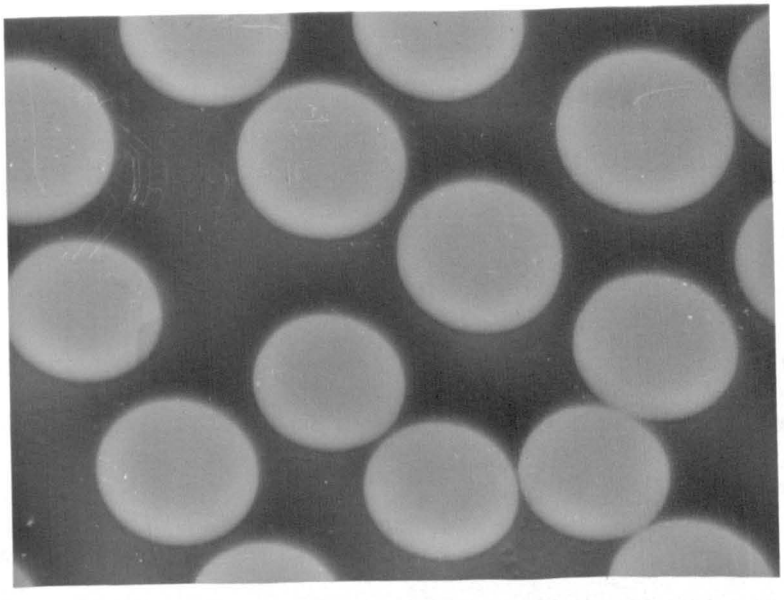

shown in Figure 2-6 which is an SEM photograph of untreated fibre sections. The darker area in the centre of each fibre is attributed to the increased density of the material in this region.

The Bledski analysis provides a satisfactory explanation of the effects of long term exposure of unstressed fibres to acid solutions on filament strength, on the basis of core area reduction. However, it does not explain how fibres can be weakened in much shorter times,in the range 1-20 minutes, by more dilute acid solutions by the simultaneous application of stress. The results of the present work,taken together with all the other available data on the formation of the core-sheath structure, show that the timescale for core-sheath formation is relatively long at 25 C. The reduction in area associated with exposures of 1-20 minutes is extremely small, and cannot be seen in the SEM. Hence fibre area reduction is not the basic cause of fibre weakening during stress corrosion crack propagation.

2-4 Experiments with continuous exposure to the acid solution during the tensile test.

Before proceeding to tests where the fibres were exposed to the acid under load, an intermediate experiment was carried out. In this series of tests the fibres were exposed to the acid solution in an unstressed condition. They were then tested in tension in the Instron 1185 machine with the acid environment still surrounding the fibre bundle. A 2 hour exposure period was used and results from various acid concentrations are shown in Table 2-4.

These results highlight the importance of stress as an important factor in fibre weakening. During the relatively short duration of

the tensile test (approximately 3 minutes), the gradually increasing load has led to substantial fibre weakening, even with the most dilute acid tested. The data do not show a strong dependence on acid concentration over the range studied, since in all the tests involving the acid a similar strength reduction was observed. The reduction was similar to that obtained in the simple ageing tests with molar hydrochloric acid at an exposure time of four hours.

TABLE 2-4 EQUEROVE 2347 BUNDLE TESTS. SPECIMENS EXPOSED TO ACID SOLUTIONS WITHOUT STRESS FOR 2 HOURS. TENSILE TESTS CONDUCTED WITH CONTINOUS EXPOSURE TO THE ACID ENVIRONMENT.

SPECIMEN NUMBER	ACID STRENGTH	GAUGE LENGTH mm.	MAXIMUM LOAD,N
1	WATER	47	1290
2	0.2M	50	740
3	0.4M	48	689
4	0.6M	40	550
5	0.8M	47	635
6	1.0M	40	651

It is considered that the majority of the weakening seen in these bundles occurred during the tensile test itself. This suggests that a second mechanism of fibre weakening exists, in which the combined effects of the environment and the stress lead to an enhanced rate of fibre failure.

2-5 Experiments with simultaneous exposure of bundles to acid solutions and stress.

In these tests the bundles were desized with acetone, washed with water, and were then subjected to tensile loading in a creep rupture rig, as shown in Figure 2-3. The acid solution was added to the enclosure surrounding the loaded bundle by means of a pipette. For the reasons outlined earlier it was necessary in these tests to measure fibre weakening in terms of the time for the bundle to break.

To evaluate the separate effects of applied stress and acid concentration on the failure times of the bundles, tests were carried out at a series of constant loads. The results from these creep-rupture tests are given in Figure 2-7, which shows the time for bundle breakage as a function of acid concentration at various loads. The data on which this plot was based are listed in Table 2-5. An impression of the repeatability of the data can be obtained by examination of Figure 2-8, where the use of a logarithmic time axis enables the individual points for each curve to be plotted. Despite the experimental scatter, it is considered that the trends shown by the curves in Figures 2-7 and 2-8 are well justified.

TABLE 2-5 STATIC FATIGUE RESULTS.

LOAD, Kg.	SPECIMEN NUMBER	ACID STRENGTH	FAILURE TIME, min.
75	116	0.0005M	>10000
75	115	0.001M	>10000
75	114	0.001M	>10000
75	123	0.00125M	2772
75	122	0.00125M	>10000
75	120	0.0025M	19
75	121	0.0025M	17
75	118	0.005M	13
75	119	0.005M	10
75	110	0.01M	9
75	112	0.01M	7
75	113	0.1M	2
75	117	0.1M	2
75	124	0.3M	1.75
75	126	0.5M	1.1
50	41	0.5M	8.6
50	68	0.5M	10.4
50	42	0.1M	9.5
50	53	0.1M	7.5
50	125	0.1M	8.0
50	127	0.05M	12.0
50	128	0.05M	13.8
50	129	0.02M	11.5
50	148	0.02M	19
50	39	0.005M	>50
50	49	0.005M	67.5
50	147	0.01M	58
40	99	0.005M	>10000
40	100	0.005M	8184
40	56	0.01M	8
40	57	0.01M	330
40	145	0.025M	90

40	55	0.1M	61.5
40	59	0.15M	38
40	60	0.15M	38
40	58	0.25M	41
40	51	0.5M	33.5
40	69	0.5M	18
40	80	0.5M	35
40	94	1.0M	30
40	95	1.0M	36
40	96	1.0M	35
40	97	1.0M	38
40	45	1.0M	21.5
30	132	0.05M	1056
30	64	0.10M	690
30	131	0.10M	1206
30	130	0.15M	504
30	67	0.25M	204
30	75	0.5M	183
30	76	0.5M	126
30	77	0.5M	162
30	46	1.0M	75
30	61	1.0M	88
20	150	0.2M	2094
20	149	0.3M	816
20	71	0.5M	468
20	151	0.75M	312
20	44	1.0M	131
15	140	0.1M	>10000
15	144	0.4M	5316
15	143	0.6M	1176
15	142	0.8M	966
15	152	0.9M	510
15	141	1.0M	570
10	73	0.5M	5892
10	150	0.9M	3060
10	48	1.0M	1620

Inspection of these data shows that there are several features worthy of note. Unexposed bundles would stand a load of 120-130 Kg. for up to 1 minute before the strand broke in the gauge length. At lower loads the unexposed fibres were stable virtually indefinitely until the acid environment was introduced. At loads in the region of half of the dry strength of the bundle, tests were possible over a wide range of acid concentrations varying between .005M and M. At loads in the region of one tenth of the dry bundle strength, the only tests of consequence were those with acid concentrations close to 1.0M, and

FIGURE 2-7. Static fatigue data for E glass fibre bundles in HCl.

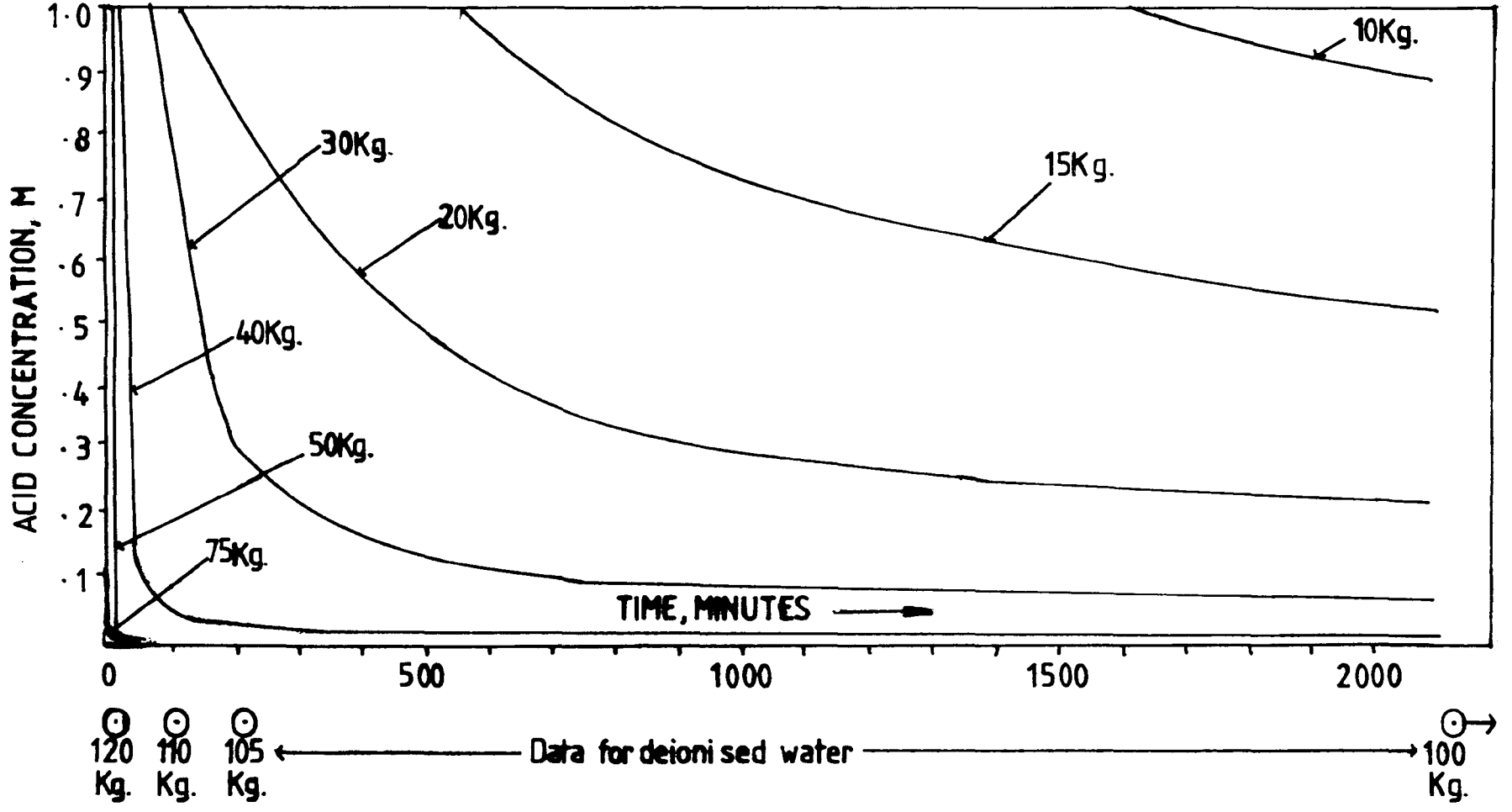

FIGURE 2-8. E glass static fatigue data, shown with logarithmic time scale and normalised stress.

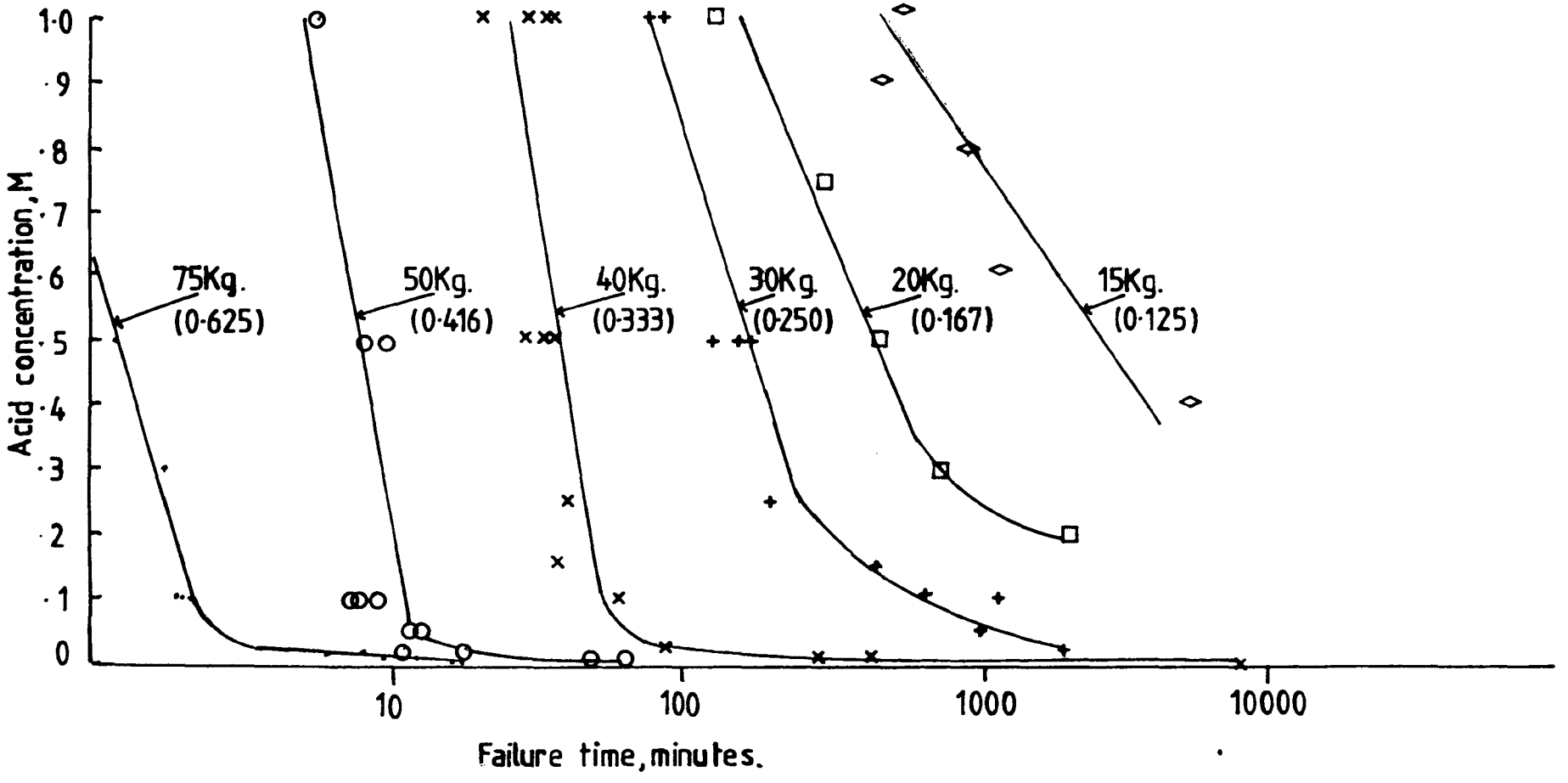

even then the failure times were extremely long. It is evident that the combined effects of stress and exposure to an acid solution had a very rapid, deleterious effect on bundle strength. In the higher load regimes bundles exposed to acid solutions were weakened by very dilute acid. However, for any given stress level there is a limiting concentration below which weakening does not occur within the the critical timescale. Aveston and Sillwood[6] have shown that in very long term exposure tests pure water was capable of weakening E-glass fibres that had been exposed under load. The timescale for this weakening was, however, of the order of years. In the present work interest was centred on much shorter timescales. The experimental programme was designed to identify combinations of acid concentration and load which gave bundle failure times in the range 1-2000 minutes. In Figure 2-7 the relative insensitivity to acid concentration at the higher loads and the existence of a lower limit to the acid concentration, below which significant weakening does not occur, leads to the occurrence of a characteristic "knee" in the plots. A similar "knee" is seen in a plot of load against failure time, at constant acid concentration, as shown in Figure 2-9.

2-6 Interpretation of static fatigue results.

The short term static fatigue curves obtained in these studies can be shown to conform with the equation:

$$(\sigma/\sigma_s)^n = t_s/t \qquad (2\text{-}1)$$

which Wiederhorn[8] has assigned as the basic equation of the "universal fatigue curve". In this equation σ_s and t_s are normalising factors, where t_s is the time required for the fibres to fracture when exposed to a standard stress, σ_s.

Figure 2-9. Load vs failure time profiles.

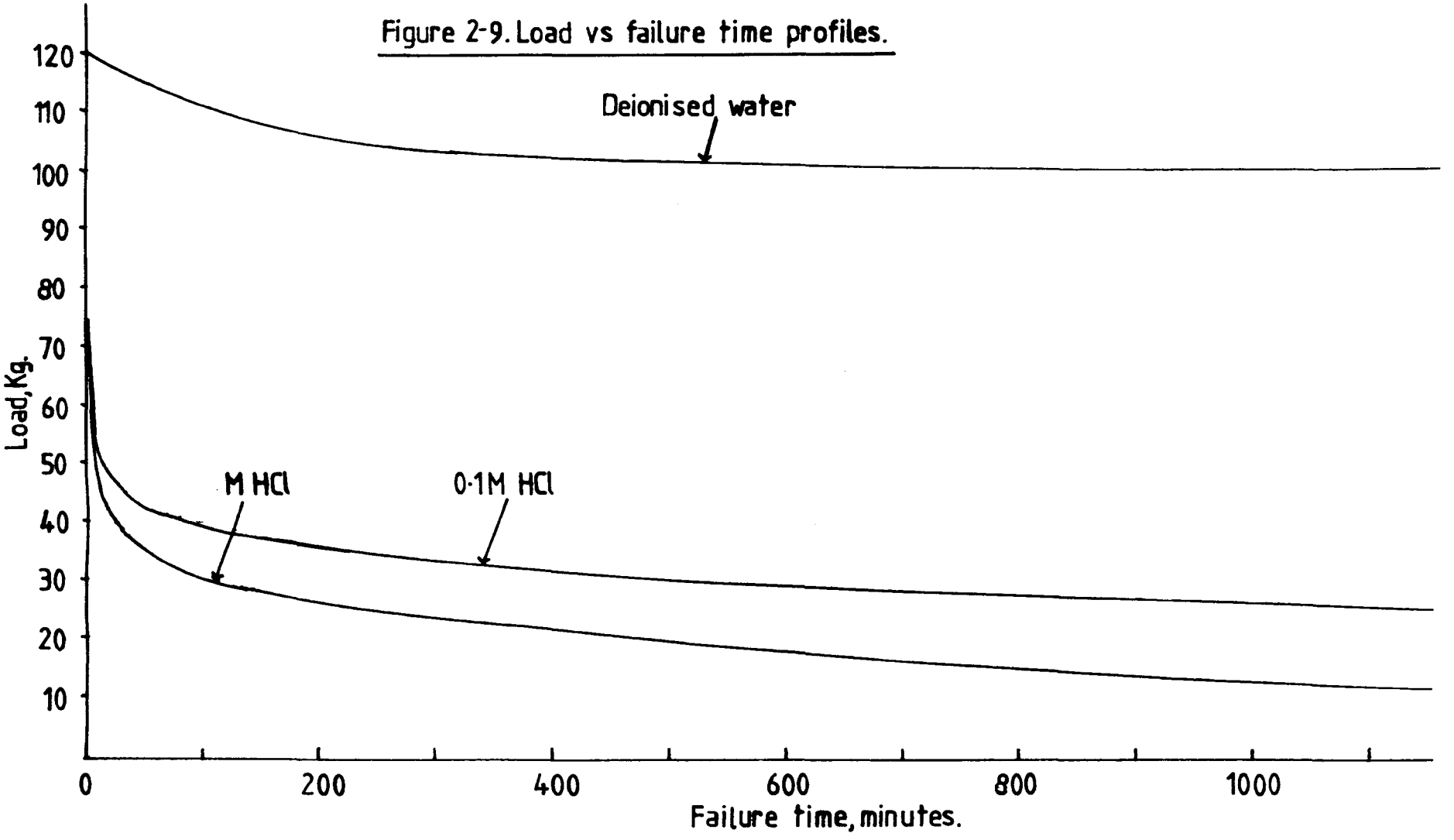

The equation may be derived on the assumption that the characteristic time to failure of fibres, exposed simultaneously to an acid solution and a load, is associated with the growth of microcracks in the fibres. In applying fracture mechanics to this situation use is made of the empirical Paris equation[53]. This relates the crack propagation rate to the stress intensity, K_I:

$$da/dt = \alpha K_I^{\,n} \qquad (2\text{-}2)$$

where a = crack length and α and n are material constants. For a given crack length, a, da/dt is constant.

Since t_s is inversely proportional to da/dt and K_I is proportional to σ_s it follows that:

$$1/t_s = C\sigma_s^{\,n} \qquad (2\text{-}3)$$

where C is a constant. For any other failure time t, a similar equation applies:

$$1/t = C\sigma^n \qquad (2\text{-}4)$$

Dividing (2-3) by (2-4) gives:

$$t_s/t = C\sigma_s^{\,n}/C\sigma^n$$

which is equivalent to equation (2-1). This equation predicts that a plot of $\log t_s/t$ vs $\log\sigma/\sigma_s$ should be linear, with a slope of n.

The data from Figure 2-7 has been used to generate this plot for three acid concentrations, 1.0M, 0.5M and 0.1M. In deriving the plot a standard load of 75 Kg. was used to provide the normalising factors. The result is shown in Figure 2-10. The line drawn through the data has a slope corresponding to an n value of 4.8. This compares with the value of about 4 obtained by Price[15] by the direct measurement of crack velocity in a range of E-glass polyester composites. The glass volume fraction in these composites was about 0.5.

FIGURE 2-10. Log t_s/t vs log σ/σ_s for E-glass fibres in HCl.

○=M △=0·5M ×=0·1M

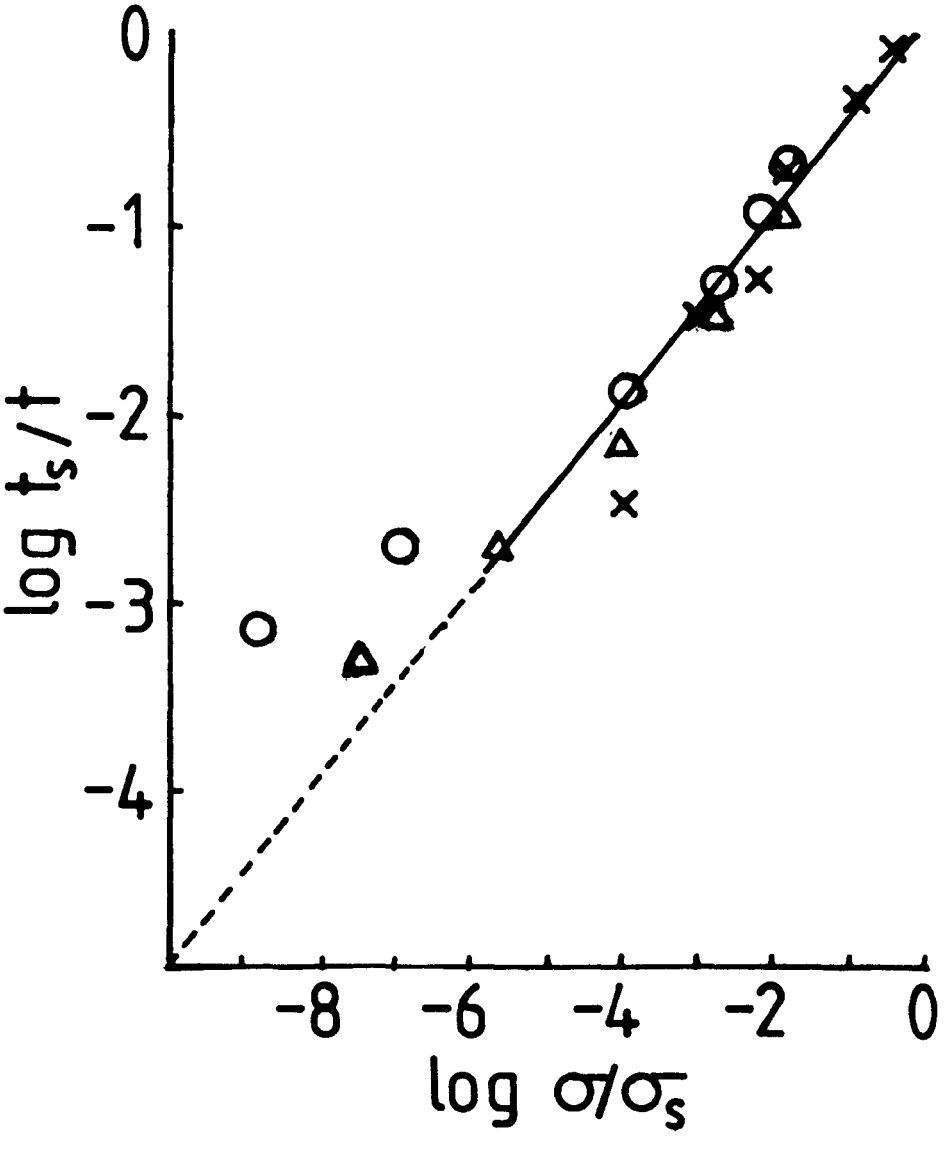

Close examination of Figure 2-10 shows that all the points fit the linear relationship well for failure times up to about 10 hours. At longer times the data for the 1.0M and 0.5M acid deviate to give failure at shorter times than predicted by the line. This is attributed to the effect of the other fibre weakening mechanism, i.e. core area reduction, supplementing the crack growth process.

In the relatively short timescales that prevail as stress corrosion cracks propagate in a composite it is considered that stress-enhanced microcrack growth is the dominant fibre weakening process. As the cracks grow their rate of propagation increases because of the increased stress intensity at the crack tip. If the stress at the crack tip reaches the tensile strength of the material the crack propagates at near sonic velocity and the fibre breaks. In an acid environment the crack propagation rate in the fibres depends strongly on the applied load. At high loads the degree of stress intensification available after a short growth period is such that at the crack tip the cohesive strength of the original glass is exceeded. The fibre fracture surface accordingly shows the characteristic mirror zone (region of corrosion-assisted slow crack growth), and river lines (region of fast fracture of uncorroded glass). At lower loads a more modest degree of stress intensification is available and almost all of the fibre damage occurs by the slower process of corrosion-assisted growth. This leads to a much extended mirror zone and results in the very smooth, featureless surfaces that characterise the highly planar surfaces seen on typical stress-corroded composite specimens from low-stress tests.

These effects are illustrated in Figure 2-11, (a) and (b), which shows fracture surfaces of fibres from bundle tests. Figure 2-11(a)

FIGURE 2-11. FRACTURE SURFACES OF BROKEN FIBRES.

(A)

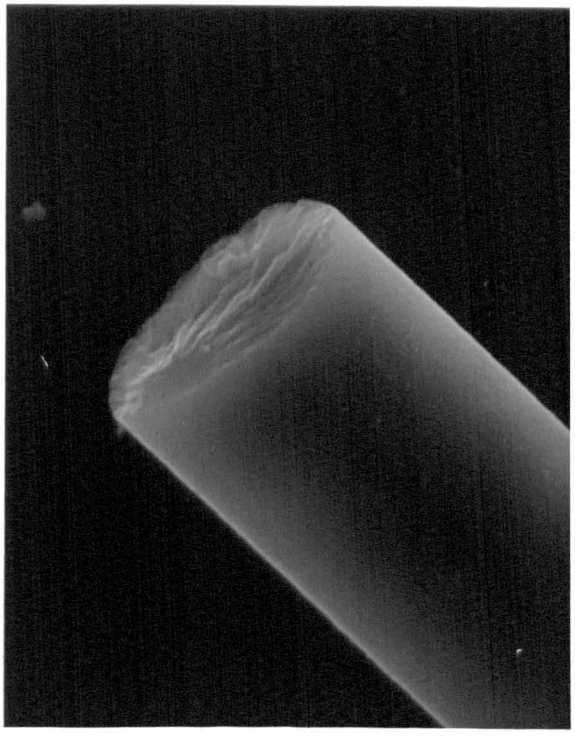

(B)

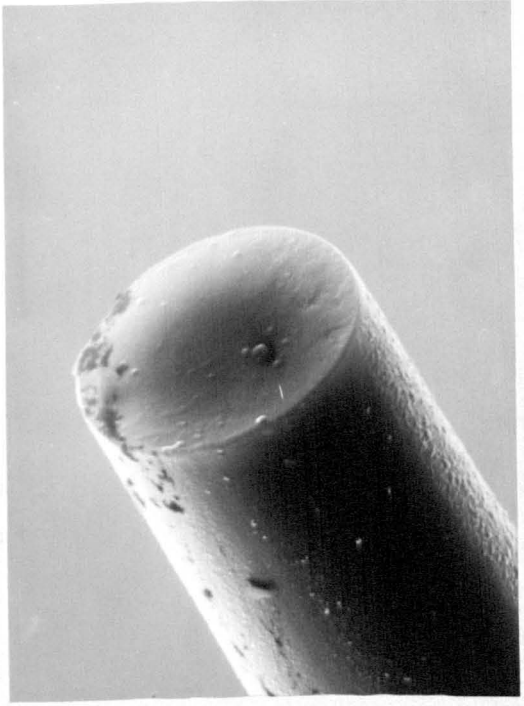

represents the high load short failure time situation. Figure2-11(b) is typical of the low load slow growth situation. The appearance of these fibre fracture surfaces shows the features descibed above and correlates well with the appearance of fibres in fractured composite specimens produced under conditions of high and low stress. This supports the view that the fibre failure process under stress involves crack growth. It also indicates that the bundle tests are representative of the fibre failure process that occurs in composites during stress corrosion.

The origin of the microcracks in the fibres has been the subject of much speculation since Griffith[16] first discovered the great increase in strength that could be achieved by forming glass into fine monofilaments. Metcalfe and Schmitz[10] examined the effect of gauge length on fibre strength and concluded that there can be no simple, generalised, statistical model for describing flaw distributions in fibres. This is because there is a distribution in flaw severity, a distribution in flaw spacing, and a distribution in the spread of flaw spacing. Empirical fits to a distribution such as the Weibull distribution can be found for specimens of constant gauge length[18]. However this treatment is inadequate if the number of flaws in the test volume is very small, or if the distribution is multimodal, with different types of flaw causing failure under different environmental conditions. This latter situation is a very plausible one in the stress corrosion situation, since it does not follow that the flaw that would fail at high load is necessarily the one that would grow at low load in a composite.

Microcracks in glass fibres almost certainly originate from flaw sites in the fibre. Examination of freshly desized fibres in the SEM

at moderate and high magnifications does not reveal any obvious flaw sites. The fibres appear to be smooth and featureless, as shown in Figure 2-12. This absence of visual defects is well known and has led to various suggestions concerning the nature of the flaws in the fibres. The most commonly quoted possibility is that of sub-microscopic cracks with widths of near atomic dimensions. Because of their shape such cracks would develop very high crack tip stresses on loading. Metcalfe and Schmitz[19] do not rate this possibility very highly, since they estimate that such micro-cracks could only be a few Angstroms long for the fibres to exhibit high strength in their as-found condition after manufacture. Bledski[12] has shown how industrially manufactured fibres can have a high residual surface stress. This can be linked with another suggestion from Metcalfe and Schmitz (ibid) that incipient flaws exist at points of high local residual stress on the fibre surface. A third possibility concerns local inhomegeneities on the fibre surface, including occluded dust particles picked up by the molten glass filaments during extrusion.

Irrespective of the nature of the flaws, it follows that the mean strength of a fibre population will be lower than that of the unflawed material to an extent dependent on the number and severity of the flaws present in the fibres. In the present study the principal interest is not so much on this weakening as on the additional weakening caused by exposure to an aqueous acid environment.

In the experimental work a clear difference has been noted in the effect of the acid when the fibres are exposed in the unstressed as opposed to the stressed state. Unstressed fibres exposed to molar acid for long periods develop the core-sheath structure. The sheath is very weak and, following Bledski's argument, the weakening is mainly due

FIGURE 2-12. DESIZED FIBRE WITH FEATURELESS SURFACE

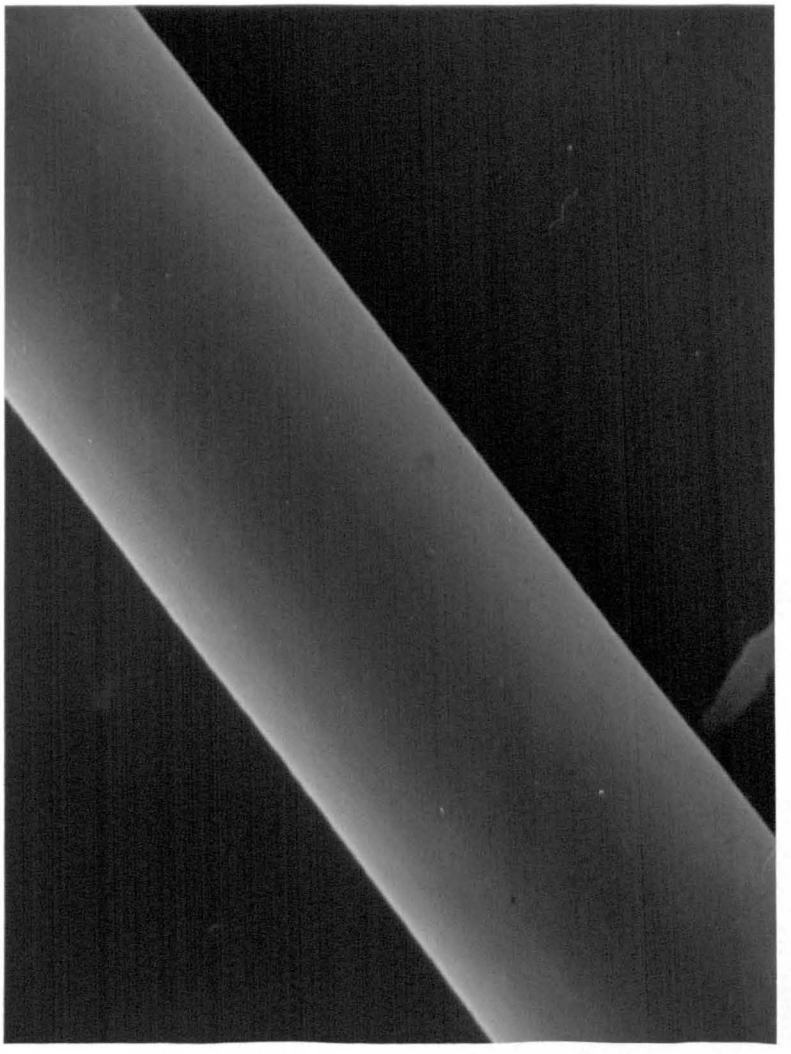

to the loss of area by the load-bearing core. This process does not occur to a visible extent in the much shorter times during which fibre weakening occurs when the fibres are exposed to the acid under load. Evidence will be presented in Chapter 3 to show that with short term exposures, even with molar acid, demineralisation is confined to the surface layers of the fibres . With a ten-minute exposure for example, the depth to which demineralisation can be detected is certainly less than 0.05 microns. With more dilute acid fibre weakening is only observed at higher loads and again, within the timescale required for fibre fracture, there is no evidence of subsurface demineralisation. It follows that if stress-assisted weakening is associated with demineralisation of the glass, then this must be a "skin" effect rather than an area reduction effect.

2-7 Stress-assisted corrosion.

The data from the static fatigue tests show that the applied stress is a very powerful driving force for crack growth in the fibres. It is capable of promoting crack growth, even in pure water, over a range of times varying from minutes to years, depending on the level of the applied stress.

It is known that freshly desized fibres contain flaws which reduce their strength. Table 2-3 shows that these flaws do not become more severe as a consequence of exposure to acid solutions for short times. However, applying a stress strongly activates flaw growth on a short timescale, and to explain this effect it is necessary to show why the environment apparently becomes more aggressive in the presence of the stress. Metcalfe and Schmitz[9] suggested a mechanism of fibre weakening that is widely quoted in the literature. This mechanism involves the

modification of the surface layers of the E-glass by an ion-exchange process. Network-modifying cations such as Na^+ and Ca^{2+} are replaced in the network by hydrogen ions. Because the H^+ ions are smaller than the metal cations, network shrinkage occurs and sets up surface stresses which are additive with the applied stress. Their evidence for this was that spontaneous cracking of the fibre surface was observed after prolonged exposure to the acid. However, Bledski[12] has shown that the spontaneous cracking only occurs when the fibres are removed from the environment and dried.

Metcalfe and Schmitz noted that, in their work, only glasses with more than 5% alkali could build up enough stress to crack spontaneously. This finding is not supported by data from other sources[9,12,35] and it is now commonly accepted that E-glass will crack spontaneously after prolonged exposure to acid. Figure 2-13 shows two different crack patterns, observed in the present work by exposing Equerove 2347 filaments to molar HCl. Bledski has observed very similar crack patterns.

Nevertheless, the principle of surface shrinkage as a source of surface stress was considered to be worth examining. At the same time it was decided to examine the growth kinetics of the core-sheath structure, since the weight of evidence points to surface demineralisation as a contributory factor, both in fibre ageing and in static fatigue failure. An experimental programme was therefore carried out to examine these aspects of the problem in detail.

2-8 Core-sheath growth measurements. Experimental procedure.

FIGURE 2-13. SPONTANEOUS CRACKING OF E-GLASS FIBRES AFTER PROLONGED EXPOSURE TO M HCL.

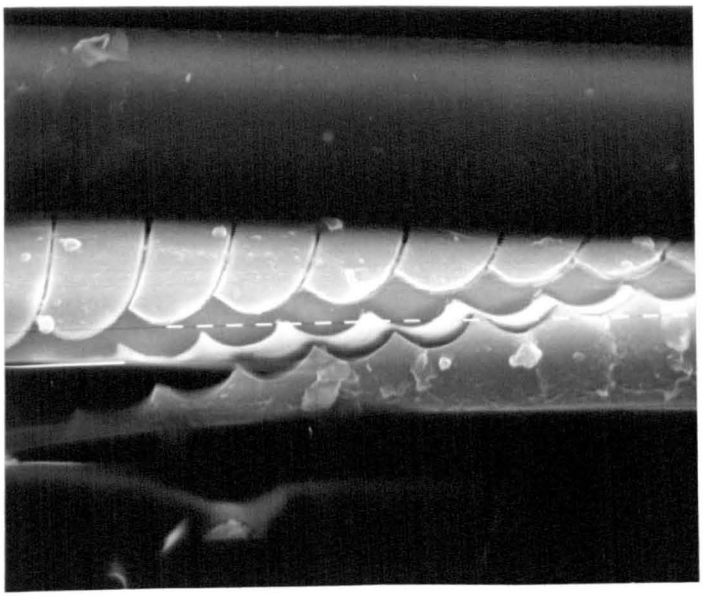

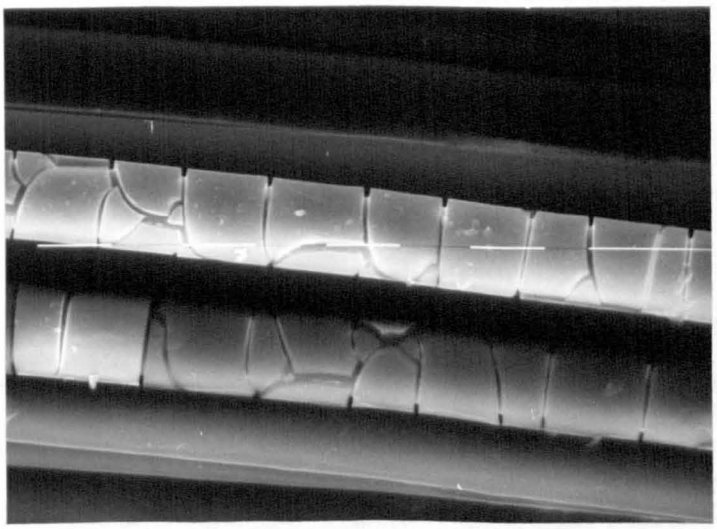

50mm. lengths of Equerove 2347 roving were cut and washed successively with acetone and deionised water, to remove the size from the fibres. The efficacy of this treatment can be seen in Figure 2-14, which compares SEM micrographs of the original and washed fibres. The cut ends of the fibres were treated with epoxy resin to hold the ends together. The specimens were placed in a test environment, which was held at 25deg.C - 0.1deg.C for the duration of the test. The test environment was a large excess of aqueous hydrochloric acid, and a variety of concentrations, in the range 0-1M, were used. At each concentration tests were made for various exposure times, up to and including 16 days.

After exposure the specimens were cut and mounted for examination in the SEM. Samples were required for observation both perpendicular and parallel to the fibre axes. For the parallel case the fibres were directly attached to an SEM stub with epoxy glue and sputter-coated with carbon. Perpendicular viewing was necessary to reveal the core-sheath structure. This was achieved by incorporating the fibres in a standard resin mounting block, followed by grinding and polishing down to 1.0 micron diamond paste. Some difficulties were encountered in wetting the desized fibres with the mounting resin, but eventually the technique shown in Figure 2-15 was developed, which worked well. Figure 2-5 shows the cross section of fibres exposed to 1.0M HCl for 16 hours, in which the core-sheath structure is clearly seen. By 20 hours in MHCl a small but significant proportion of the fibres began to show cracking of various degrees in the sheath, including the spiral cracking shown in Figure 2-13.

FIGURE 2-14. DESIZING OF E-GLASS FIBRES BY WASHING WITH ACETONE

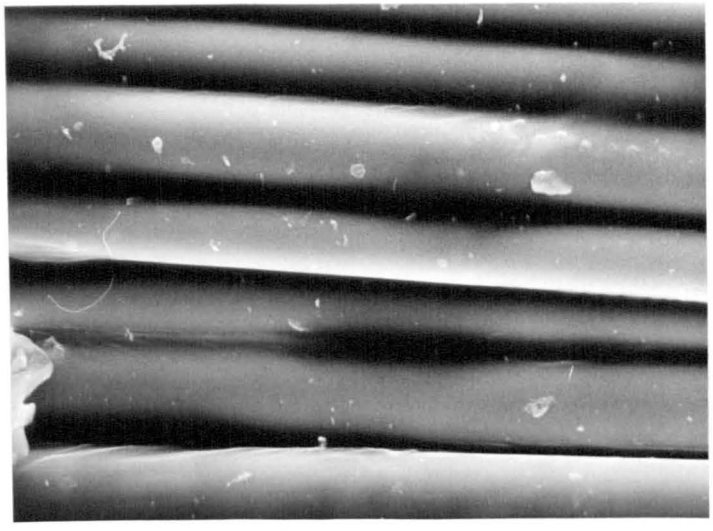

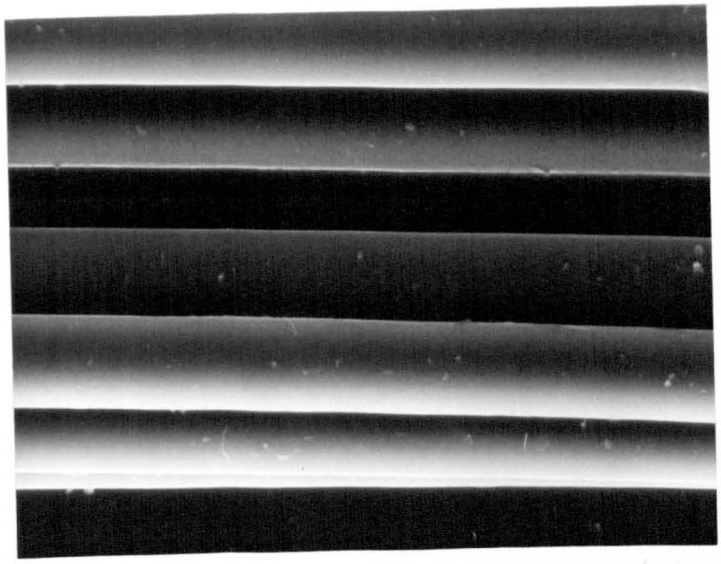

FIGURE 2-15: METHOD FOR OBTAINING FIBRE CROSS-SECTIONS.

1.Short length of 2 mm. I.D. silicone rubber tubing slit axially and stretched, to enable fibre bundle to be placed inside. When released, tube reassumes cylindrical shape.

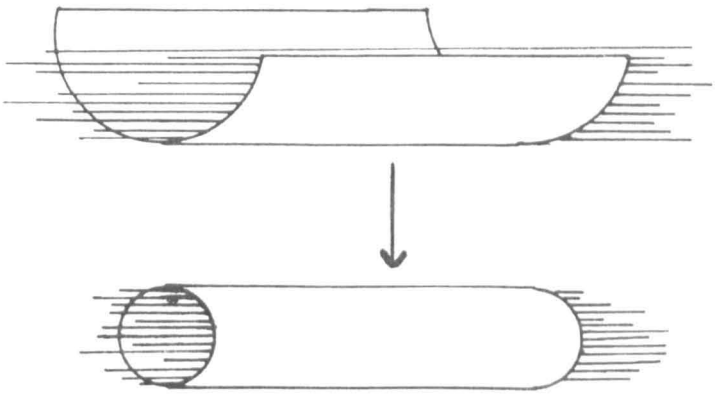

2. Tube + bundle placed inside glass sleeve with short length of silicone tube protuding. Further length of larger diameter silicone tubing, fitted with screw clip, pushed over glass sleeve:

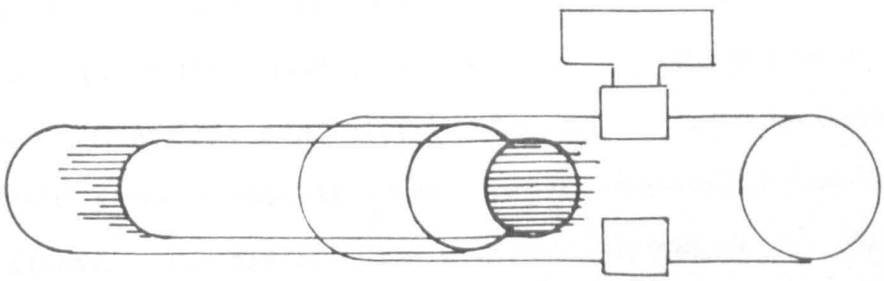

3. Assembly mounted vertically, fitted with funnel and charged with catalysed resin. Allowing the resin to flow through the bundle gives good wetout. When the resin has set, the cast rod containing the fibres is easily released from the silicone tubing, and can be sectioned, mounted and polished in the usual way.

2-9 Fibre diameter measurements.

To estimate the mean diameters of the sheath and core in the specimen cross sections a statistical method was used for some of the data. The most densely populated areas of each mount were photographed, and the diameters of 200 fibres were measured with a 'VIDEOPLAN' image analyser. This involved tracing the outline of each fibre with a light pen. The software in the system computed the area of each outline traced in this way, and assigned a diameter by assuming that the area was circular. The error in drawing around each fibre was calculated by drawing around a circle of known diameter (similar to that of the photographed fibres) and was found to be 0.6% (standard deviation).

The stastical analysis of these data was also carried out by the 'VIDEOPLAN' software. The data were interpreted by summing the measured values. The Gaussian formula was used to derive mean, modal, and median values for each set of measurements. In the present work the mean values were considered to be the most relevant. These were used to explore the growth profiles of the sheath, and to asses any radial dimension changes associated with core-sheath development. Figure 2-16 shows a typical output for an analysis of the freshly desized fibres. The distribution of fibres diameters is slightly skewed. However the shape of the distributions of core and sheath diameters was broadly self-consistent for specimens exposed to a wide range of acid concentrations and exposure times. Figure 2-17 shows the distributions of core and core + sheath diameter for fibres exposed to molar HCl for 16 hours.

Figure 2-16. Untreated fibre diameter distribution.

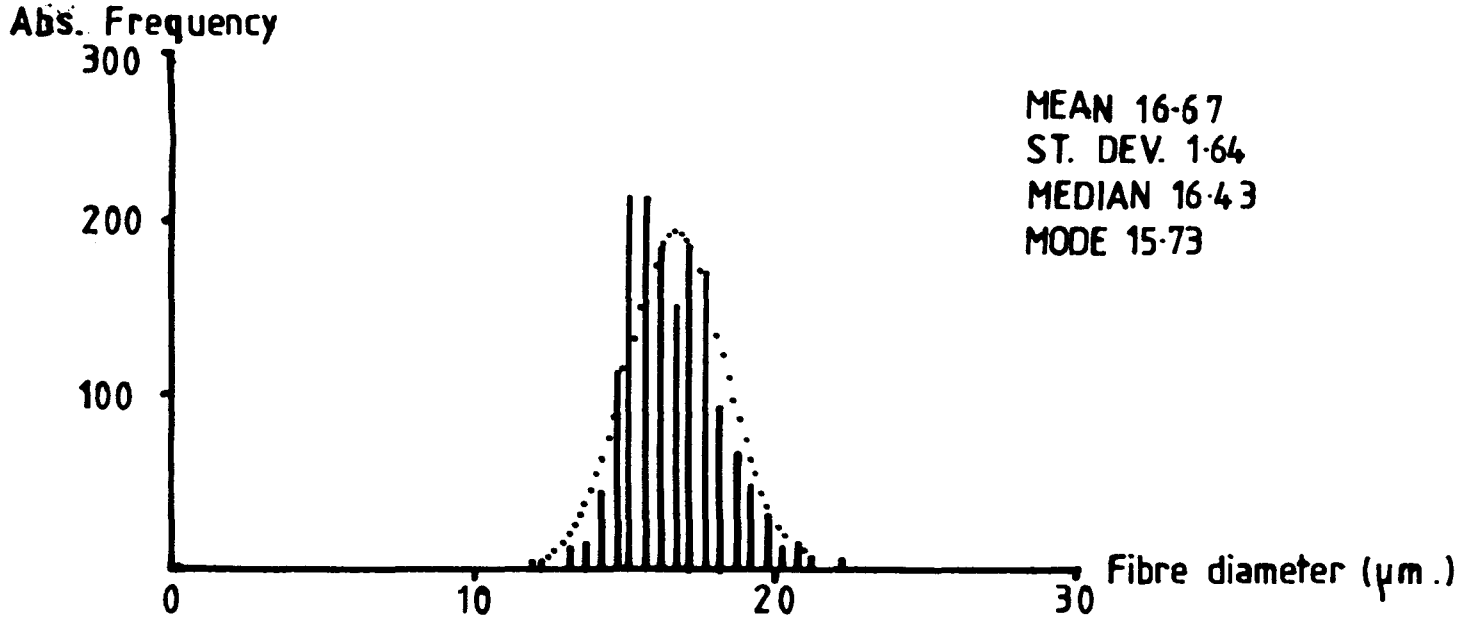

Figure 2-17. Core and sheath size distributions at 16 hrs. in M HCl.

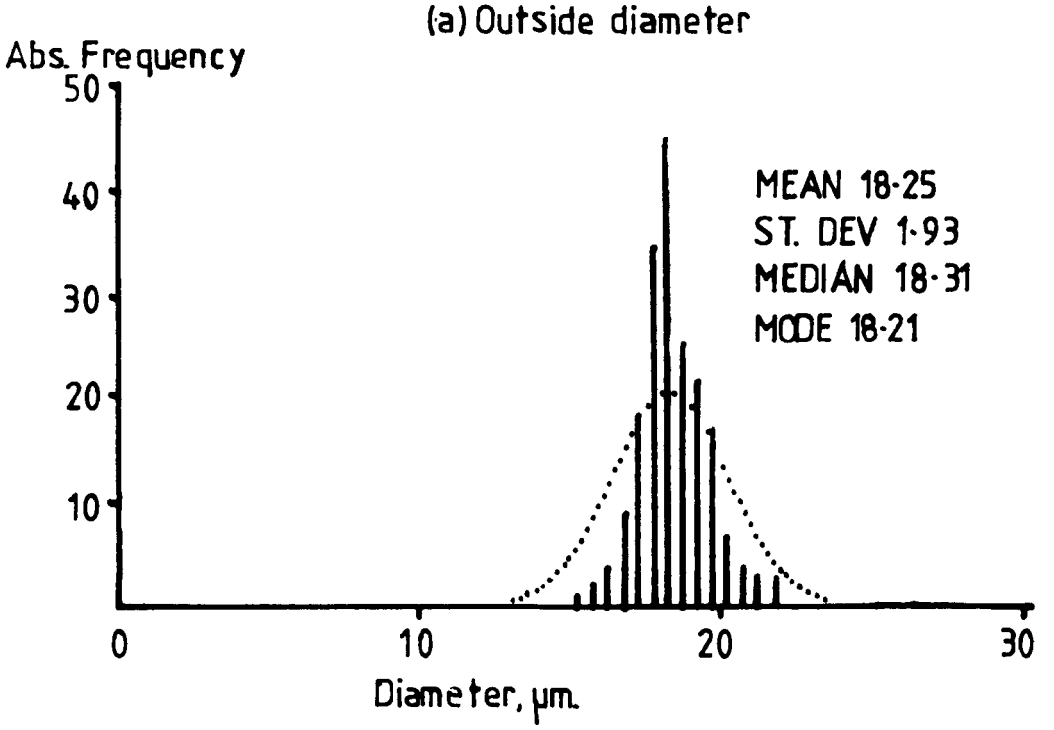

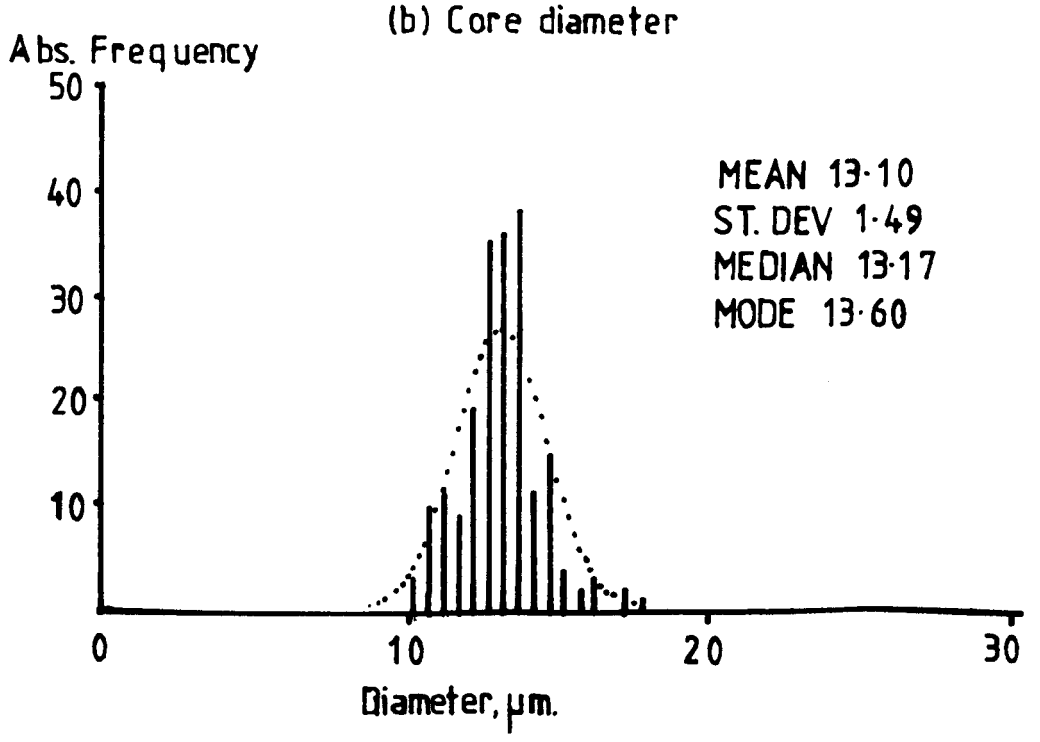

Additionally, a more direct method of measurement was used to provide data to supplement that obtained from the 'VIDEOPLAN'. This involved the direct measurement of core and sheath diameters from SEM photographs. For each data set mean diameters were obtained for 30-40 fibres measured in this way. These data were of particular value in confirming the shape of the sheath growth profile, as discussed below.

2-10 Results of fibre shrinkage measurements.

In Figure 2-18 the 'VIDEOPLAN' data is used to show the variation in outer diameter for fibres exposed to molar HCl for times up to 168 hours. At this time the sheath represents more than 50% of the total fibre area. As can be seen there is no significant change in the mean outer diameter of the fibres. Since each point on the plot is based on 200 individual measurements this is considered to represent a convincing demonstration that radial shrinkage does not occur during fibre demineralisation.

Because of its amorphous nature glass is usually considered to be isotropic, and it would therefore seem unlikely that axial shrinkage would occur. Indeed, for the Bledski explanation of spontaneous cracking to occur as the sheath is drying, it would seem necessary for the hydrated sheath to expand, as diffusing water enters the structure. Intuitively this seems reasonable, especially as gel-like layers of siliceous material have been detected on the surface of glass specimens[29].

On the basis of these results it is considered very unlikely that a change in the volume of the depleted layer is the primary cause of crack nucleation in the stress corrosion of E-glass fibres. Even if

Figure 2-18. Outer fibre diameter after exposure to MHCl.

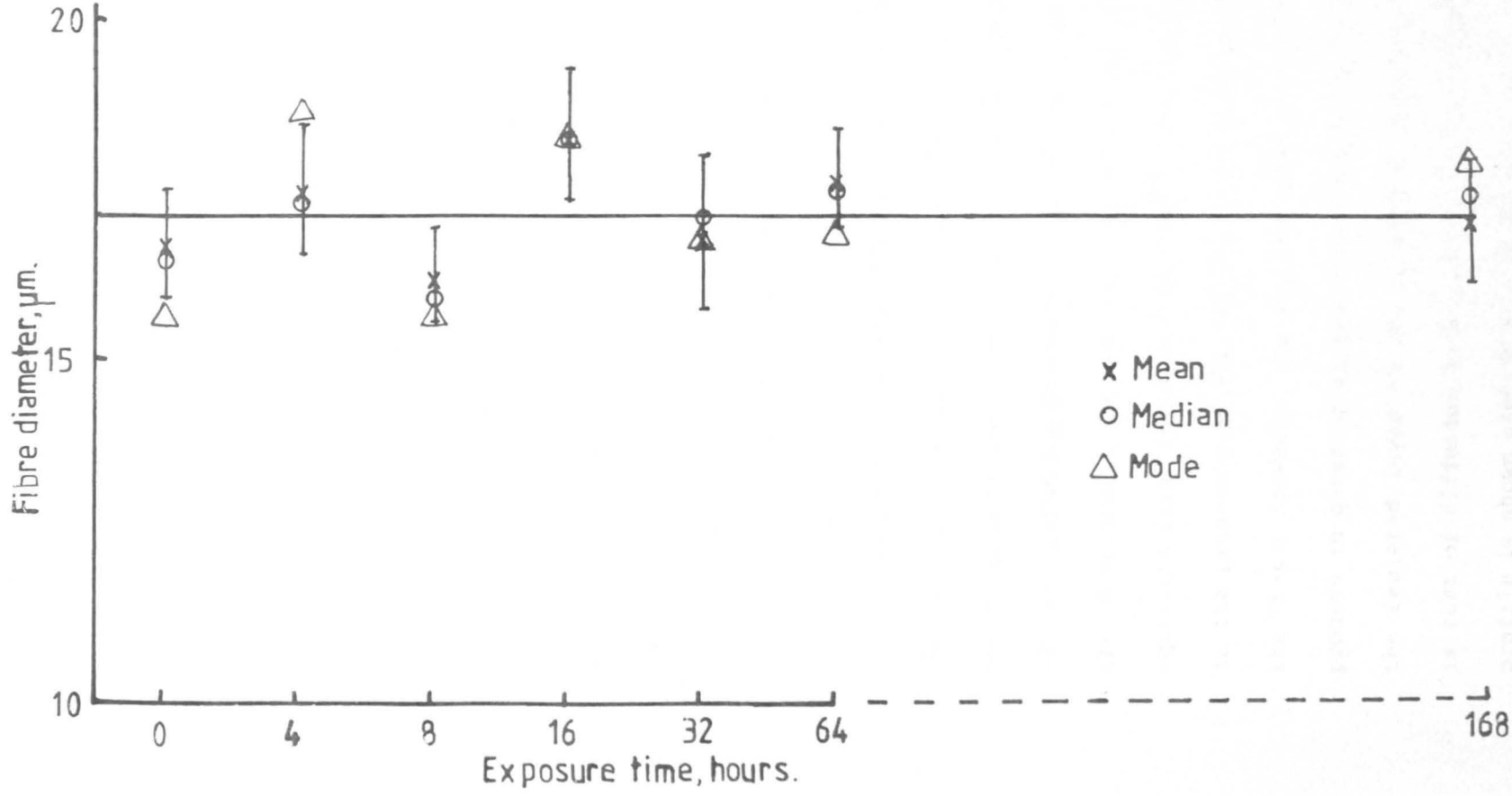

surface shrinkage had been detected it is known that substantial growth of the depleted layer is necessary before spontaneous cracking occurs[9]. A particularly noteworthy feature of fibres in the surfaces of freshly fractured stress-corrosion composite specimens is that they show very little evidence of general corrosion. As will be shown later, this is in accordance with the skin-weakening mechanism discussed above.

2-11 Results of core-sheath growth measurements.

Figures 2-19 and 2-20 show the increase in sheath width and sheath area plotted as functions of time, for fibres exposed to MHCl for up to 384 hours. A good fit to the core diameter profile is given by the empirical equation:

$$d = 18.1 - 1.8 \ln t \qquad (2\text{-}5)$$

where d is the core diameter, and t the exposure time.

For mechanistic reasons,which will be discussed in more detail in Chapter 3, there is reason to believe that the rate of growth of the sheath is diffusion-controlled. Diffusion processes are involved in all the following Chapters of this Thesis, and the argument requires the development of specific solutions to the general diffusion equations first formulated by Fick[86]. For the geometries of importance in the present work the derivation of these solutions is discussed in the Thesis Appendix. During the formation of the sheath the diffusion process in question is that involving the movement of the acid through the depleted layer to the unreacted glass underneath. The geometry is that of diffusion into a semi-infinite cylinder. The sheath growth profile is shown plotted as a function of exposure time in Figure 2-20. At first sight this profile appearcd to have the correct shape for a

Figure 2-19. Core diameter vs time.

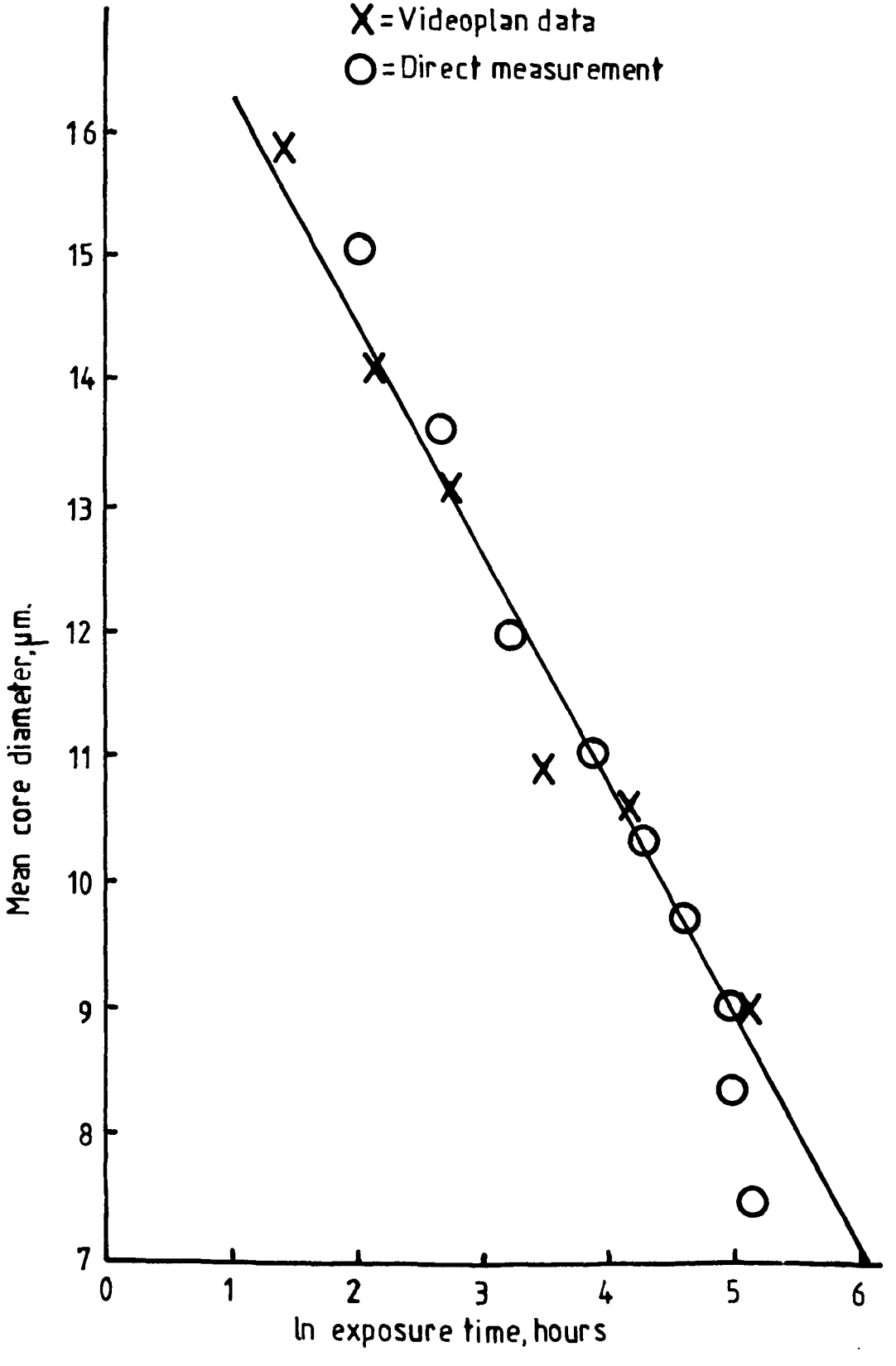

Figure 2-20. Diffusion profiles for growth of sheath in M HCl.

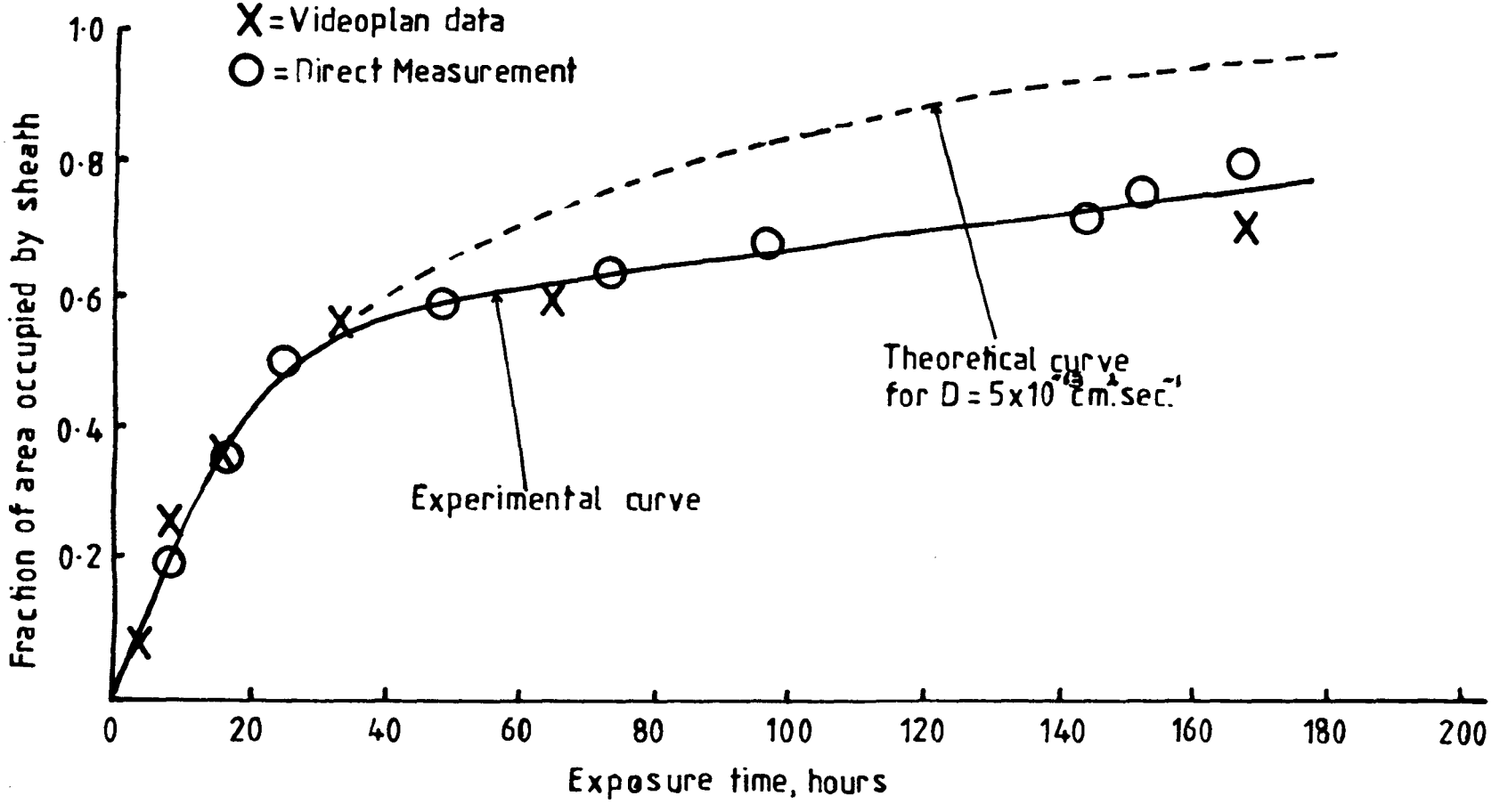

simple diffusion model. An attempt was therefore made to fit the data to the diffusion equation for this geometry, using the method described in the Appendix. The solution is expressed in terms of the total uptake of diffusant by the cylinder,(Mt), as a fraction of the total uptake when the cylinder is saturated with diffusant (M). In the present argument these can respectively be represented by the annular area occupied by the sheath, and by the total area of the fibre. A theoretical diffusion profile was derived that gave the best fit to the initial part of the experimental data plotted in Figure 2-20. The dotted line in the Figure shows this profile, which corresponds to a diffusion coefficient of 5×10^{-13} cm.^{2}/sec. It can be seen that the predictions fit the data very well for the earlier part of the curve. At exposure times of greater than about 40 hours,however, the rate of depletion is arrested to a greater extent than would be predicted by simple diffusion. The results are evidently representative of a more complex diffusion situation, in which the diffusion coefficient varies with penetration depth.

This leads to the notion that in static fatigue, the fibre weakening process is associated with the demineralisation of the fibre surface, rather than with the gross corrosion of the fibre. In Bledski's model of fibre ageing, the reduction of the load-bearing area of a fibre is due to sheath growth. For an effect to be noticed a relatively thick depleted layer must be formed. In contrast to this, the static fatigue failure of fibres can occur within a timescale of a few minutes, so that there is no possibility of forming a thick depleted layer. If fibre demineralisation is involved at all in the static fatigue mechanism, it can only occur in a very thin depletion zone at the fibre surface. The subsequent demineralisation of the subsurface layers is a complex diffusion-controlled process, which, by its nature proceeds

more slowly as the distance from the surface increases. The next objective was therefore to consider how these facts could be used to explain the very pronounced effect of an applied stress in activating the growth of cracks during static fatigue.

2-12 Fibre weakening mechanisms. Ageing and static fatigue.

In static fatigue the exposure time to the acid environment needed to promote fibre fracture can be very short, and may only be a few minutes. Depending on the time available for surface leaching, and the acid concentration in the fibre environment, it is possible that the surface demineralisation may be partial or complete. The progressive removal of the CaO and Al_2O_3 from the glass network by the leaching process will give a continuous distribution of strength, varying from the high level of the original glass to the low level of the fully demineralised material. Figure 2-19 shows that the rate of demineralisation of the subsurface glass is substantially slower than that of the surface material. This exponential decrease in sheath growth with time can be attributed to the ease with which the cations can react with hydrogen ions and diffuse out through the siliceous layer which forms on the surface of the fibre. The demineralisation rate is therefore a maximum at a fresh surface and then decreases exponentially with time. The effect of exposing an unstressed fibre to an aqueous medium for a short time will thus be to promote the growth of a more or less uniform surface film of fully or partly demineralised material which is weaker than the glass substrate. The further growth of this film is immediately reduced, however, by the rate-controlling diffusion process. In a very short exposure of an unstressed fibre the layer is too thin to reduce the load-bearing cross section of the fibres, or to extend significantly the severity of the strength-

determining flaws. The strength of the fibres is therefore reduced only marginally, if at all.

The factor that dominates the static fatigue process is the application of a stress. At a fibre surface the local stress will be non-uniform if the fibres contain flaws. Since the exact nature of the flaws is not known, they can conveniently be defined as those local regions of the fibre surface where stress intensification exists when a load is applied. This stress intensification can be due, for example, to sub-microscopic or larger cracks, or to local regions of residual stress that are additive with the uniform stress applied by the load. When a fibre is simultaneously exposed to a load and an aqueous environment the uniform demineralisation process will commence. It is evident that the flaw sites, being regions where the local stress is highest, will be subject to preferential material fracture as soon as the demineralisation reduces the strength sufficiently. At high loads this would require very little demineralisation. At lower loads very much more demineralisation would be needed. The key point is that the fracture of the weakened material would immediately expose a fresh element of surface to the aqueous medium. This would be demineralised at the maximum reaction rate. The flaw would grow more quickly than the surrounding surface, because the continuously exposed surface would not be subject to the growth inhibition experienced by a thickening surface film. Additionally, the stress intensity for a sharp crack increases as its length increases, so that a crack growing in this way soon gains ascendancy as the main centre of stress intensity, and in due course fibre fracture occurs at this point.

This hypothesis accounts for the main features of stress-assisted crack growth in fibres exposed to various aqueous media and is depicted

in Figure 2-21. High stresses are needed to drive cracks where the environment is deficient in acid, because the demineralisation only occurs to a small extent, and the material weakening is minimal. With very low stresses severe demineralisation is required, and the stress intensification at the growing crack tip may never reach the level needed to fracture the uncorroded glass. The observed fracture surface is therefore very smooth, since the crack can only extend slowly, as the corrosion reduces the local strength of the material by severe demineralisation. In the unstressed condition there is no driving force to activate the local stresses in short time exposures. With strong acid , (1M), and long exposure times the complete demineralisation associated with the core-sheath structure weakens the surface to the extent that weak residual surface stresses can trigger spontaneous cracking of the fibre surface.

FIGURE 2-21. STATIC FATIGUE OF E-GLASS FIBRES ON EXPOSURE TO AQUEOUS ACIDS.

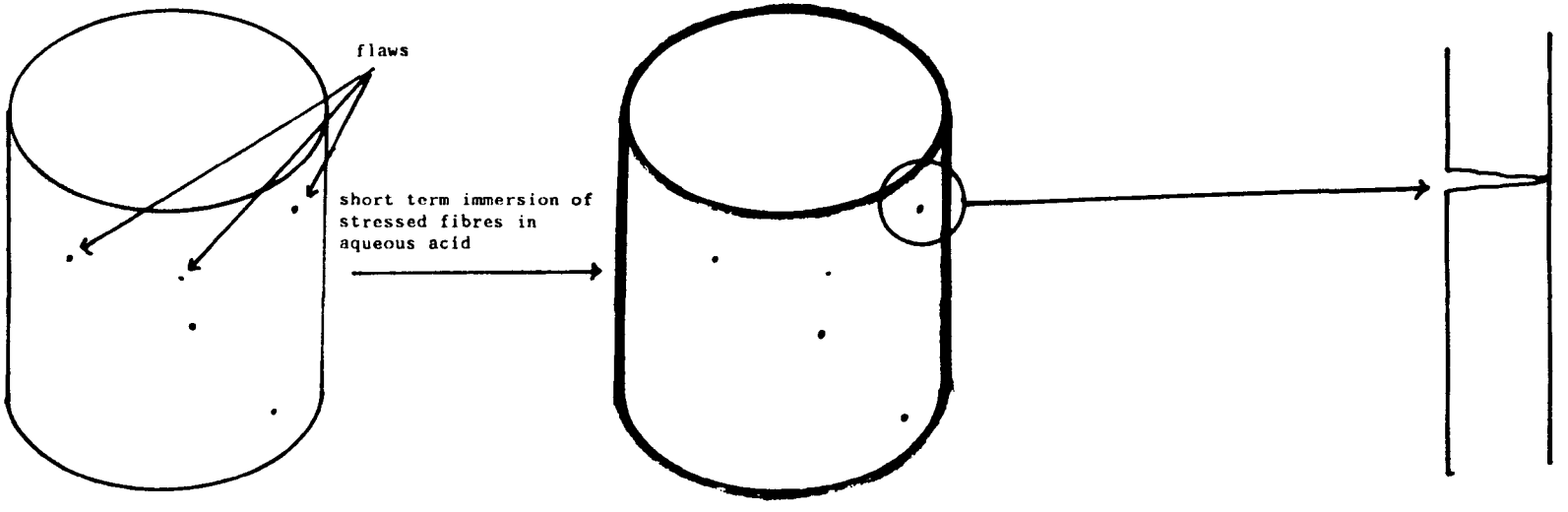

1. Original fibre with distribution of surface flaws. Detailed nature of flaw not known but must be very small. flaws act as stress concentrators.

2. Very thin fully or partially demineralised layer starts to grow on surface. Initial growth rate slows because it is diffusion-controlled.

3. Weakened thin layer cracks at flaw. High stress intensity at crack tip, where fresh surface of unreacted glass is exposed to the acid. Demineralisation commences at high initial growth rate.

CONTINUED OVERLEAF

FIGURE 2-21. (continued from previous page).

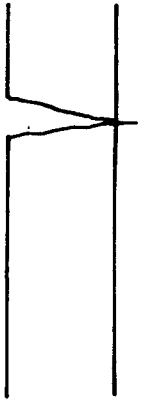

4. High stress at crack tip causes freshly weakened material to crack. Crack extends into the glass more quickly than the rate of growth of the sheath.

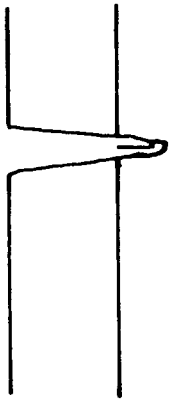

5. Demineralised layer grows rapidly round the crack

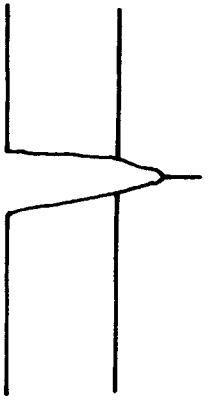

6.....which then cracks again.

7. Crack grows by repeated sequence of steps 5. and 6.

CHAPTER 3. WEAKENING OF GLASS FIBRES---STRUCTURAL ASPECTS.

A central feature of the crack initiation and propagation processes discussed in the previous Chapter is the hypothesis that the attack of a freshly exposed glass surface, by aqueous solutions, occurs at a rate which decreases as the attack proceeds. The attacked surface is weakened to an extent that depends on the acidity of the attacking medium. In this Chapter a mechanism is advanced which accounts for the weakening of the fibres by the leaching action of aqueous acids. In support of this mechanism data is presented showing the results of surface and subsurface decalcification measurements, on fibres exhibiting the core-sheath structure. Further data was also obtained on fibres from the static fatigue tests, which did not have a visible sheath. SEM and TEM methods were used in these experiments. For the TEM work a new technique for preparing suitable specimens from the fibres was developed and this is described and discussed in detail.

3-1 Glass structure.

E-glass is a silica-based glass, with a significantly different composition than soda-lime glass ,as shown in the Table below.

TABLE 3-1 GLASS COMPOSITION

Constituent	%w in E-glass	%w in soda-lime glass
SiO_2	52.4	72
$Al_2O_3.Fe_2O_3$	14.4	0.5
CaO	17.2	11
MgO	4.6	3.5
$Na_2O.K_2O$	0.8	1.3
B_2O_3	10.6	

Current theory depicts the structure of silica-based glasses in terms of the random network model, proposed by Zachariasen[24] in 1932. In this model the oxides are categorised as network formers (SiO_2, Al_2O_3, B_2O_3) and network modifers (Na_2O, K_2O, MgO, CaO). In E-glass the principal network former is silica, and the basis of the structure is an irregular array of SiO_4 tetrahedra. Pure silica will form such an array to create the random network shown in Figure 3-1(a). This contrasts with the regular array shown in Figure 3-1(b) which represents the crystalline quartz structure. A key property of glass is the very rapid increase in viscosity that occurs on cooling, which hinders the development of a crystalline structure. Rapid cooling thus favours the formation of an amorphous glass. Both the structures shown in Figure 3-1 (a) and (b) are rigid, because of the three dimensional nature of the bonding, and as a consequence of this these materials are hard and brittle.

The melting point of silica is very high (2300°C.) To reduce this to a more practical level for glass making and glass forming activities, fluxing agents such as alkali or alkaline earth oxides are added to the glass. These are the network modifiers and they act by breaking some of the bridging bonds in the silica tetrahedra. This gives the structure shown in Figure 3-1(c), using CaO as an example. It can be seen that the overall reaction is:

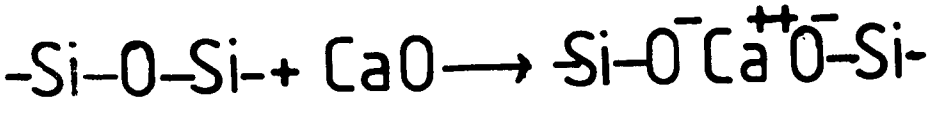

REACTION 3-1.

FIGURE 3-1. WEAKENING OF RANDOM NETWORK BY ACID LEACHING. TWO DIMENSIONAL REPRESENTATION OF STRUCTURES.

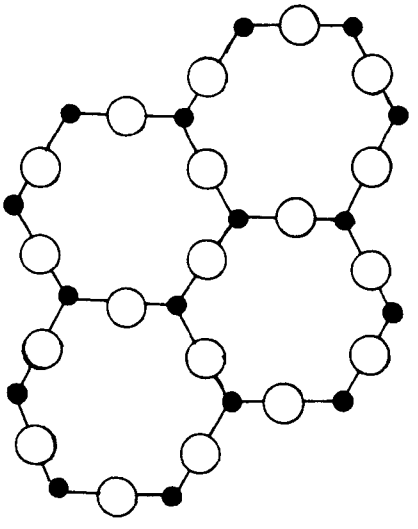

(a) Crystalline silica
• Silicon
○ Bridging oxygen

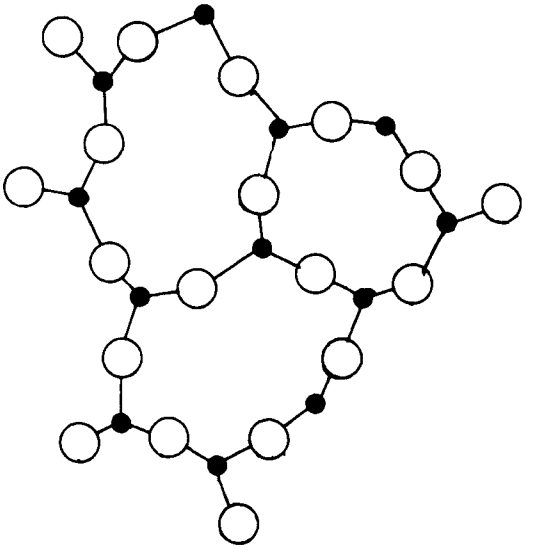

(b) Random network in amorphous silica

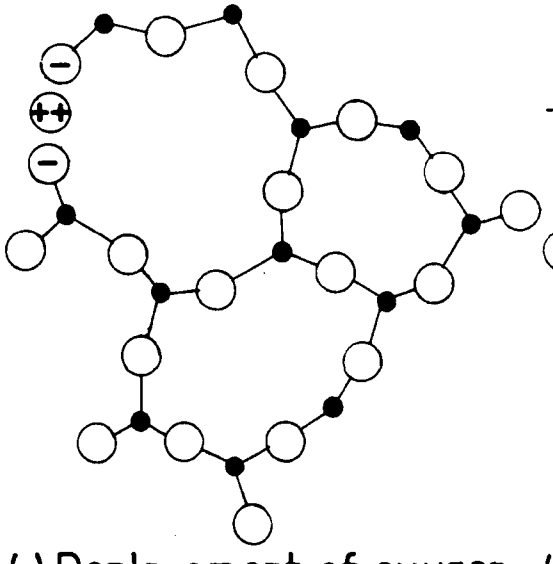

(c) Replacement of oxygen bridge by $O^{-}Ca^{++}O^{-}$ ionically bonded unit.

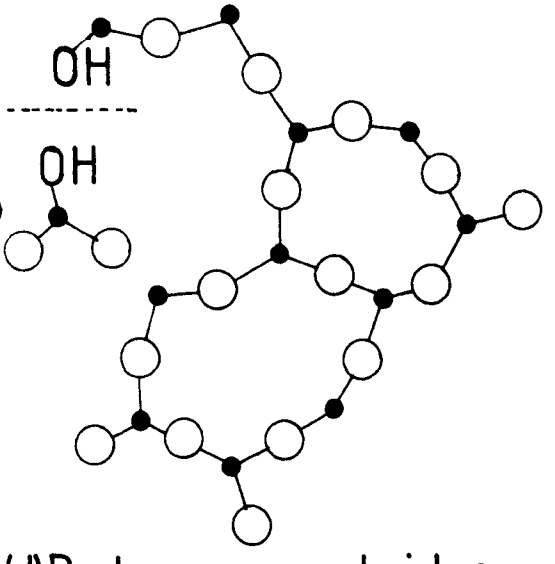

(d) Broken oxygen bridge resulting from calcium leaching.

The result is that some of the covalent oxygen bridges between the Si atoms are replaced by ionic bonds. A similar reaction occurs with Na_2O

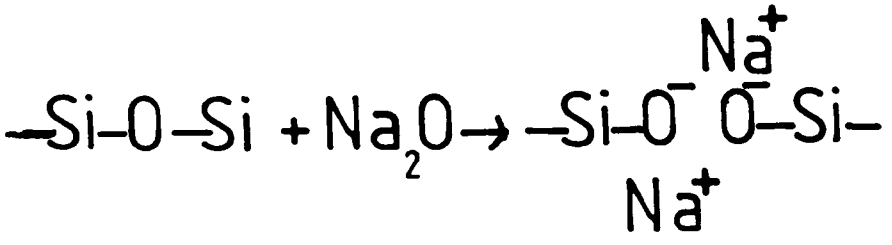

REACTION 3-2.

The calcium and sodium ions fit into interstices in the silica network. These can become mobile in certain circumstances, wheras the anionic oxygen sites in the network are clearly immobile.

The negatively charged oxygen atoms in the structure are termed non-bridging oxygen atoms (NBO's). Although the ionic bonds between the cations and the negatively charged NBO's do make a contribution to the overall strength of the structure, it is not as rigid as the fully bridged network. The glass is weakened in proportion to the number of network oxygen atoms converted into NBO's. A much more severe weakening effect is observed if the sodium or calcium ions are removed from the structure by the leaching action of an aqueous solution :

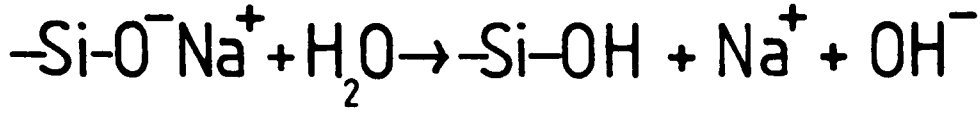

REACTION 3-3.

This leaves the weakened structure shown in Figure 3-1(c) which has many broken bridging bonds compared with the original network shown

in Figure 4-1(b). It is suggested that this is the basic cause of the weakening that occurs as a consequence of the demineralisation of the glass.

3-2 Leaching of sodium from soda-lime glass.

The leaching of sodium from soda-lime glasses by water is of high practical interest in other fields of research. It is important, for example, in relation to the encapsulation of highly radioactive waste, for the dating of ancient glass objects, and for the study of glass electrode performance in electrochemistry. Very sensitive surface analysis techniques are available for determining the sodium leaching profiles of bulk glass specimens. In interpreting the results of leaching measurements made by these methods, two alternative mechanisms have been advanced to account for the observed profiles. These are the water diffusion model of Smets[25,26], and the ion exchange model of Doremus[27].

In the Smets model the attack commences at the glass surface, by a process in which ionic bonds associated with NBO's are eliminated, by reaction with water, as shown in reaction 3-3 above. The sodium and hydroxide ions pass into the bulk solution, leaving behind a weakened siliceous layer. In this layer the NBO's have been converted into uncharged silanol groups. Initially the rate of attack is determined by the rate of reaction of the surface with the water. As the layer builds up, however, further leaching is slowed because of the requirement that molecular water must diffuse through the siliceous layer to reach the fresh glass in the subsurface layers. This diffusion process is held by Smets to be rate-determining, and represents a diffusion situation in which the diffusing substance is immobilised

by reaction with the substrate. The diffusion equation for this situation is:

$$\partial C/\partial t = \partial/\partial x(D\partial C/\partial x) - \partial S/\partial t \qquad (3\text{-}1)$$

where : C = concentration of diffusing substance, S = concentration of immobilised diffusant at distance x in time t, and D is the diffusion coefficient. Implicit in this equation is the variation in diffusion coefficient with diffusion depth.

In the Doremus model the initial reaction at the glass surface is an ion exchange reaction between hydroxonium ions (H_3O^+) and sodium ions bonded to NBO's :

$$-Si-O^-Na^+ + 2H_2O \rightarrow -Si-O^-H_3O^+ + Na^+ + OH^-$$

REACTION 3-4.

Although the demineralising agent in this reaction is the hydroxonium ion, the charged H_3O^+ ion in the reaction product can dehydrate to yield the uncharged silanol moiety shown in reaction 3-3. The water molecules thus liberated will tend to coalesce and assist in the formation of the continuous aqueous phase that is typical of the fully demineralised, water-saturated gel that is the ultimate result of glass leaching. The Doremus model can account for the morphology of water-leached soda-lime glasses in terms of three distinct zones:

(a) An outer zone, which consists of the water-saturated gel, within which ionic mobilities are similar to that in aqueous solutions.

(b) A depletion zone, which is a very thin region at the interface, where depletion occurs in accordance with reaction 3-4.

(c) The unattacked glass below the interface. Water cannot penetrate into the network until demineralisation has occurred, and the attack is therefore confined to the interface region.

A characteristic feature of this type of attack is that the interface surface at the depletion zone becomes fully demineralised as it moves forward. The rate of growth of the outer zone (i.e. the sheath) is governed by the rates of diffusion of the H_3O^+ and Na^+ ions in the partially demineralised depletion zone. Doremus has shown[27,29] how this can be modelled as an interdiffusion process, with the movement of the interface defined by a variable diffusion coefficient D^*. This is determined by the intrinsic diffusion coefficients of the diffusing species (Na^+ and H_3O^+) and their concentrations in the interface surface. The diffusion equation is:

$$\partial C/\partial t = \partial/\partial x(D^* \partial C/\partial x) \qquad (3\text{-}2)$$

If the concentrations of the sodium and hydrogen ions in the interface surface are represented by C_{Na} and C_H such that at all times:

$$C_{Na} + C_H = 1$$

$$\text{then : } D^* = D_H D_{Na}/[C_H D_H + (1-C_H)D_{Na}]$$

$$= D_H/[1 + C_H(D_H/D_{Na} - 1)] \qquad (3\text{-}3)$$

Experimentally it has been found[25,26,28,29] that the surface leaching profiles of bulk glass exposed to water for various times conforms with a common pattern. The glass develops a sodium-depleted layer bounded by a very steep concentration gradient. Figure 3-2 shows a typical example. The shape of the profile is consistent with the three-zone morphology described above. The steepness of the concentration gradient in the depletion zone is very significant in relation to the proposed mechanism of crack propagation during static fatigue.

Figure 3-2. Sodium profile in water-leached soda-limeglass. Data of Smets and Tholen[26]

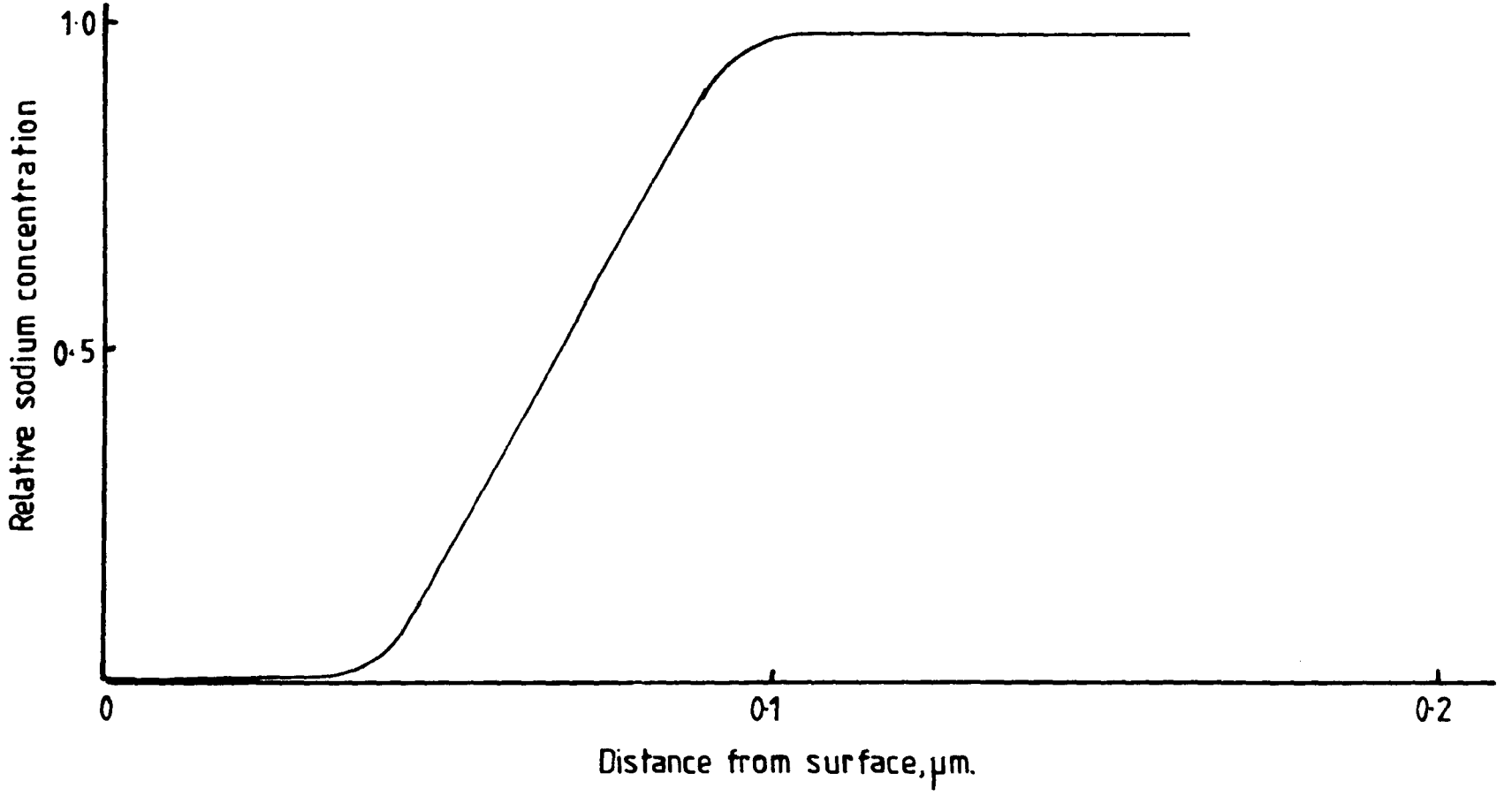

It shows that the demineralisation is essentially a surface phenomenon that proceeeds to completion before the interface moves forward into the subsurface layers of the glass. Equation 3-2 gives a good approximation to the experimental data shown in Figure 3-5. The high degree of demineralisation needed before the interface moves forward into the glass can be seen by examining the variation in D^* with C_H. Doremus gives D_{Na} as $10^{-16} cm^2.sec^{-1}$. and D_H as $10^{-13} cm^2.sec^{-1}$.. Substituting these values in equation 3-3 gives the following results:

C_H	D^* $cm^2.sec^{-1}$.
0	10^{-16}
0.4	1.7×10^{-16}
0.8	5.0×10^{-16}
0.9	10^{-15}
0.99	10^{-14}
0.999	10^{-13}

It can be seen that the order of magnitude of D^* only changes when C_H is greater than 0.9 and that a rapid increase occurs as the demineralisation approaches completion.

Formally, this type of attack is one of the "moving boundary" situations discussed by Crank[23]. The response is characteristic of a system where the diffusion coefficient is initially very low and rises discontinuously to infinity. This occurs when all the anionic sites in the depletion zone have been occupied by the diffusant. The use of the variable diffusion coefficient in the Smets equation, 3-1, would give an equivalent fit to the experimental data in Figure 3-2.

It should be noted that these arguments have been developed in relation to the leaching of soda-lime glass by water. It is now proposed that a similar mechanism applies to the leaching of E-glass by aqueous

acids. The rest of this Chapter is concerned with a critical examination of this proposition.

In interpreting results, such as those in Figure 3-2, Doremus defined the "thickness" of the depleted layer as the distance from the surface where the leached element is at half of its surface concentration. For soda-lime glass this gives a profile which is linear with the square root of the exposure time, up to 400 hours. For greater times the thickness of the leached layer is constant. This is attributed to surface etching in the alkaline medium that results from reaction 3-1, and involves the final dissolution of the siliceous layer. When the rate of advance of the diffusion front (which decreases with distance from the surface) is equal to the rate of surface dissolution, the front no longer advances with respect to the actual surface. The apparent diffusion depth thus remains constant. This accounts for the constant depth of the sodium-depleted layer in leached soda lime glass specimens. It follows that the growth of a thick layer of demineralised silica, (i.e. a sheath), will not take place in solutions which are alkaline, or which become alkaline as the leaching proceeds. This is an interesting difference from the behaviour of E-glass demineralisation in acid solutions. The presence of the acid prevents the dissolution of the silica and enables a completely demineralised fibre, with a diameter of 10-20 microns,to be formed on very prolonged exposure to acid.

3-3 Calcium leaching from E-glass.

The leaching of soda-lime glass by water is a well recognised problem. For most practical applications of glass, e.g. for window manufacture or container applications, this is not a serious con-

straint. The nature of diffusion processes is that the rate of penetration slows markedly away from the contact surface, and the rate of loss of surface and bulk strength is negligible for reasonably thick objects. This is not the case , however, for very fine glass filaments with diameters in the range 5-50 microns. The sensitivity of thin layers of sodium-rich glass to leaching by water makes it unsuitable for use as fine monofilaments. It is for this reason that E-glass, which contains very little alkali, is widely used for the manufacture of fibre reinforcement.

In E-glass the sodium is virtually all replaced by calcium, and this glass has a much higher resistance to leaching by water. One reason for this may be the possibility of balancing the charge on the divalent calcium cation by a pair of anionic non-bridging O^- sites in the glass network, thereby producing a stronger system of ionic bonds than is possible with the monovalent sodium ions. This is illustrated in two dimensions below :

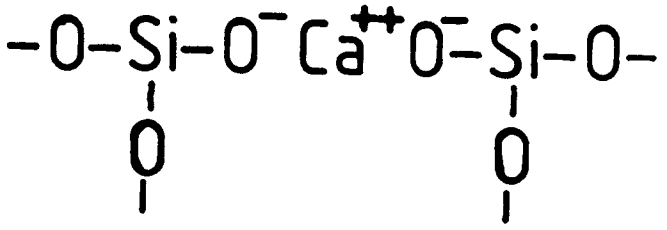

Water is not very aggressive to the calcium cation in this structure and the removal of calcium, whilst not zero, is minimal. Mineral acids such as hydrochloric acid, however, are readily able to abstract calcium from the structure by the reaction,again shown in two dimensions in reaction 3-5 below.

Simple chemical considerations indicate that the rate of calcium removal would be expected to correlate with acid concentration, particularly with dilute solutions in the range 0-1M. Evidence that this

is so is available from the work of El-Shamy and Morsi[30] on the extraction of sodium and calcium from various powdered glasses by mineral acids of different concentrations.

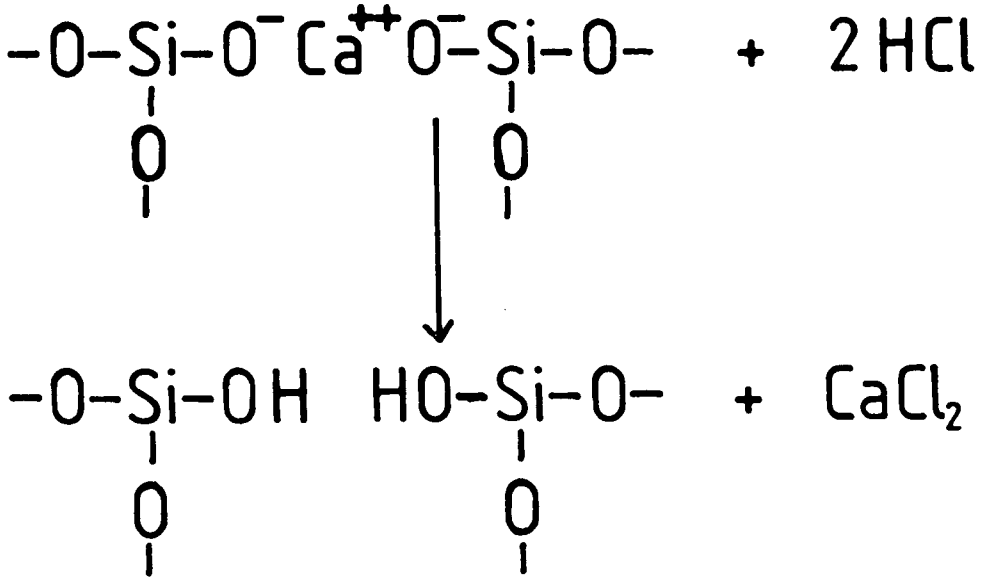

REACTION 3-5.

3-4 Aluminium leaching from E-glass.

The above argument is a simplified picture of the true situation with E-glass, because the presence of Al_2O_3 in the formulation provides additional protection against the loss of cations by aqueous leaching. The Al_2O_3 can react with CaO by the reaction :

$$Al_2O_3 + CaO = Ca(AlO_2)_2$$

In the glass this leads to the formation of $[AlO_4]^-$ tetrahedra, which which can substitute for some of the SiO_4 tetrahedra in the network. Because of the net negative charge on the AlO_4 unit a balanced number of cations must be associated with each unit to preserve electrical neutrality. In two dimensions this gives the structure shown on the next page:

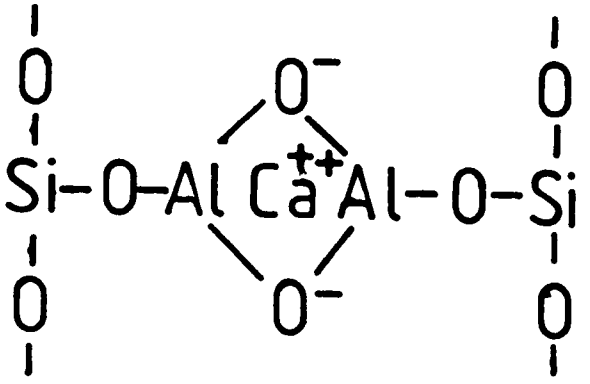

This structure provides a means of accommodating fluxing agents in the glass without removing the bridging oxygens from the network. The Ca^{2+} ions are much less mobile than when linked to NBO's and are very resistant to leaching by water. If however this structure is attacked by acid, dissolution of the entire unit is likely, leading to very severe disruption and weakening of the network. Chemically the dissolution reaction is :

$$Ca(ALO_2)_2 + 8HCl = CaCl_2 + 2AlCl_3 + 4H_2O$$

Again, it is easy to see how pure water would be expected to have only a small leaching effect on this unit, but that acid action would demineralise the structure to an extent dependent on concentration.

It is also clear why the demineralised network is weaker than the bridged network, and that the strength of the material would be expected to decrease monotonically with the extent of demineralisation.

3-5 E-glass fibre weakening mechanisms.

It is important to recognise the fact that the above discussion relates primarily to surface effects associated wuth the exposure of flat glass specimens to aqueous solutions. The same general features would be expected to apply to E-glass fibres exposed to similar solutions. The leaching models are based on the concept that the attack

at a freshly exposed glass surface proceeds by a demineralisation process, resulting in the loss of calcium and aluminium from the glass. The initial rate of surface attack leads to the formation of the demineralised layer, and subsequent subsurface attack occurs at a much slower, diffusion-controlled rate.

This is all in accordance with the ideas advanced in Chapter 2 for the very large increase in crack propagation rate for fibres exposed simultaneously to an aggressive environment and a tensile load. However, in seeking confirmation of the existence of the theoretical demineralisation profiles at the fibre surface, there are problems. All the publishcd work discussed above on the measurement of leaching profiles had been carried out on relatively large glass specimens with very flat surfaces. These had been etched with aqueous HF, prior to leaching, to reveal a pristine glass surface. The very sensitive surface analysis techniques, such as secondary ion mass spectrometry and resonant nuclear reaction spectrometry, used to examine the leached surface, could not easily be adapted for use with glass fibre specimens. In the present work the mechanical testing of the fibre strands was supplemented by SEM and TEM examination of fractured fibres. It was from these data that evidence for compositional changes in the surface and subsurface layers was sought. The methods used to study the surface depletion of E-glass fibres are described below.

3-6 Measurement of leaching profiles with E-glass fibres.

The characteristic feature of a demineralisation process in which the depletion occurs at the glass surface is that the depleted layer is bounded by a very steep concentration gradient at the interface, as has been found with water-leached soda-lime glass. E-glass speci-

mens with a core-sheath structure provide qualitative visual evidence of a sharp concentration gradient at the sheath boundary. It was considered, however, that a more quantative demonstration of the existence of this steep gradient was needed. This would further justify the suggestion that surface demineralisation was an essential prerequisite for stress-corrosion of the fibres. Evidence of surface attack was therefore sought by examination of acid-leached E-glass fibres.

A preliminary survey was made with the SEM. Cross-sections of fibres that had been mounted, ground and polished were carbon-coated to minimise charging problems. Specimens were also prepared in which fibres in the as-found condition were mounted longitudinally on an SEM stub, for examination after carbon coating. Energy dispersive X-ray analysis (EDAX or EDX) was used to study composition differences between the sheath and the core of acid-leached fibres.

As applied here this technique is only semi-quantitative and has very limited resolution, since the effective spot size is about 1 micron in diameter. The mean diameter of the Equerove 2347 fibres was about 17 microns, so that accurate profiling in the region of the core-sheath boundary was not possible. Despite these limitiations, the technique shows that the sheath is severely demineralised compared with the core. In Figure 3-3 EDAX spectra from the centres of the core and sheath are contrasted and show this effect. Very similar spectra were observed by Jones et. al.[9], by Lhymn and Schultz[72] and by Bledski[12].

An impression of the extent and depth of the demineralised layer is obtained by examining EDAX spectra taken from longitudinally mounted fibres. Figure 3-4 shows spectra from fibres that had been

FIGURE 3-3. EDAX ANALYSIS IN SEM OF CORE AND SHEATH FROM FIBRES SHOWN IN FIGURE 2-5.

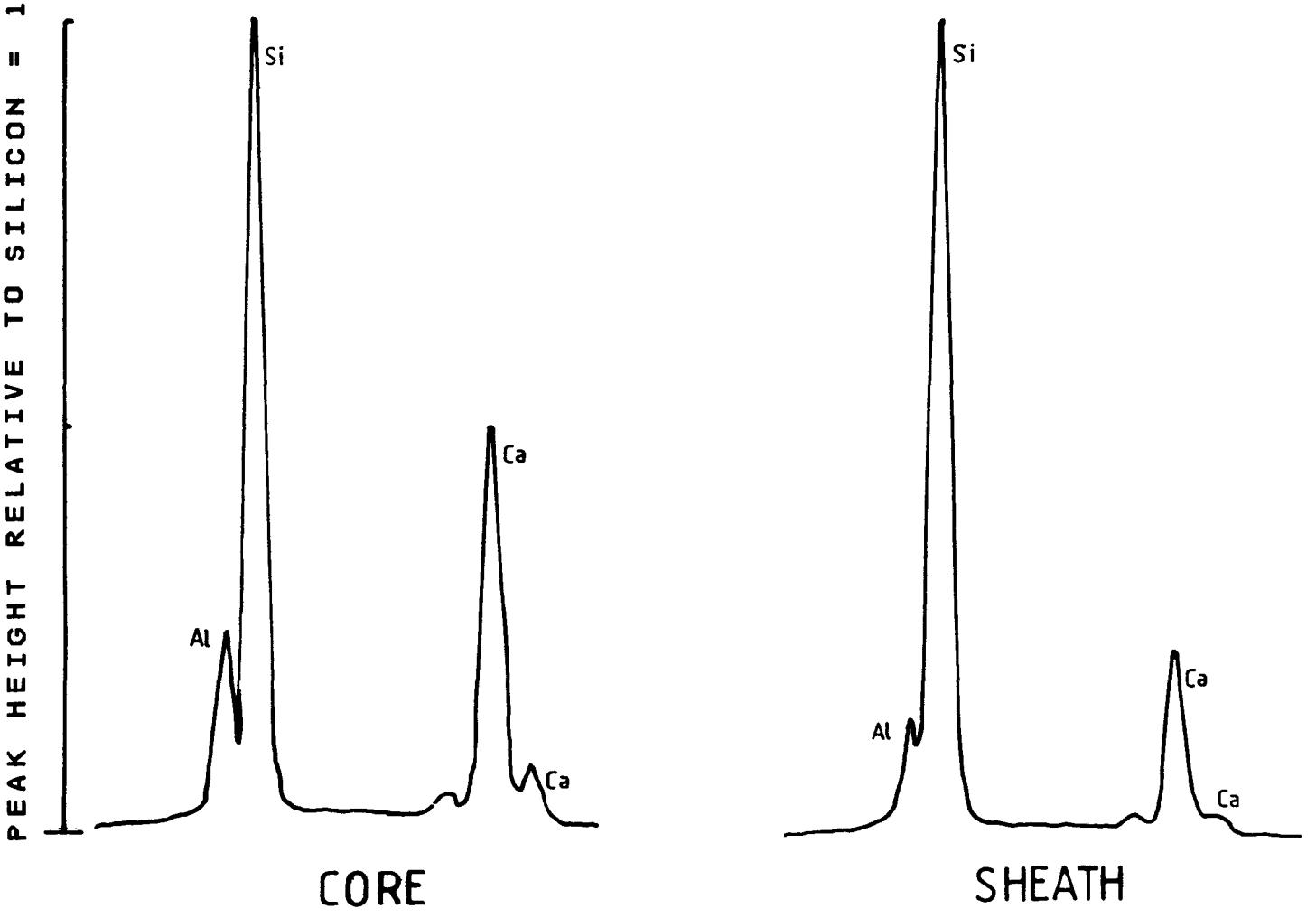

FIGURE 3-4. EDAX ANALYSIS IN SEM OF HORIZONTALLY MOUNTED FIBRES. EFFECT OF ACID CONCENTRATION FOR 7 DAY EXPOSURE.

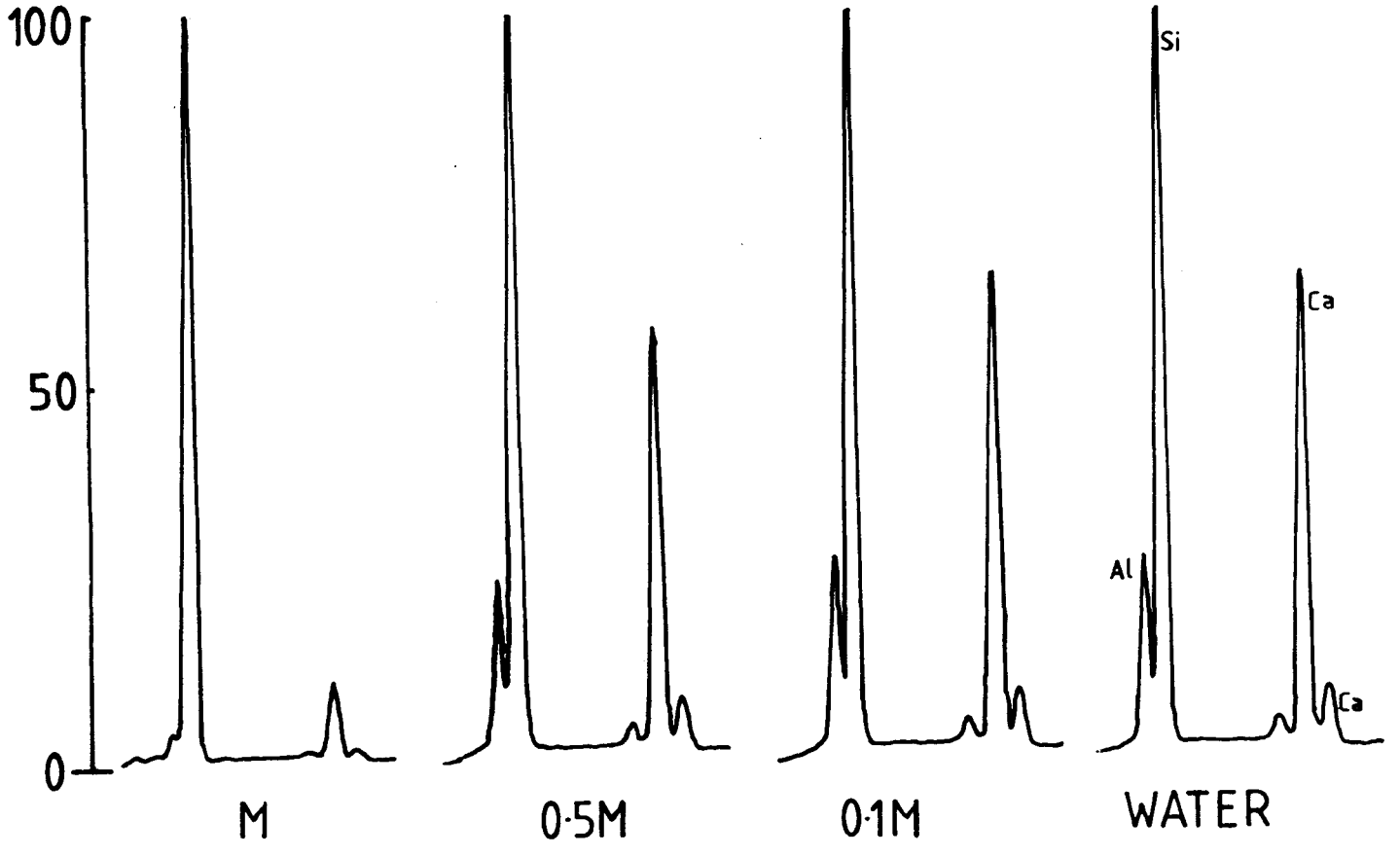

exposed unstressed to acids of various concentrations for 7 days at 25°C. The extent of demineralisation can be related to the calcium peak heights in the spectra. It can be seen that the gross demineralisation associated with the developement of a visible core-sheath structure was only observed at concentrations greater than 0.1M. Further experiments showed, in fact, that the critical concentration for the development of this structure lies between 0.4M and 0.6M at 25°C.

The SEM techniques just described cannot achieve sufficiently high resolution to show the presence of a steep concentration gradient. This is especially true for fibres which have only been exposed to acid for relatively short times. With such fibres the depletion layer is very thin and there are no visual indications of a core-sheath structure. Attempts were therefore made to see if the inherently higher resolution available with TEM methods could be used to examine glass fibres. A method for preparing suitable specimens had to be worked out before this could be done and this is described in detail below.

3-7 TEM examination of glass fibres.

The improvement in analytical resolution in the TEM, compared with the SEM, is primarily due to the use of a more intense, focussed beam with a nominal spot size of 100 Angstrons. The problem is that samples for examination by imaging in the TEM must be transparent to the electron beam, although this is not strictly necessary for energy dispersive X-ray analysis. For practical reasons the technique is restricted to samples that can be prepared and mounted on 3mm. diameter grids. For imaging the effective thickness of the specimen must be

less than 0.1 microns. For EDX analysis the limiting thickness is about 1 micron.

Specimen thinning is almost always a difficult and time-consuming feature of TEM work. This is despite the availability of a variety of sophosticated etching and erosion methods, such as ion-beam thinning and atom milling. To make high resolution analyses of glass fibre cross sections it was necessary to find a way of obtaining radial slices from the fibres with a thickness not exceeding about 1 micron. The difficulty of doing this with a very brittle material can be judged from a scale diagram of such a slice, as shown below for a 17 micron diameter fibre.

In seeking a way of obtaining suitable specimens, various methods were tried. Simple grinding of the fibres in a pestle and mortar generated a powder. This powder was examined with an optical microscope. The fibre fragments were found to be either large and rod-shaped, or very small and irregular. There was no sign of any thin, flat, radial chips of the type required.

In another trial a standard thinning method was evaluated. A bundle of fibres was mounted along the axis of a 3mm.diameter resin rod, using the resin mounting method described in Figure 2-12. Thin slices of this rod were cut off, using a slitting wheel. Attempts to thin the centres of these slices, containing the fibre bundles, were made with a commercial atom beam thinning unit. This technique is known to be very effective for preparing thin metal foils for TEM examination. It was found that the polymer was eroded by the atom beam more effectively than the glass. It was possible to mill a hole through a slice,

but the glass fragments in the slice were not thinned appreciably. The result was that the glass fragments either fell out of the slice, or remained precariously attached to the thinned polymer as large rod-shaped fragments.

Finally, a method was found which could be used to obtain suitable glass fragments for TEM examination. This was an adaption of a replication technique. From the SEM work specimens were available that had been mounted and polished to reveal the cross sections of the fibres. It was found that by contacting the polished surface with a thin film of replicating resin, in the presence of a solvent, a bond was established between the film and the resin mount. Peeling the replication film away from the mount surface pulled loose material off the surface, including thin fragments of glass from the fibres. In normal TEM practice the replica is required to reveal the topography of the surface. The first two or three sheets of replication film are used to clean the surface and are rejected. The fourth and subsequent "clean" replicas are used to examine the surface topography. In the present application it is the cleaning operation that provides the fibre fragments for analysis. A fuller description of the replication technique is given below.

3-8 Replication technique for obtaining thin cross-section fibre fragments.

The mounted fibre bundle was ground and roughly polished down to 6 micron diamond paste. This yielded fibre cross sections showing many surface cracks, as shown in Figure 3-5. The polished specimen was dried and wetted with one drop of methyl acetate. A 5mm. square of acetyl cellulose replication film was placed over the bundle ends in

FIGURE 3-5. ROUGH POLISHING OF FIBRE CROSS-SECTIONS, SHOWING CRACKS.

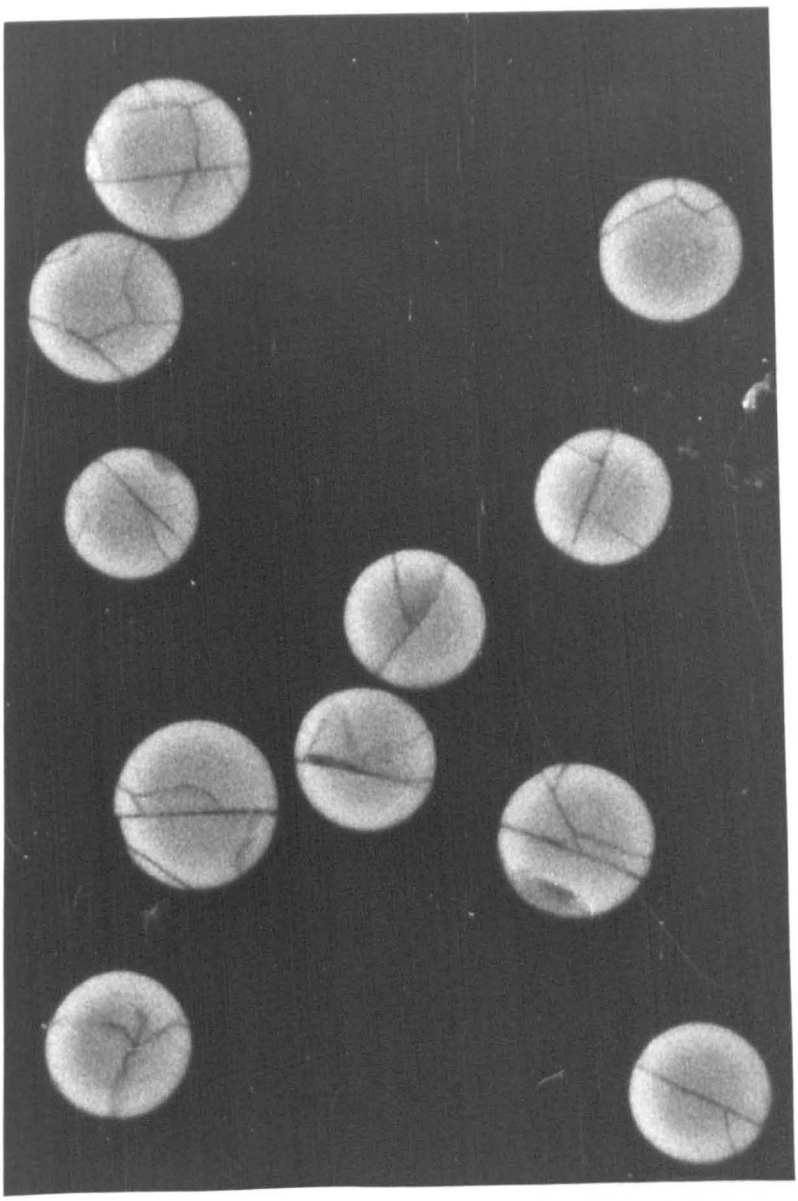

the mount, and was pulled down by surface tension. After a few minutes most of the solvent had evaporated and the film was firmly attached to the to the mount. It was easily possible to free a corner with tweezers and to pull the film off the mount. The film was flattened by clamping between two microscope slides at 80°C. for 30 minutes.

The flat film was then tacked down, replica side up, to a microscope slide by means of tiny pieces of transparent adhesive tape. The replica was carbon-coated in a commercial, high-vacuum coating unit. This provided a reasonably thick, tough, fine-grained carbon film. It was particularly important to form a tough film in this process. Low vacuum carbon-coating units are available, but are not suitable for this application, because the carbon film they produce is not strong enough for subsequent handling.

The coated replication film was removed from the slide and placed, replica side down, on another slide which had been heated and coated with a thin layer of molten paraffin wax. The melting point of the wax was 45°C. After the wax had solidified the entire slide was immersed in methyl acetate in a beaker held at room temperature. The acetyl cellulose dissolved, leaving the carbon replica affixed to the wax. By bringing the methyl acetate slowly to 50°C. in a water bath, the carbon replica was released and floated up to the liquid surface. With care it could be picked up intact on a 3mm. diameter copper grid.

At this stage the replica was often folded,or rolled up. It could be straightened by refloating it succesively in baths of acetone and water. The difference in surface tension between these media caused spontaneous, quite violent unrolling of the film on the water surface.

Finally the film was picked up on a clean 3mm. grid for TEM examination.

There are a large number of operations involved in this specimen preparation method. The very delicate nature of the carbon replicas required many attempts before suitable specimens could be obtained. A feature of this method is that it does not yield complete fibre cross sections. Figure 3-6 is a photomicrograph of a typical example. The original full cross section of the fibres can clearly be seen in the replica. The fragments of core and sheath adhering to the film have remained in position during the replication operation. These were the type of fragment examined in the subsequent TEM work. They have a thickness in the range 0.1-1.0 microns.

3-9 TEM analysis of fibre fragments: determination of optimum analytical conditions.

Figure 3-6 shows fragments of core and sheath from static fatigue specimen #26. This specimen had been exposed to molar HCl under a load of 30 Kg. and had failed by fracture at 16 hrs. The core-sheath structure can clearly be seen on the micrograph.

The micrograph also shows that several fragments of both core and sheath were available for analysis. These fibre fragments were not sufficiently thin to be fully transparent to the electron beam. However, some transparent areas could be found, near to the specimen edges. These areas did not show any structural features and did not yield diffraction patterns, other than the single broad ring commonly seen with amorphous material. Neither the core nor the sheath showed any evidence of crystallinity, and appeared to be amorphous and

FIGURE 3-6. FRAGMENTS OF CORE AND SHEATH FOR TEM EXAMINATION.

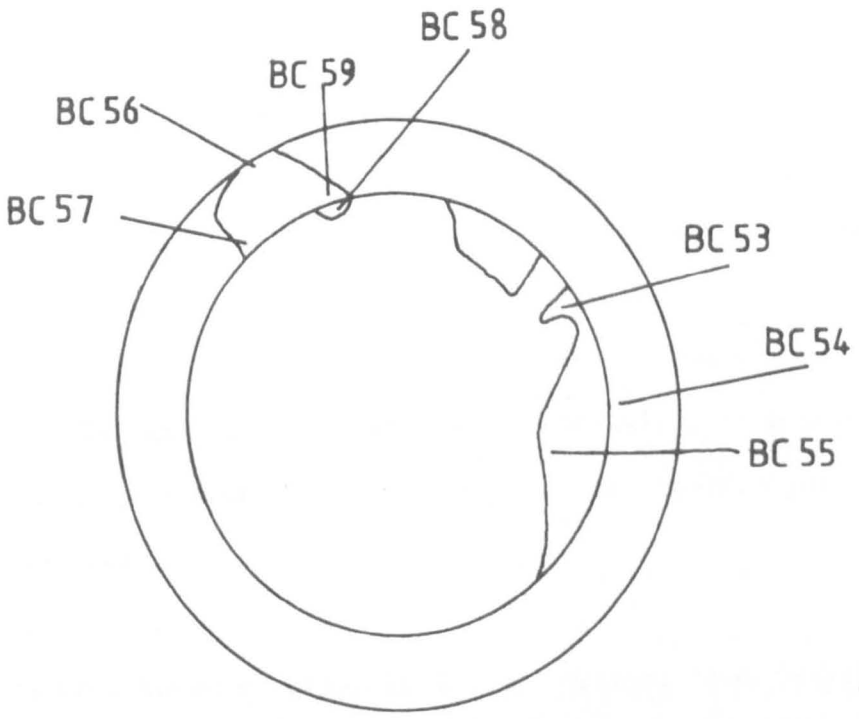

QUALITATIVE EDX ANALYSIS

SHEATH : SILICON ONLY (BC 56, 57, 59)

CORE : SILICON, ALUMINIUM, CALCIUM (BC 53, 54, 55, 58)

isotropic. This is fully in accordance with the random network structures discussed earlier in this chapter.

Initially, EDX analyses were made with the microscope in TEM mode. This provided a qualitative survey of the distribution of elements in the structure. Figure 3-6 shows the areas examined and gives the qualitative results obtained.

These results suggested that the sheath consisted of almost fully demineralised silica, whilst the core consisted of unreacted E-glass.

In order to look for more quantitative evidence of a sharp concentration boundary at the core-sheath interface, it was necessary to change the operating mode from TEM to STEM. Using a fine electron beam (spot size 200 Angstroms) and a magnification of 62500, a series of spot analyses were made. The two fragments examined were representative of the core and the sheath respectively. The positions at which these analyses were made showed up as erosion spots on the specimens, as shown in Figure 3-7. The results from the analyses are illustrated by the calcium and silicon profiles shown in Figure 3-8. It can be seen that the data show a steep calcium concentration gradient at the core-sheath interface. A similar profile is obtained from the aluminium data.

There are, however, problems in interpreting these results. The most serious of these was that the level of calcium in the E-glass core was not as high as would be expected. It was suspected that the material might undergo composition changes during analysis as a consequence of the exposure to the intense beam used for the analysis. This suspicion was later justified. It was therefore considered necessary

FIGURE 3-7. STEM ANALYSIS OF #26 FIBRE REPLICA.

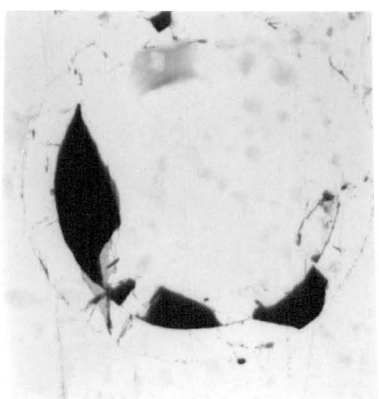

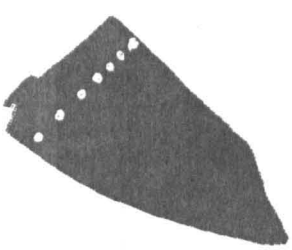

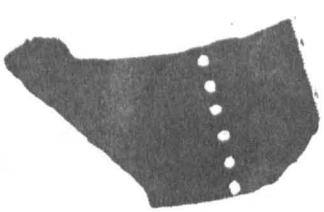

FIGURE 3-8. STEM EDX ANALYSIS OF CORE AND SHEATH FRAGMENTS SHOWN IN FIGURE 3-7

CALCIUM AND SILICON PROFILES

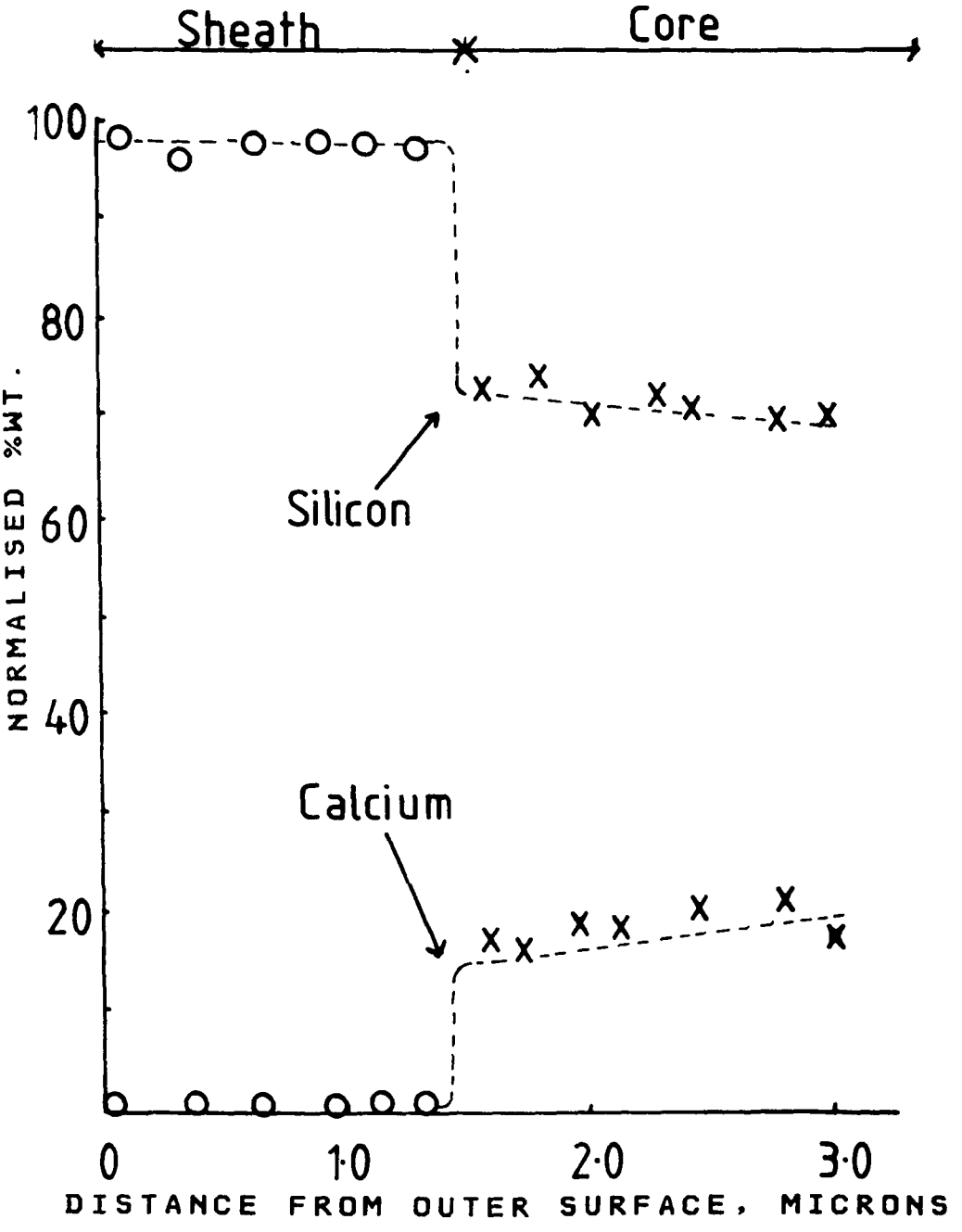

to make an evaluation of the conditions under which the microscope could be expected to give the best analytical results.

A specimen of unreacted E-glass, suitable for analysis in the TEM, was needed. A strand of roving was heated with a gas burner to remove the size, and on further heating yielded a molten bead of glass. This was picked up with a piece of silica tubing, so that it formed a seal at one end of the tube. With the E-glass in a molten state it was blown into a bulb, which, with continued blowing, thinned and eventually burst. This yielded a large number of very thin flakes of the glass which were collected. The flakes were of relatively uniform thickness, in the range 0.25-0.75 microns. It was straightforward to mount one of these flakes on a 3mm. grid for TEM examination. This E-glass specimen was used to explore the influence of beam intensity on glass erosion, and to see what influence this had on the EDX analysis of the material.

With the microscope in the STEM mode, two different ways in which the specimen can be examined by EDX analysis are: (a) average analysis of a relatively large area that is continually scanned by the beam, and (b) spot analysis from the small area exposed to the stationary beam. The chance of beam damage with method (a) is much less than with (b), because the beam is only localised at any point on the surface for a very short time whilst scanning. It follows that data from the two methods must be in agreement for surface erosion to be under control. Composition changes as a consequence of beam damage can also be revealed by making replicate analyses at the same point on the specimen surface.

After much experimentation it was found possible to identify conditions under beam damage was minimised. Analysis by methods (a) and (b) were in agreement, as were replicate measurements by method (b). It was necessary to defocus the beam slightly to achieve this situation, although the spot analyses could be made with a nominal spot size of 100 Angstroms. The magnitude of the beam damage effect can be seen in the data listed in Tables 3-2 and 3-3 below. The improvements achieved by slightly defocussing the beam are shown in these Tables.

The thickness of the E-glass flake was estimated to be 0.3 microns. It had a relatively flat surface and gave a reasonably uniform take-off angle for the EDX detector. A series of spot analyses across the surface were made, using the optimum beam conditions for the analyses. These were compared with an "average" analysis of the same area, to yield the results shown in Table 3-3. The analyses were obtained at a magnification of 12500,with a spot separation distance of 1.2 microns.

Comparison of the results of the "average" and spot analyses in the Tables shows that very consistent results can be obtained under these conditions. It should be noted that the EDX software normalises the X-ray emission data, to add up to 100%. Elements such as boron do not appear in the analysis. The system was not accurately calibrated to yield absolute values for the composition of the glass (see Table 3-1). This was not considered essential for the present purpose. The relative values obtained from the analyses were sufficient to examine the variations in composition in the vicinity of the core-sheath interface.

TABLE 3-2 SPOT ANALYSIS OF E-GLASS FLAKE SPECIMENS WITH 100 ANGSTROM DEFOCUSSED BEAM. DISTANCE BETWEEN SPOTS = 1.2 ANGSTROMS.

Beam conditions	Composition (arbitrary units)		
	CaO	SiO2	Al2O3
Method(a);"average" analysis	31.2	54.0	12.7
Method (b);200 second sequential spot analyses traversing the specimen.	31.1	53.49	12.73
	31.92	53.84	12.50
	31.18	54.53	12.31
	30.75	53.86	13.15
	31.84	54.28	12.36
Mean of 200-second analyses	31.3 .51	53.9 .40	12.61 .34

TABLE 3-3.EDX ANALYSIS OF E-GLASS FLAKE SAMPLE UNDER DIFFERENT BEAM CONDITIONS.

Beam conditions	Composition (arbitrary units)		
	CaO	SiO2	Al2O3
Method (a);"average" analysis	31.1	54.9	12.1
Method (b);500 Angstrom spot size; 100-second analysis	21.7	66.5	10.6
Sequential 10 second analyses of same area	27.4	58.67	12.45
	24.3	61.28	11.93
	22.5	64.1	11.5
	17.2	73.5	8.8
	18.9	69.6	10.5
	18.8	70.4	10.1
Method (b);500 Angstrom spot size; sequential analyses from another area			
5 seconds	30.7	54.0	12.6
5 seconds	27.9	58.8	12.3
10 seconds	25.2	63.2	11.2
Method (b);100 Angstrom size;1 increment defocus; sequential 50 second analyses from same point point on surface	32.0	53.2	12.8
	32.1	54.1	11.7
	29.8	53.4	13.6
	31.5	53.7	13.3
Mean value for 100 Angstrom spot results.	31.4 1	53.6 4	12.9 .8

3-10 Resolution of STEM system with defocussed 100 Angstrom beam.

The beam defocus required to control specimen erosion during spot analysis inevitably leads to a downgrading of the resolution of the microscope. A convenient way of checking this is to sublime some molybdenum trioxide crystals onto a grid. The sublimed oxide forms very thin plate-like crystals with very well-defined, sharp edges. These can be used to check the resolution of the defocussed beam.

The high X-ray yield from molybdenum provided good counting statistics and enabled linescans to be made both at optimum focus and at the one increment defocus condition. The crystal used for this analysis is shown in Figure 3-9. The two linescans obtained from this crystal are shown in Figure 3-10.

The rise time of the Mo K shell X-rays is a measure of the resolution of the system. This is usually defined in terms of the spread of the profile between 10% and 90% of the profile height. Figure 3-10 shows that at optimum focus the 100 Angstrom spot gives a resolution of .04 microns. At 1 increment defocus this is downrated to 0.1 micron. It should be noted that this is substantially better than that available in the SEM.

3-11 Specimen surface geometry: effect of take-off angle on EDX results.

Consistent values for the calcium content of unreacted E-glass were found to be critically dependent on surface geometry. This had a very big effect on the EDX take-off angle. The E-glass flake sample was used to demonstrate this by comparing "average" area analyses with the

FIGURE 3-9. MOLYBDENUM TRIOXIDE CRYSTAL USED FOR TEM RESOLUTION TESTS.

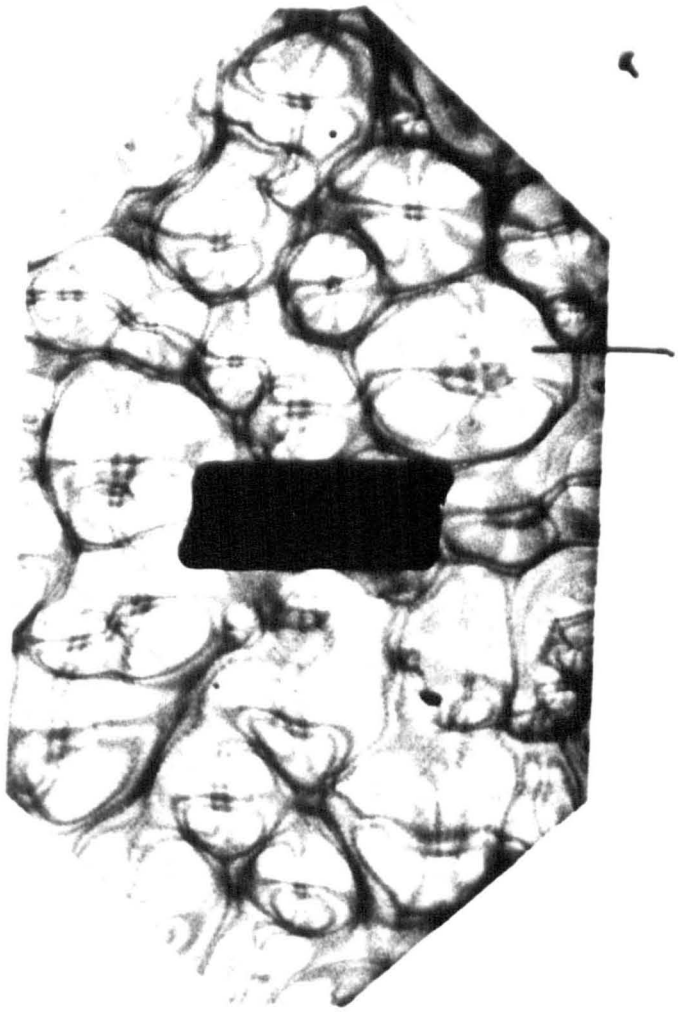

FIGURE 3-10. MOLYBDENUM K-X-RAY LINESCANS WITH FOCUSSED AND DEFOCUSSED BEAM.

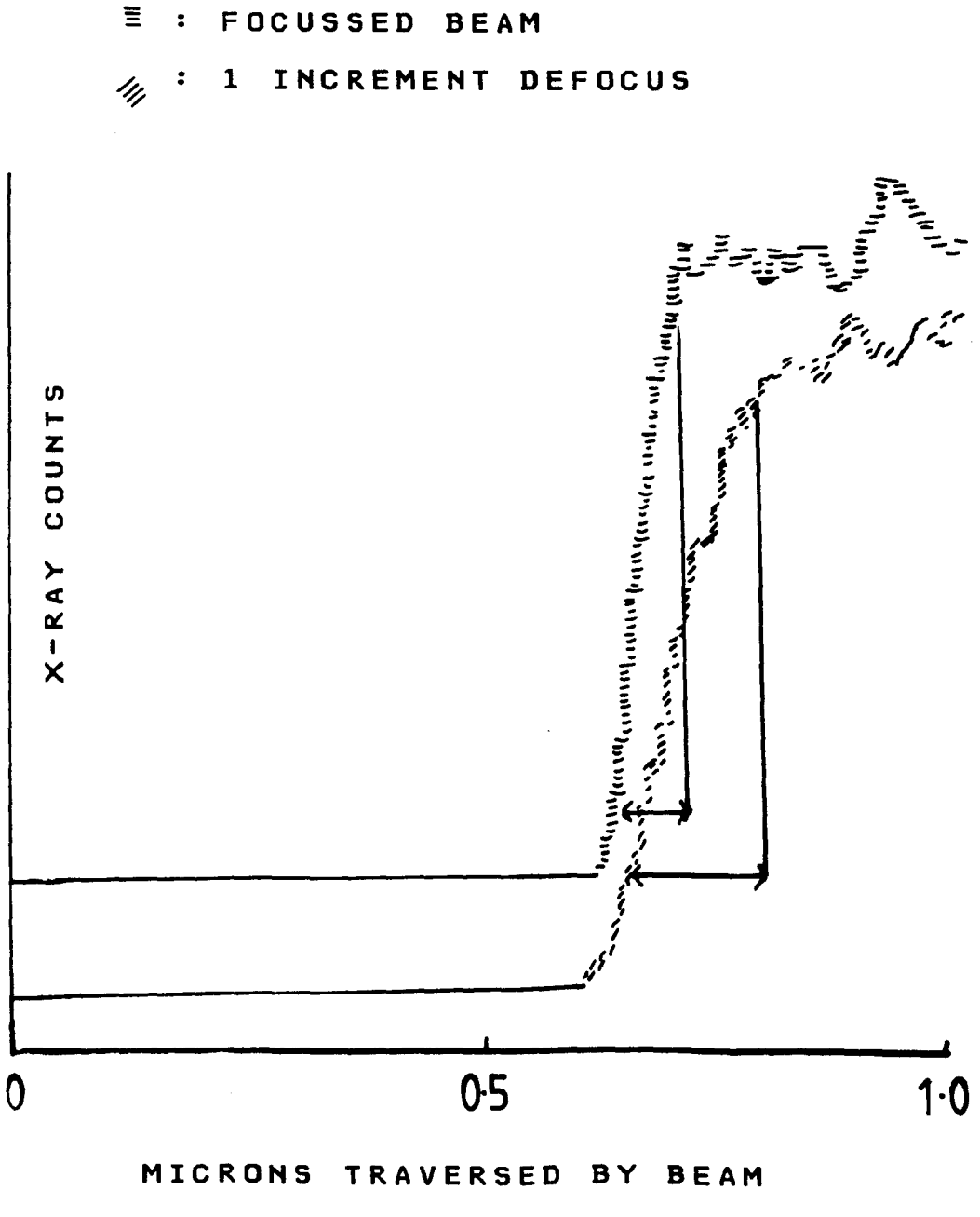

microscope in the STEM mode, using different specimen tilt angles. The results are given in Table 3-4 and it is evident that the effect is very large, especially at negative tilt angles.

TABLE 3-4

Effect of specimen tilt on EDX results on e-glass flake specimen.

Beam conditions	Composition (arbitrary units)		
	CaO	SiO2	Al2O3
Average area analysis	38.2	48.4	10.9
20° tilt	32.5	53.3	12.4
40° tilt	30.3	54.7	12.8
58° tilt	29.3	55.2	13.2
-10° tilt	46.0	46.5	9.3
-15° tilt	60.4	28.38	6.0

In seeking data relating to concentration gradients in the vicinity of the core-sheath interface, it was therefore necessary to screen candidate fragments to ensure that they were reasonably flat. Even with this precaution, it was not found possible to obtain analyses in which the composition of the unreacted glass in the fibre core was the same for all the specimens examined. Despite these difficulties, however, it was considered that the results could be used to judge the extent of demineralisation at the two critical regions, i.e. the fibre surface and the core-sheath interface.

3-12 Results of TEM examination of acid-leached E-glass fibres.

Another replica from specimen #26 (see Table 2-1) was prepared. In this replica a fragment was identified in which both the sheath and core elements were intact. This is shown in Figure 3-11. A series of spot analyses were made, using the optimum conditions to avoid beam damage. The areas covered by the analysis are also shown in Figure

FIGURE 3-11. STEM ANALYSIS OF REPLICA FROM #26 CONTAINING INTACT CORE-SHEATH BOUNDARY.

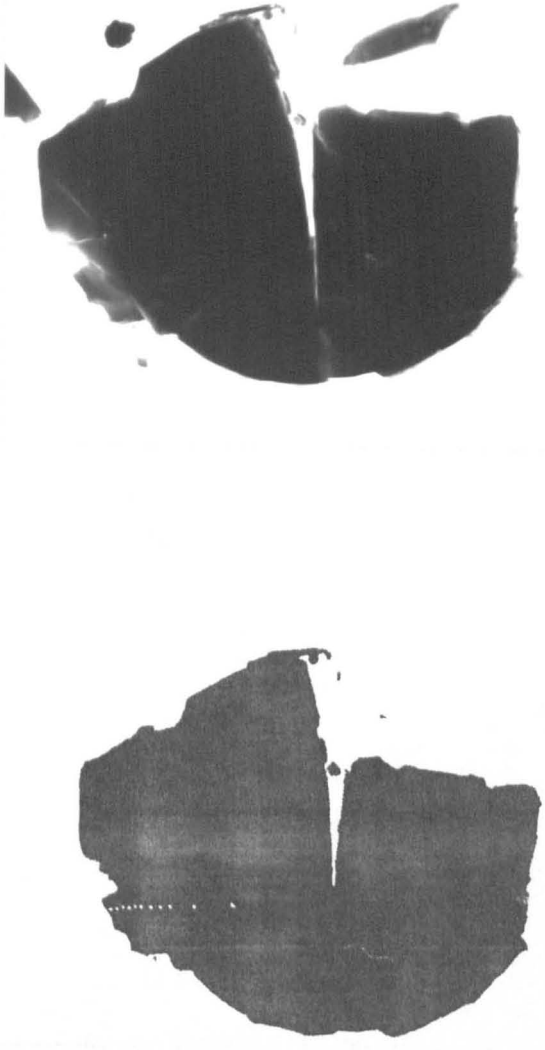

FIGURE 3-12. CALCIUM PROFILE ACROSS CORE-SHEATH BOUNDARY.
STEM ANALYSIS OF FIBRE FRAGMENT FROM #26.

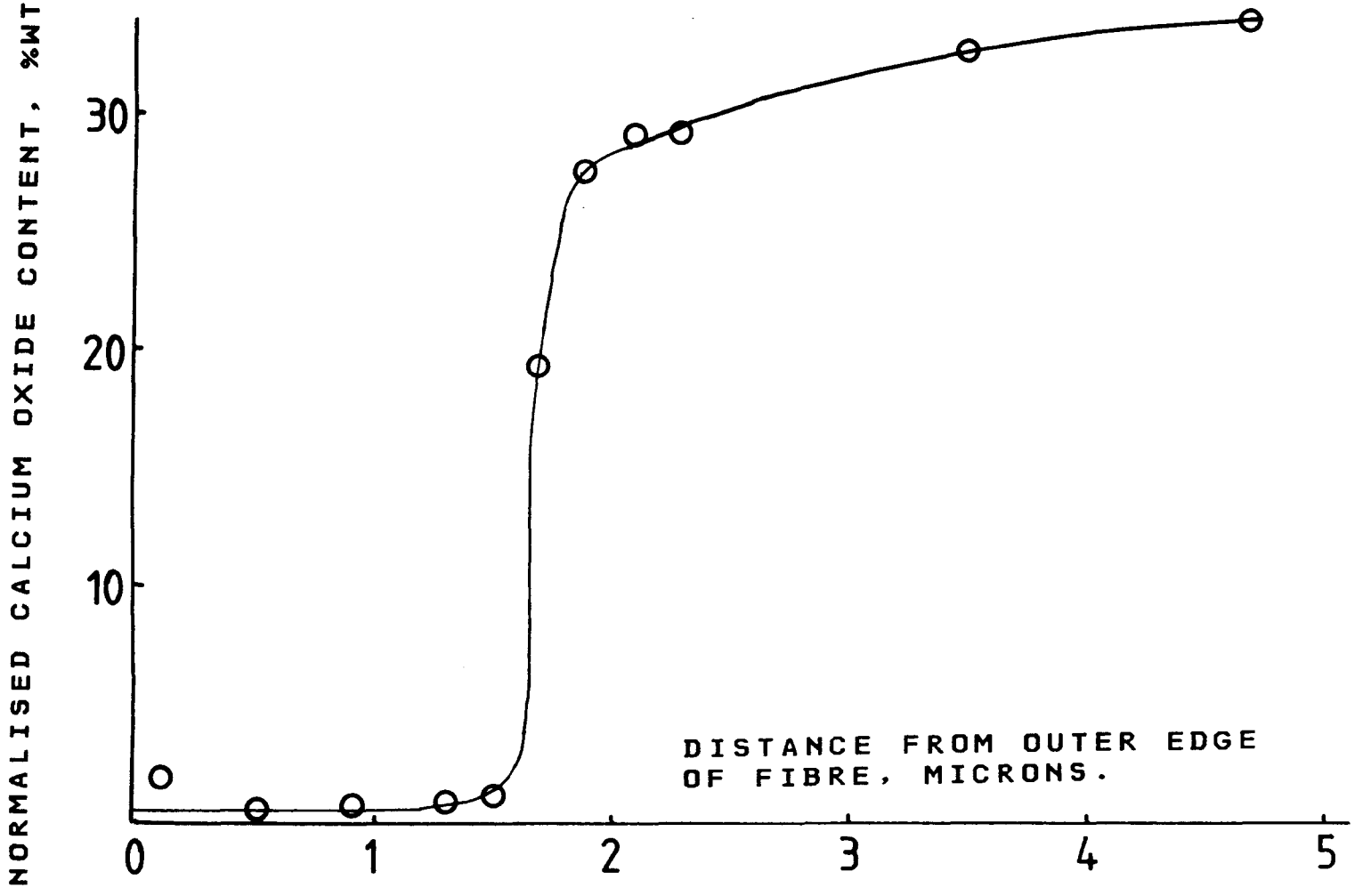

3-11. The results are plotted in Figure 3-12. They show that extreme depletion of calcium has occurred in the sheath, which is bounded by the expected very steep concentration gradient. The steep gradient coincides with the visual boundary for the core-sheath interface. The abnormally high calcium concentrations deeper in the core are almost certainly due to variations in take-off angle, associated with the shape of the specimen surface. The profile bears a striking similarity to those from water-leached soda-lime glasses, as obtained by Smets, Doremus and others (loc. cit.). This result, taken with the earlier data from #26, strongly supports the contention that acid attack is confined to the surface of the unreacted glass.

Another replica examined by the TEM method was #61 (see Table 2-5). The fibres in this specimen had been exposed to M HCl,under a load of 30 Kg., and had fractured at 88 minutes. The core-sheath structure could not be seen in the cross sections, as shown in the replica micrograph in Figure 3-13. TEM analyses of a fibre fragment from this replica were carried out, as shown in Figure 3-13. The results are shown plotted in Figure 3-14. The findings are clouded to some extent by the take-off angle problem, which again has led to inconsistent levels of calcium in the core. However, the presence of a very steep concentration gradient separating a very thin, severely demineralised layer from the subsurface is clearly evident. The thickness of this demineralised layer is estimated to be less than 0.2 microns in this specimen.

Samples #61 and #26 had both been exposed to M HCl, which was known from visual evidence to cause severe demineralisation. The available evidence suggests that with acid of this concentration the surface attack proceeds until demineralisation is virtually complete. The

FIGURE 3-13. STEM ANALYSIS OF REPLICA FROM #61.

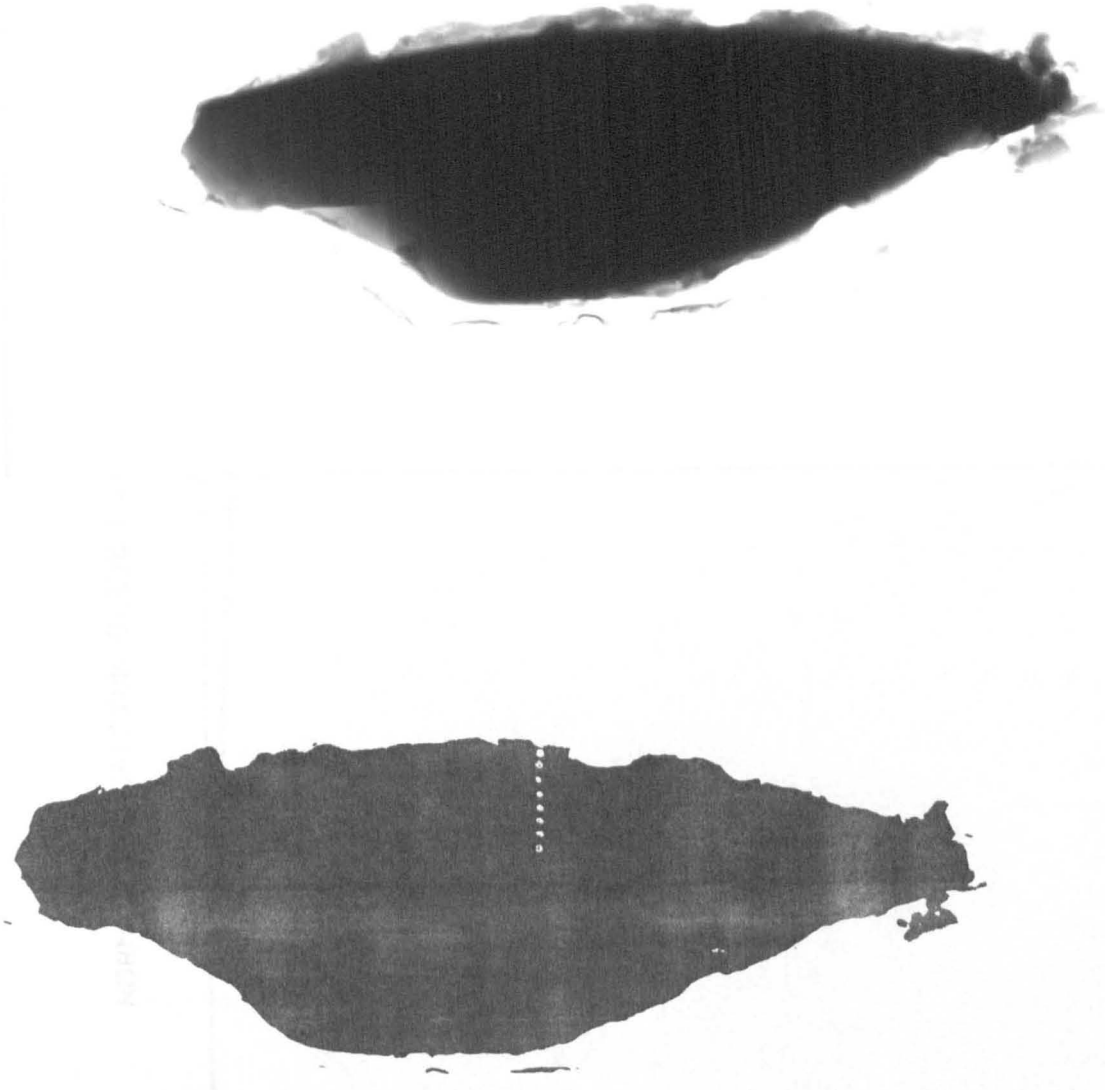

FIGURE 3-14. STEM ANALYSIS OF REPLICA FROM #61 : CALCIUM PROFILE.

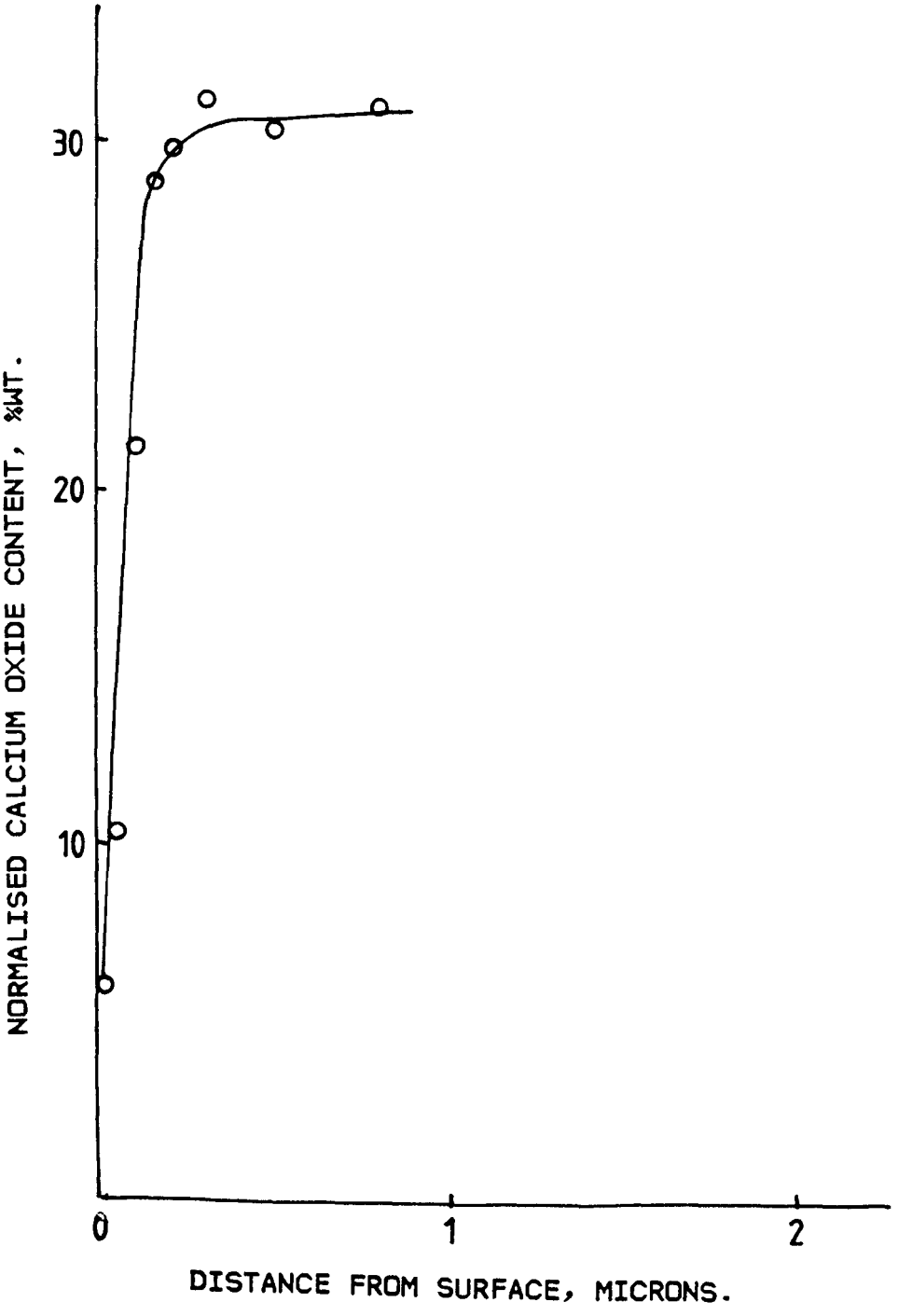

resulting siliceous surface is permeable to the aqueous acid and the attack continues at the interface with the unreacted glass. The essential feature of this process is that the glass itself is not permeable to the acid until it has been grossly demineralised.

With less concentrated acid it is suggested that the extent of surface demineralisation is limited. The surface does not, therefore, become permable to the acid. A visible sheath does not develop and the subsurface composition remains unchanged. This suggestion was tested by using the TEM method to examine fibre fragments from replica #55 that had been exposed to 0.1M HCl under a load of 40 Kg.. The strand had fractured after an exposure time of 66 minutes.

Figure 3-15 shows the appearance of this replica and also shows the locations of the spot analyses carried out on this specimen. The results are shown plotted in Figure 3-16. Despite the continuing problem with the take-off angle, it can be seen that a steep concentration gradient was not evident with this replica. Substantial demineralisation, if it had occurred at all, was confined to a very thin surface layer, with a thickness of less than 0.1 microns.

3-13 Comments on results of the TEM analyses.

The attempts made to refine the qualitative TEM method have highlighted some of the difficulties in obtaining truly quantitative results from EDX analysis. The technique finally adopted overcomes problems associated with beam damage, albeit at some cost in resolution. With perfectly flat specimens with a well-defined, constant take-off angle, good quantitative data could be obtained from E-glass

FIGURE 3-15. STEM ANALYSIS OF REPLICA FROM #55

FIGURE 3-16. STEM ANALYSIS OF REPLICA FROM #55 : CALCIUM PROFILE.

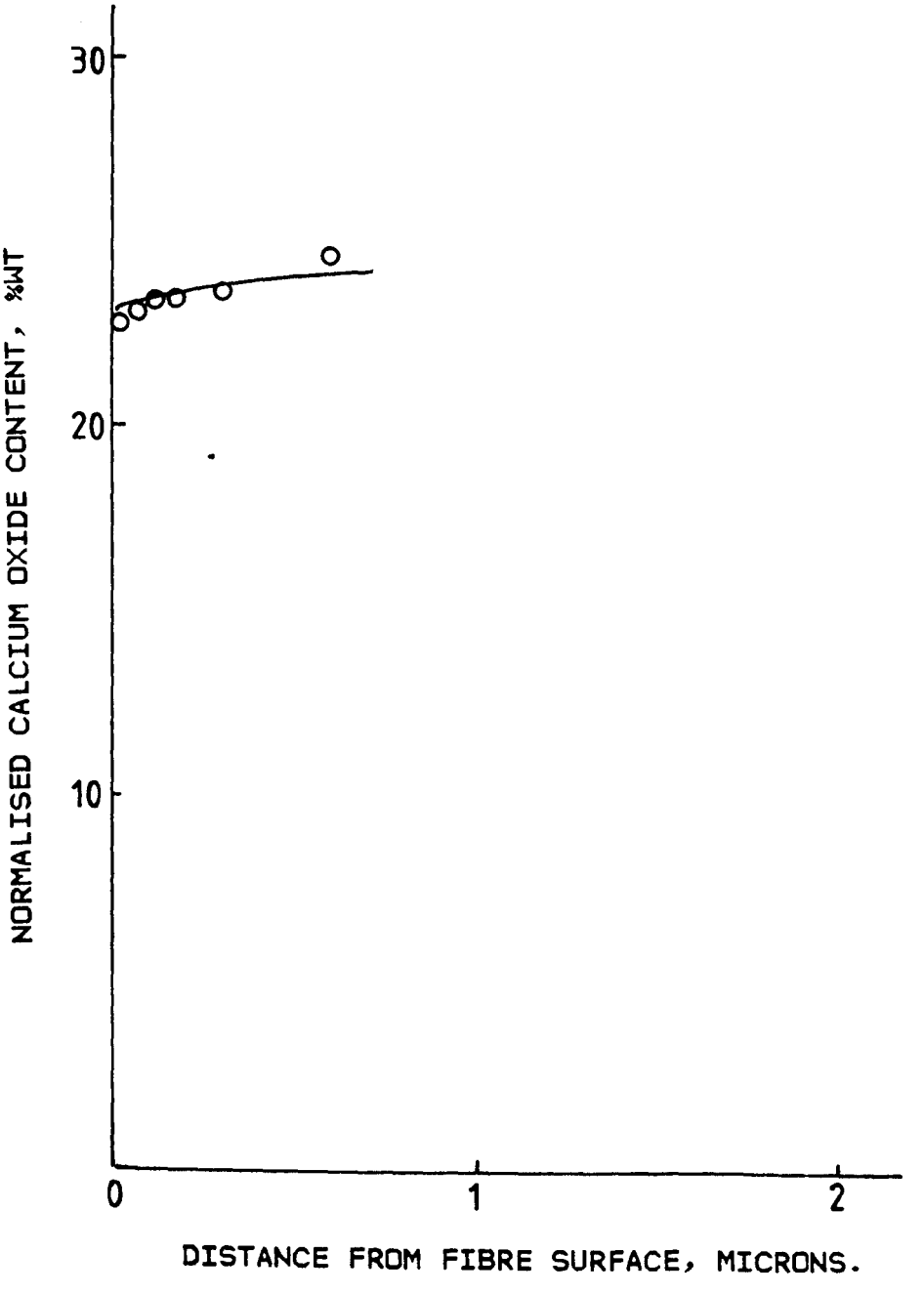

specimens. The fibre fragments examined in this work did not fully conform with this last requirement.

Nevertheless, the trends revealed by the analyses are considered to be well justified. The results clearly show that the severe demineralisation, associated with the corrosion of the fibres by the more aggressive acid media (0.5 - 1.0 M), only occurs within a narrow zone at the fibre surface. With less concentrated acid the attack does not lead to complete demineralisation of the surface. The acid does not permeate through the partly demineralised surface and a visible core-sheath structure does not develop.

The structural weakening of the glass caused by the demineralisation was discussed earlier in this Chapter. It is considered that the analytical data obtained from the TEM work strongly supports the suggestion that surface weakening in the presence of a stress is the primary cause of the stress corrosion failure of E-glass fibres. This contrasts with the failure mechanism that applies to strands that fracture as a consequence of exposure to stress alone, i.e. without acid being present. In this case the fibres undoubtably fail by an instantaneous flaw mechanism, so that the fibre strength is critically dependent on the flaw distribution in the original fibres.

CHAPTER 4. AQUEOUS AND ACID DIFFUSION MEASUREMENTS IN POLYESTER RESINS.

The fibre weakening mechanisms discussed in the two previous Chapters relate to the failure of E glass fibre bundles by a stress-corrosion process. In considering the more complex problem of the stress-corrosion of polyester resins reinforced with E-glass, the presence of the polymer matrix introduces further variables into the system.

In a glass fibre/resin composite that has been well wetted out, the individual fibres are separated by the resin. The thermosetting resins covered in this research programme are generally considered to be resistant to short term corrosive attack by mineral acids. If, therefore, the resin webs separating the fibres are capable of presenting an impermeable barrier to the corrosive medium, it is evident that corrosion problems will not be encountered. Alternatively, if the acid is able to pass through the resin barrier, the fibre weakening mechanisms discussed previously can operate and stress corrosion of the composite becomes possible. In this situation it is also evident that the rate of fibre weakening could be strongly influenced by the rate at which the acid gains access to the fibres.

In stress-corrosion problems interest is centred on events occurring at the tip of a crack that is propagating slowly through the material. In an E-glass /polyester composite it is the rate of weakening and sequential failure of the glass reinforcement that determines the rate of crack growth. It has been shown in a previous Chapter that the extent of fibre weakening depends critically on the stress level and on the concentration of acid to which the fibres are exposed. In

the present Chapter the objective is to establish whether or not diffusion of the acid through the resin can create a sufficiently aggressive environment for fibre weakening to occur. If the results show that this is not the case then it must be assumed that matrix cracking is the principal mode of acid transport to the fibre surfaces.

4-1 Diffusion processes.

It is well known that polyester resins will take up moisture from the environment and that this uptake occurs by molecular diffusion[80,87,92]. Net diffusion into the polymer continues until the resin is saturated with water. At this point the rate of diffusion into the polymer is balanced by the rate of diffusion out of the polymer. The process is characterised by two parameters:

(a) SOLUBILITY,S, representing the maximum amount of diffusant that the substrate can hold. It has the dimensions %wt.. At any given temperature the solubility of e.g. water in a given polymer is a fundamental material property. In the region of room temperature the solubility of water in polyester resins is typically in the range 0.5-3.5%wt..

(b) DIFFUSIVITY,D, representing the rate of uptake of diffusant. This is dependent on temperature, pressure and the concentration of diffusant in the specimen environment. It is expressed in terms of a diffusion coefficient,D, with dimensions cm^2/sec. Strictly the diffusion coefficient can only be applied to those systems where the uptake of the diffusant is associated with the random movement of molecules through a permeable network. The driving force for the uptake is the existence of a concentration gradient,dc/dx, and the diffusion coefficient is featured in the two laws formulated by Fick[86].

Fick's first law relates the diffusive flow, expressed as the flux J, to a constant concentration gradient:

$$J = -D\ dc/dx \qquad (4\text{-}1)$$

The stipulation that dc/dx is constant implies that the system is in a steady state condition.

Fick's second law, which has much more relevance in the present work, is concerned with the behaviour of the system before the steady state condition is achieved. It covers, for example, the situation in which the aggressive solution starts to diffuse through a newly exposed surface at the tip of a propagating stress-corrosion crack in a composite material. Equation 2-4 is a statement of Fick's second law and this is restated below :

$$\partial c/\partial t = D\ \partial^2 c/\partial x^2 \qquad (2\text{-}4)$$

The general statement of the diffusion law given above requires specific solution to enable the behaviour of a particular system geometry to be described. Solutions relevant to the present work are discussed in the Thesis Appendix.

Water is known to diffuse into polyester resins in accordance with Fick's laws[92]. The diffusion coefficient is sensitive to temperature. For polyesters the diffusion coefficient lies in the range 10^{-8} - $10^{-10} cm^2.sec^{-1}$. at room temperature.

4-2 Acid and water diffusion.

The ability of a polymer to take up water does not imply that mineral acids are also capable of dissolving in the polymer. Even if the acid does diffuse through the polymer network at the molecular level,

it would be expected to do so to a different extent and at a different rate than that of water. The consequence of this is that diffusive transport of aqueous acid through a polymer web separating two fibres, is likely to involve a gradual increase in the concentration of the acid available at the next fibre surface. For a given depth of diffusion into the resin this would be predictable, if the respective solubilities and diffusion coefficients for the water and the acid were known.

Before alternative measurement methods could be examined to assess their suitability for measuring acid diffusion it was necessary to define the minimum sensitivity required. This is determined by the extent to which acid diffusion must occur to promote fibre weakening. As has been shown in Chapter 2 this is critically dependent on the stress level. It is considered that the most likely condition for diffusion to be important is the low stress situation, where the crack propagation rate is relatively slow. This statement is based on the assumption that matrix cracking is favoured by the sudden release of strain energy when a fibre fractures. The lower the applied stress, the less strain energy is stored in the fibres, reducing the chance of matrix cracking. Inspection of Figure 2-8 suggests that at low stress the critical concentration of acid at the fibre surface is in the range 0.1-1.0 M. This must be achievable by diffusion within the relevant timescale if diffusive transport of the acid through the resin is to be held responsible for fibre weakening.

This gives the sensitivity with which the solubility and diffusivity measurements must be made. To maintain continuity with the previous work, attention was given to measurements with 1.0 M aqueous solutions of hydrochloric acid. In planning the experiments

it was assumed that the solubility and diffusivity of hydrochloric acid would be similar to or lower than water. It was also desirable to try to choose specimen sizes that would saturate in a reasonable time, say within one to three months, when exposed to the acid. Calculation showed that this would only be achieved with specimens weighing less than 100mg.. At a saturation level of 2.5%wt. 0.1 M HCl the maximum amount of HCl in these samples would be 100×10^{-6}gm..

The method chosen for measuring the acid uptake by the resin therefore had to be capable of high sensivity. After consideration it was decided to use a radioactive tracer method for the experimental work, for the following reasons. Radioactivity measurements involve the detection of individual disintegrations on an atomic scale and can easily meet the sensitivity requirement. Perhaps a more important factor, however, is that the radioisotopes available for use in the present work (^{36}Cl and ^{3}H) do not occur naturally. Because of this the full sensitivity of the method can be used without interference from contaminants in the specimens or the environment. Since the source of the diffusing material is uniquely tagged it provides unambiguous evidence of the movement of material from the diffusant solution into the polymer. Finally, it enables the diffusion of different molecular species to be followed simultaneously. This is of high interest in the present study, because the behaviour of both the water and the hydrochloric acid present in the diffusant can be monitored.

4-3 Diffusion measurements.

The aim was to determine the concentration of acid that could build up by the simultaneous diffusion of both water and HCl in the resin. Equation 4-2 shows that for Fickian diffusion this concentration is a

function of both time and diffusion depth. It is evident that a full understanding of the system requires that the solubilities and diffusivities of both of the diffusing species are known. The measurement experiments must therefore be designed to yield both of these properties. A wide range of experimental strategies are available for the measurement of diffusion coefficients. These have been extensively reviewed by, inter alia, Crank[23], Barrer[93], and Jost[94]. In many systems it is easily possible to allow diffusion to occur for a definite time, and then to determine the diffusant concentration in the substrate, as a function of diffusion distance. This provides a direct measure of the concentration gradient. By making similar experiments with different diffusion times the term $\partial c/\partial t$ in equation 2-4 can be estimated, thus providing all the data needed to calculate D. The analysis of concentration-distance profiles in a material also forms the basis of the well-known Matano-Boltzmann method for the measurement of diffusion coefficients. This method was used by Marshall[87] to measure water diffusion coefficients by a radioactive tracer method, using tritium to label the water. A limitation of this method, however, is imposed by the boundary conditions for the solution of equation 4-2. This limitation stipulates that the diffusion front must always be confined within the specimen boundaries. This is because the concentration gradient in equation 4-2 is specified for the non-steady state situation. As soon as the diffusion front reaches the finite boundary of the system, the concentration gradient decreases. If the diffusion process is allowed to continue, the specimen will eventually become saturated with diffusant, and the concentration gradient will fall to zero. These different situations are depicted in Figure 4-1,(a)-(c), which shows the effect on the concentration gradient when the diffusant reaches the specimen boundary.

FIGURE 4-1. DIFFUSION PROFILES FOR SEMI-INFINITE PLATE.

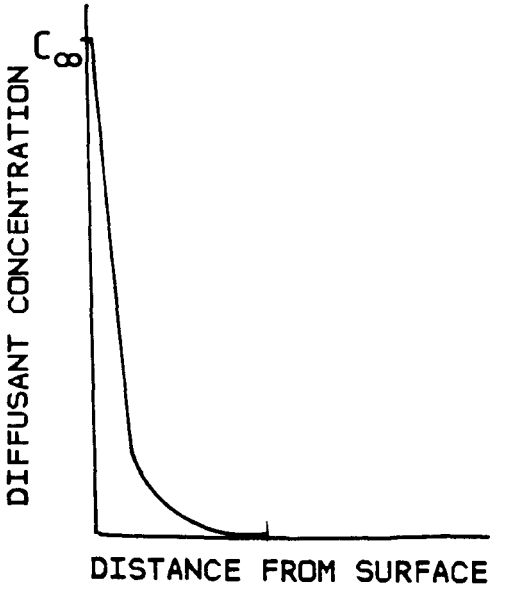

(A)CONCENTRATION-DISTANCE PROFILE FOR SHORT TIME.

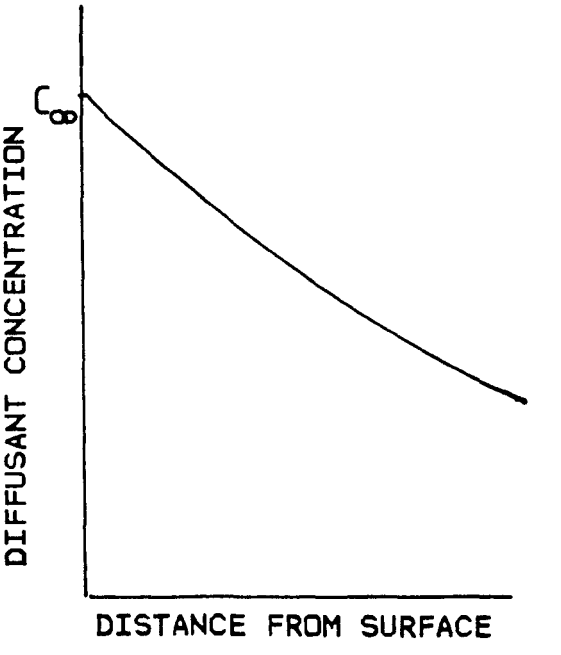

(B)CONCENTRATION-DISTANCE PROFILE FOR INTERMEDIATE TIME.

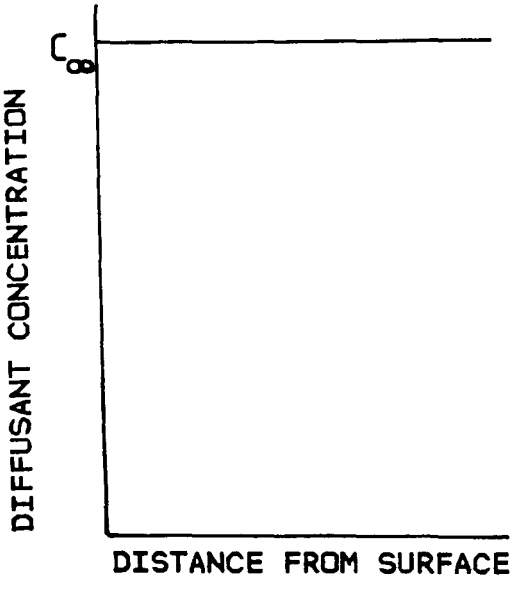

(C)CONCENTRATION-DISTANCE PROFILE FOR LONG TIME.

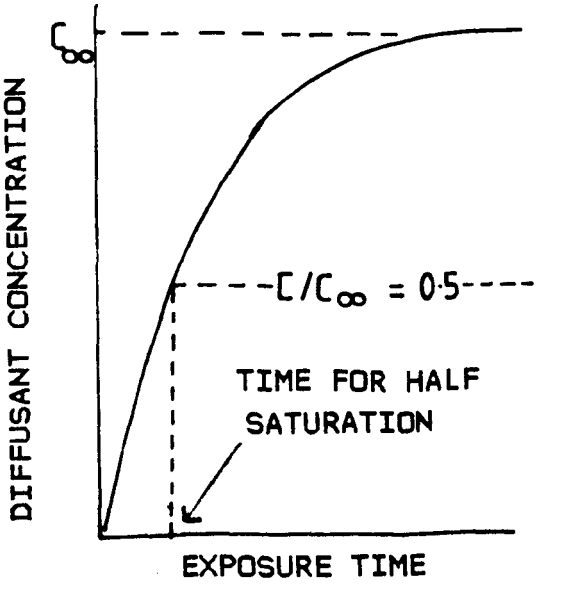

(D)CONCENTRATION-TIME PROFILE FOR TOTAL UPTAKE METHOD.

For experimental consistency in the present work it was considered essential to link the diffusivity measurements with the solubility measurements. An alternative approach, which would make this possible, was the use of the "total uptake" method (Crank,loc.cit.). In using this method a number of nominally identical polymer specimens are prepared and weighed. The specimens are then exposed to the diffusant for various times. After exposure the amount of diffusant taken up by each specimen is measured and is used to construct an uptake curve of the type shown in Figure 4-1(d). The flat portion of this profile represents the situation in which the specimen is saturated with diffusant and provides a measure of the solubility S. The diffusion coefficient determines the rise time of the curve. A convenient measure of this rise time is the half-saturation time, $T_{0.5}$. For diffusion into a semi-infinite plate, Ellis and Found[92] have shown that a very simple solution to the diffusion equation 2-4 can be used to interpret these data. The diffusion coefficient is given by the equation:

$$D = 0.049\ L^2/T_{0.5} \qquad (4\text{-}3)$$

where L is the plate thickness.

An alternative to this is to use the whole uptake profile to derive the diffusion coefficient. This was the method used in the work described below. It is described in detail in the Thesis Appendix. The radioactive tracer measurement method was therefore used to acquire total uptake data for a number of polyester samples. The experimental details are described below.

4-4 Radioisotopes used and their measurement.

In this programme the hydrochloric acid was traced with ^{36}Cl whilst

the water was traced with ^{3}H (tritium). Tritium labelling of the hydrochloric acid was not considered to be appropriate, because in aqueous solution there is a rapid interchange of hydrogen ions between the water and the acid. This leads to the uniform distribution of the tritium between the water and the HCl molecules. Because of the overwhelming preponderance of water molecules, even in 1.0 M acid, tritium uptake by the polymer reflects water uptake, rather than HCl uptake. ^{36}Cl is therefore preferred as the hydrochloric acid label, although strictly it is only a measure of chlorine uptake.

Both of the isotopes used are beta emitters, with sufficiently long half-lives ($t_{0.5}$) to preclude the need for decay corrections. The radioactivity parameters of the isotopes are:

Isotope	Half-life = $t_{0.5}$	Maximum energy of beta particle
^{36}Cl	3 X 10^{5} years	0.714 MeV.
^{3}H	12.3 years	0.018 MeV.

The very large energy difference between the beta particles emitted by these isotopes makes it easily possible to resolve them by beta spectrometry, using a liquid scintillation spectrometer.

The essential feature of all radioactivity measurements is the estimation of the number of atomic disintegrations occurring in unit time. This disintegration rate (dpm = disintegrations per minute) is directly proportional to the amount of radioactive material present. For several reasons it is often possible only to detect a fraction of these disintegrations. Hence the measured counting rate(cpm = counts per minute)is related to the disintegration rate by the counting efficiency,E:

$$cpm = dpm \times E/100$$

where E is expressed as a percentage. For beta emitters it is a general principle that the efficiency of the counting method is dependent on the energy of the emitted particles. The familiar Geiger counter, for example, could be used to detect the ^{36}Cl particles emitted from a polymer sample with an efficiency of perhaps 10%. ^{3}H cannot be detected at all with such a counter, because the low energy beta particle cannot penetrate the window of the counter.

For the diffusion work the preferred method of measurement is liquid scintillation counting, which will detect ^{36}Cl with an efficiency close to 100%, and ^{3}H with an efficiency in the range 20-50%. In this method a special solution, known as a liquid phosphor, is used. This consists basically of toluene in which fluorescent solutes have been dissolved. The radioactive sample is dissolved or suspended in this solution. When a beta particle is emitted from the sample it is absorbed by the solution. Part of the energy absorbed is re-emitted by the fluorescent solutes as a scintillation, with an intensity proportional to the energy of the absorbed beta particle. In a liquid scintillation spectrometer the photons associated with these scintillations are detected with a photomultiplier, which converts the light pulses into an electrical pulses, suitable for amplification, pulse height analysis and counting. The two liquid scintillation counters used in this work(Tracor model 6892, Packard model 5310) both had pulse height analysis facilities capable of routing pulses into different channels for counting. This meant that the tritium could be counted in one channel and ^{36}Cl in another.

4-5 Preparation of samples for liquid scintillation counting.

The total uptake method used for the solubility and diffusivity

measurements yielded a large number of polymer specimens containing small amounts of HCl and water tagged either with ^{36}Cl or ^{3}H or both. On completion of the exposure to the radioactive diffusant it was imperative to wash the excess liquid from the specimen surface after removal from the solution. This is extremely important, because the residual liquid adhering to the surface can greatly exceed the amount of material that has diffused into the polymer. A suitable procedure was developed in which the specimens were washed by momentarily dipping them into three separate baths of inactive 0.01 M HCl. Tests on blank specimens showed that this procedure freed them from gross surface contamination.

To use liquid scintillation counting to measure the radioactivity in these specimens it was necessary to extract the radioactive material from the polymer samples and to bring it into solution in the toluene-based phosphor. This was not entirely straightforward, because the sample material was aqueous in character and insoluble in toluene. Liquid scintillation counting, however, has found very wide application in the biological and medical fields, where the majority of samples for study are also aqueous in character. To meet this need special extraction systems (Packard Inc.: biological oxidiser) and liquid phosphors (Packard Inc.: Monophase and Optifluor) have been developed and are available commercially. These provided a good starting point for the further development work needed to prepare the exposed polymer samples for counting.

4-6 Development of a combustion procedure.

Combustion of the washed samples is a very effective way of recovering the radioactivity for counting. At the high temperatures nec-

essary for the combustion the diffusants are driven out of the polymer, which is oxidised to CO_2 + H_2O. The water can easily be condensed in a cold trap, whilst the HCl, by virtue of its extremely high solubility in water, can also be recovered in the cold trap.

The Packard biological oxidiser is designed to achieve a very high throughput of samples. A diagram of the unit is presented in figure 4-2(a). 10-50 mg. amounts of the biological material are weighed into a small silica boat, and are volatilised in a furnace at 1000deg.C in a stream of oxygen. Complete combustion is achieved by passing the resultant gases over a catalyst at 900deg.C and the biological material is completely converted into water and carbon dioxide. These can be recovered by condensation in a cold trap, maintained at liquid air temperature. Subsequently, the cold trap is removed, liquid phosphor is added, and the trap is allowed to warm up to room temperature, to yield the required counting solution. Under optimum conditions this method is very rapid and can achieve turn-round times of less than five minutes per sample.

In trying to use this method without modification for the polymer samples major problems were encountered. The HCl given off by the exposed resin samples was found to react with the catalyst used in the oxidiser. Quantitative recovery of the HCl could not therefore be achieved by combustion over this catalyst. Experiments were therefore attempted with the catalyst replaced by quartz chips. Without the catalyst, however, the relatively large size of the specimens and the chemical constitution of the material resulted in incomplete combustion at the normal oxygen flow-rate. Attempts to correct this by increasing the oxygen flow-rate led to explosive combustion and it was therefore decided that a complete redesign of the combustion system

FIGURE 4-2. POLYMER COMBUSTION UNITS.

(A) PACKARD BIOLOGICAL OXIDISER.

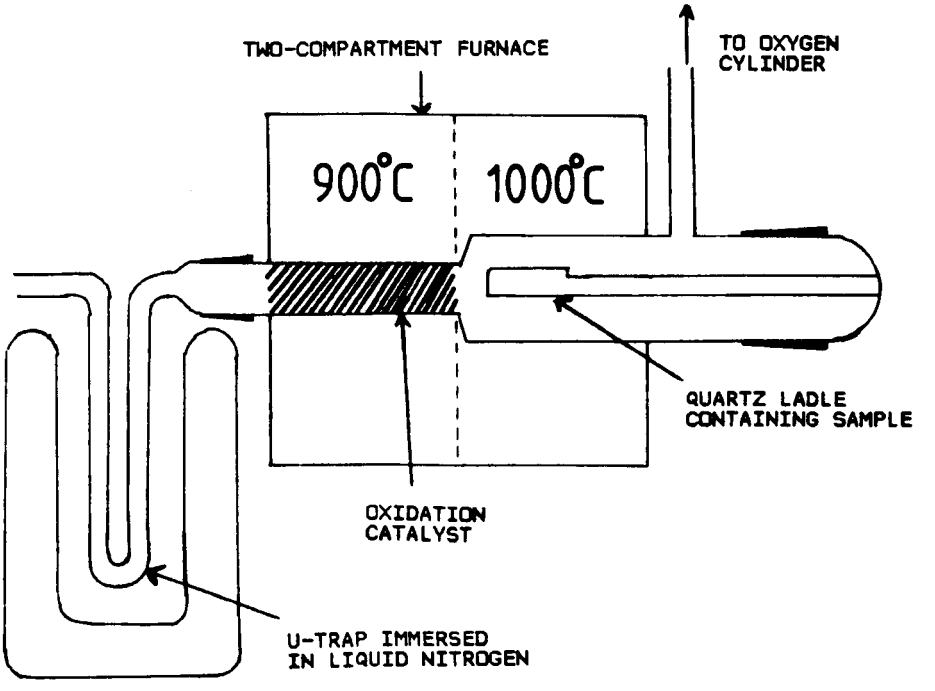

(B) REDESIGNED COMBUSTION UNIT

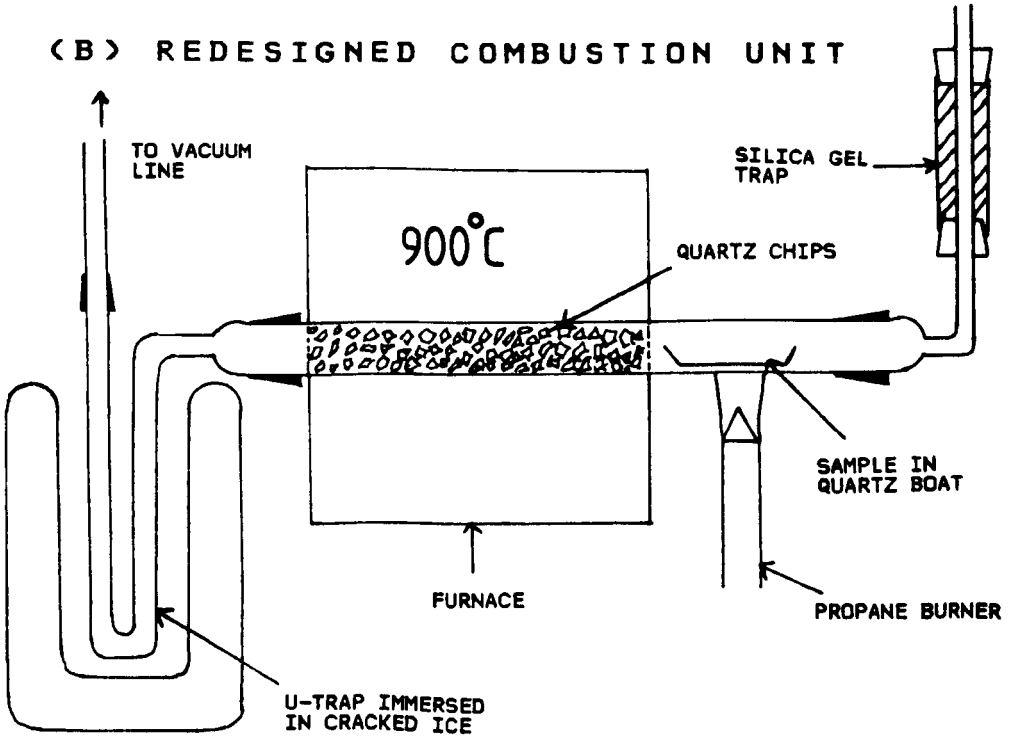

was needed. Eventually it was found that the system shown in Figure 4-2(b) gave satisfactory performance. This features combustion in a stream of air, rather than oxygen, and the use of the propane burner to volatilise the sample enabled this to be done sufficiently slowly to ensure complete combustion. The system is capable of handling much larger samples than the Packard unit, but has the disadvantage that much longer turn-round times are involved. Typically, sample preparation took one hour for specimens weighing 50-100 mg..

For the method to be viable, it was essential that the very small amounts of tagged diffusant taken up by the polymer samples were completely recovered in the cold trap of the unit. It would be very easy to lose some or all of the tagged material, either by absorption in the combustion tube, or by incomplete condensation in the cold trap. In radioactive tracer work the normal way of avoiding this is to add a large excess of inactive material to the sample to provide a "carrier". In applying this method 0.1ml. quantities of .01 M HCl were used to provide this carrier.

It was necessary to find the optimum flow of air through the modified unit that would give satisfactory combustion, but which would also give efficient condensation in the cold trap. The performance of the unit was checked in a series of experiments at different flowrates. In each experiment a measured volume of tagged M HCl and a 50 mg.inactive polymer specimen were burned off in the unit. Comparison of the added with the recovered radioactivity levels showed that there was a sharp cutoff in flow-rate above which full recovery was not achieved. A rotameter was therefore fitted to the unit to ensure that the air flow-rate was always within the full recovery range.

A stepwise summary of the whole procedure, showing how the inactive carrier is used, is as follows:

1. The combustion unit is primed by a burn of 0.1 ml. inactive .01 M HCl to get some liquid into the cold trap.
2. The washed polymer sample from the diffusion test is burned.
3. The system is flushed with another burn of 0.1ml. of .01 M HCl.
4. The cold trap is removed from the liquid nitrogen bath and 20 ml. of Monophase liquid phosphor is added. The solution is mixed by shaking as it gradually warms up to room temperature.
5. A 15 ml. aliquot is taken for counting in a polyethylene counting vial.

This method was found to be very effective, with negligible contamination of the unit between samples.

4-7 Slow extraction and reverse diffusion specimen preparation methods.

The majority of the solubility and diffusivity data reported below were obtained by the combustion method. As the programme developed, however, interest in methods of specimen preparation that involved less operator time were examined. It was essential that any new methods introduced at a later stage should yield results that were consistent with those from the combustion method. This was carefully checked before the two methods described below were used in practice.

The first alternative method involved the slow extraction of the diffusants from the polymer into 15 mls. of the Optifluor liquid phosphor, to which 0.2 mls. of .01 M aqueous HCl had been added. The extraction was carried out by immersing the washed, exposed polymer

specimens in the phosphor in a counting vial. The high energy ^{36}Cl beta particles from within the polymer are readily able to escape into the phosphor, to generate scintillations. The HCl penetration into the polymer can therefore be assessed immediately. The low energy tritium beta particles, on the other hand, are absorbed by the polymer itself and do not reach the phosphor. The tritium counts therefore increase slowly with time, and eventually stabilise as the water in the specimen equilibrates with that in the phosphor. The massive excess of water in the phosphor led to essentially complete recovery of the tritium after about one week at room temperature. The second alternative method involved the reverse diffusion of the radioactive material into an aqueous solution similar to that of the tagged diffusant. True diffusion is a dynamic phenomenon, with diffusant molecules moving both into and out of the substrate. When the saturation condition is achieved the two rates of flow , i.e inward and outward, are equal. The diffusion is therefore reversible. This situation is only achieved if two conditions are satisfied:

(a)The diffusion is occurring by the random movement of the diffusant through the polymer network at the molecular level,

(b)There is no reaction between the diffusant and the substrate, since this would immobilise the diffusant molecules.

Subjecting the exposed polymer to reverse diffusion thus provides a measure of the amount of mobile diffusant that has been taken up by the resin. This is a useful measurement, because it is only the mobile diffusant that is available to attack glass fibres encapsulated in resin.

In using this method the washed, exposed polymer specimens were immersed in 2 mls. of aqueous 0.1 M HCl. After one week the specimen was removed and placed in a second 2 mls. of the inactive acid sol-

ution. Each 2 ml. of solution produced in this way was dissolved in 15 mls. Optifluor for counting. The counts from two or three extractions on each specimen were combined to give the total specimen counting rate. In fact, in all the specimens examined by this method, 95% of the activity was recovered in the first extract.

As stated above, much of the work reported below was carried out by the combustion method. Data obtained by the other two methods, including the tritium measurements, gave results that were fully consistent with the combustion data.

4-8 Precision limitations.

The precision and sensitivity of all radioactivity measurements are limited by the statistical nature of the decay process, the background counting rate and the overall counting efficiency of the system. The background is due to the combination of electronic noise, originating in the photomultiplier, the presence of naturally occurring radioactive impurities in the sample and the counter, and cosmic radiation.

Errors in net counting rates due to the counting statistics of the sample and the background were minimised by increasing the counting times, where appropriate, up to a maximum of ten replicate 50 minute counts. Errors due to this cause were less than 1% for high counting rates, and were not larger than 10% for low counting rates.

As mentioned earlier, liquid scintillation counters give high counting efficiency for both tritium and ^{36}Cl. However, the liquid phosphor is very sensitive to scintillation quenching when the sample contains material which is either strongly coloured, or which can in-

terfere with the fluorescence process. Quenching is a major topic in liquid scintillation counting. Not only does it reduce sensitivity, but it can also invalidate the simple linear relationship between counting rate and radioactivity level. To achieve quenching control in the present work the compositions of all the liquid phosphor samples were matched with those of similar samples containing known amounts of ^{36}Cl and tritium. In all cases, therefore, the counting efficiency was obtained by direct measurement, using a standard sample with the same composition as the test sample.

4-9 Radioisotope specific activity and sensitivity.

Radioisotopes in general are expensive and constitute a health hazard. ^{36}Cl, for example, is both more expensive and more hazardous to use than tritium. Thus, although extremely high sensitivity can be achieved by using the pure, "carrier-free" isotope, it is normal to dilute the tracer with its inactive analogue to match the activity level to the needs of the experiment.

In the present case it was known that the solubility of water in polyester resins was in the range 0.5%wt.-3.5%wt. It was therefore decided to use tritiated water with a specific activity of 10 microcuries ml^{-1}, and ^{36}Cl labelled hydrochloric acid with a specific activity of 1 microcurie ml^{-1}. In all of the following experiments the diffusant solution was 1.0 M HCl. It was anticipated that differential diffusion would lead to a reduction in the acid content of the fluid diffusing into the polymer. It was estimated that, at the specific activities chosen, the presence of 0.001M HCl could be detected in the fluid dissolved in a 50 mg. polymer sample saturated with diffusant. This gives a reserve sensitivity factor of 100 on the

minimum concentration of 0.1M that has been shown to be necessary to weaken fibres under the low stress conditions of current interest.

4-10 Polyester resin specimens.

Polyester resins are made by the condensation of dibasic acids with polyhydric alcohols to form linear polymer chains with repeating ester units. These chains can be cross-linked with styrene to produce a structure with three-dimensional bonding. The polymers are known as thermosetting resins and tend to be hard but brittle. Scott-Bader Crystic 272 is an example of such a resin. It is made by condensing isophthalic acid and maleic anhydride with propylene glycol and is cross-linked with styrene. This resin is widely used in industry as a general purpose resin for the manufacture of grp.

To link the present work with studies carried out in earlier programmes[15,63], data was required on four resin systems. Three of these were modifications of the Crystic 272 resin. The brittleness of this material can be reduced by incorporating flexibilising agents (e.g. rubbery materials) into the resin. Proprietary resin modifiers are available from Scott-Bader for this purpose, and specimens of Crystic 272 that had been modified in this way were tested. The two modifying agents used were Scott-Bader 586 and NV 1080.

Under certain circumstances, resins made from isophthalic acid are sensitive to degradation in the presence of aqueous solutions of acids and alkalis. Alternative formulations,based on HET acid, (hexachloro-endomethylene-tetrahydrophthalic acid), are said said to be more resistant to chemical attack than Crystic 272. Beetle 870, produced by British Industrial Plastics, is a het acid resin that is

marketed as a corrosion resistant material. This resin was, in fact, the most brittle of the four tested.

The resins and modifiers are all supplied as partially polymerised liquids. Completion of the polymerisation and most of the cross-linking of the structure occurs when the material is catalysed by methyl ethyl ketone peroxide in the presence of cobalt naphthenate, which acts as a polymerisation accelerator. The final stage of the cross-linking is achieved by postcuring the polymer at a high temperature. In the present experiments 1% catalyst and 0.5% accelerator were used for the polymerisations, followed by a postcure at 80°C for four hours. The resin specimens used for the diffusion measurements were prepared by casting processes, either between glass plates, or in small bore glass tubes, or in a rotating wide bore tube. The reasons for using differently shaped specimens will be discussed presently. The identification numbers and compositions of the resins tested in the programme were:

Resin number	Resin composition
272	Crystic 272
272/586(a)	75% Crystic 272 + 25% Crystic 586
272/586(b)	50% Crystic 272 + 50% Crystic 586
272/1080	80% Crystic 272 + 20% NV 1080
870	Beetle 870

4-11 HCl solubility experiments in Crystic 272. Thin plate experiments.

The first measurements were made to examine the extent to which ^{36}Cl-labelled HCl would diffuse into Crystic 272. For this purpose thin sheets of the resin were prepared by casting between glass plates. From these sheets a number of rectangular specimens were cut, each weighing about 50 mg.. The approximate dimensions of these specimens

were 20 x 5 x 0.3mm.. They were individually immersed in 2 ml. of the ^{36}Cl tagged molar HCl in small glass tubes sealed with small rubber stoppers. Immersion times ranged from one hour to three months. In all a total of 50 specimens were tested in this way and were counted by the combustion and slow extraction methods.

Examination of the results obtained showed that the uptake of ^{36}Cl by the resin was extremely low in relation to the expected solubility of water in the resin. If the molar HCl had permeated the resin without change of concentration it would be expected that the chlorine content at saturation would be about 0.06%wt.. The results obtained had a mean value of 0.0018%wt.. Moreover, the results showed much scatter, did not gradually increase with time, and did not show a trend to level out at an equilibrium level representing the saturation solubility. It was believed that the results were not due to acid diffusing into the resin at all. The very low levels of activity detected were thought to be due to the acid becoming absorbed on the specimen surface or entering surface microcracks, particularly at the cut edges of the specimens.

To check this further, another set of long term exposures to the ^{36}Cl-labelled HCl was carried out. These experiments featured thin plates with the same rectangular dimensions as those tested previously, but with a range of thicknesses. They were made by casting between glass plates using shims as distance pieces to control the thickness. The exposure time in this experiment was 310 hours. If the measured activity levels were due to true solubility, the total uptake should increase with increasing thickness, so that the measured solubility is independent of thickness. In a parallel experiment a similar set of thin plate specimens of varying thickness were exposed

to tritium-labelled aqueous HCl for the same exposure time. After exposure the samples were counted by the reverse diffusion method to yield the results given in table 4-1.

TABLE 4-1 CRYSTIC 272 SOLUBILITY MEASUREMENTS AT 20°C WITH THIN PLATE SPECIMENS.

Plate No.	Exposure Time,hr.	Wt.,mg.	Thickness mm.	HCl,%wt. from ^{36}Cl assay	H_2O,%wt. from ^{3}H assay
1	2280	98.58	0.25	.00136	
2	2280	98.17	0.25	.00129	
3	310	96.73	0.25	.000752	
4	2280	49.28	0.12	.00282	
5	2280	47.82	0.12	.00339	
6	310	28.84	0.08	.00300	
7	1968	25.92	0.08	.00410	
8	310	99.04	0.25		1.79
9	310	46.52	0.12		1.86
10	310	30.80	0.08		1.84

These tritium measurements show that the water uptake reaches saturation within the exposure time of 310 hours. It is particularly noteworthy that the measured solubility is independent of the plate thickness, as predicted above. The water uptake is reversible, since the counts were obtained by the reverse diffusion method, and the results are therefore consistent with the known Fickian diffusion of water into polyester resins.

In contrast to this the HCl uptake, as measured by the ^{36}Cl uptake of the resin samples, was again extremely low and erratic. The uptake did not increase with specimen thickness or respond to differences in exposure time. In fact, the uptake appeared to correlate best with the surface areas of the specimens. The effect of this was to produce the trend where the % uptake appeared to decrease with increasing

specimen thickness. The conclusion drawn from these experiments was that HCl has a very low or zero solubility in Crystic 272 resin. The low levels of ^{36}Cl picked up by the specimens were probably due to adsorption or occlusion in surface cracks. The rectangular shape of the thin plate specimens and the relatively high surface area of the cut edges makes these specimens susceptible to this problem. A better geometry could be achieved by using rod-shaped specimens with a high aspect ratio. Such specimens would minimise adsorption or occlusion effects due to the cut edges of the specimens.

4-12 Solubility and diffusivity measurements with rod specimens, using ^{3}H and ^{36}Cl tagging.

To demonstrate further the difference in the solubility and diffusivity of water and HCl in polyester resins, dual tagging with both ^{3}H and ^{36}Cl was used. Rod-shaped specimens of Crystic 272 were prepared by casting the resin in 1.2mm. diameter glass tubes. 25mm. lengths of these rods were used to generate total uptake data for both water and HCl . The specimens were immersed in molar HCl tagged with the two isotopes. Tests on the 272 resin were carried out at a laboratory temperature of 20°C. Results were obtained for a range of exposure times up to 507 hours. The exposed resin specimens were counted by both the combustion and slow extraction procedures described earlier. The results are given in full in Table 4-2 and are shown plotted in Figure 4-3.

TABLE 4-2 DUAL TAGGING MEASUREMENTS ON ROD SPECIMENS OF CRYSTIC 272.

Experiment No.	Exposure Time,hr.	%wt.H_2O in resin	%wt.HCl in resin	Measurement method
138	1.37	0.082	0	combustion

139	2.50	0.215	0.00008	combustion
140	4.45	0.354	0.00032	combustion
147	6.92	0.523	0.00021	combustion
190	21.42	0.879	0.00042	combustion
153	30	1.117	0.00021	combustion
217	77	1.535	0.00074	combustion
218	78	1.654	0.00158	combustion
151	172	1.789	0.00021	combustion
191	223	1.829	0.00132	combustion
145	1.08	0.253	0.00024	slow extraction
144	3.41	0.455	0.00028	slow extraction
143	5.33	0.560	0.00020	slow extraction
142	6.08	0.595	0.00028	slow extraction
146	8.08	0.662	0.00020	slow extraction
192	24.16	1.025	0.00053	slow extraction
156	162	1.823	0.00038	slow extraction
157	162	1.844	0.00079	slow extraction
154	175	1.851	0.00059	slow extraction
155	175	1.843	0.00038	slow extraction
197	226	1.850	0.00083	slow extraction
167	507	1.889	0.00075	slow extraction

Inspection of the data in Table 4-2 shows the contrast in behaviour between the water and the acid. The HCl uptake with these specimens is even lower than with the thin plates, and shows no regular fluctuation with time. This is consistent with the lower surface/volume ratio of the rods, compared with the plates. The results obtained from the two different counting methods can be seen to be in excellent agreement.

The plotted data in Figure 4-3 show that the water profile can be fitted almost exactly to equation 4-2, with a solubility of 1.82% wt. and a diffusion coefficient of $3.15 \times 10^{-9} cm^2 sec^{-1}$. The points representing the HCl uptake can only be revealed on this plot by expanding the scale. An alternative way of presenting the ^{36}Cl results is shown in Figure 4-4. This compares the ^{36}Cl uptake with the theoretical curve that would apply if M HCl diffused through the resin unchanged.

FIGURE 4-3. DIFFUSION OF WATER AND HCL INTO CRYSTIC 272 AT 20° C.

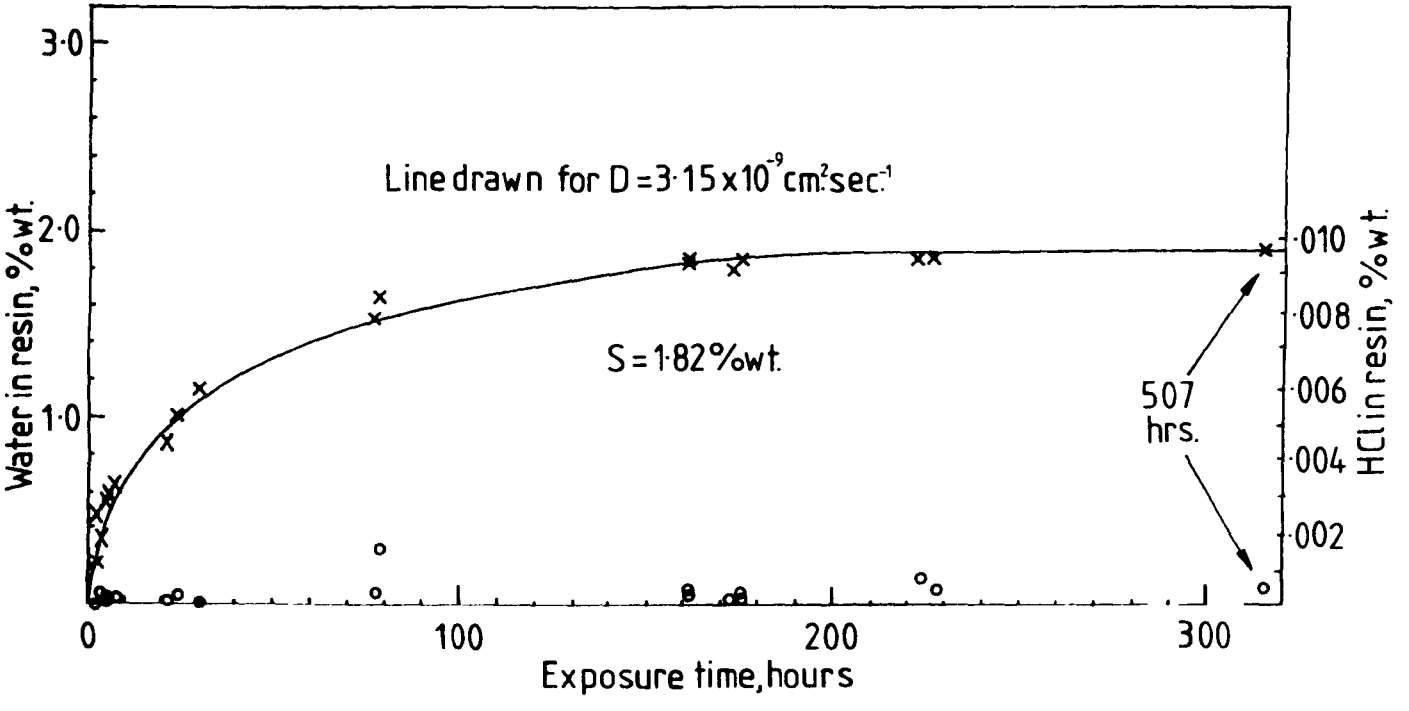

FIGURE 4-4. PREDICTED AND OBSERVED ^{36}CL UPTAKE FOR DIFFUSION OF MOLAR HCL INTO CRYSTIC 272 RESIN.

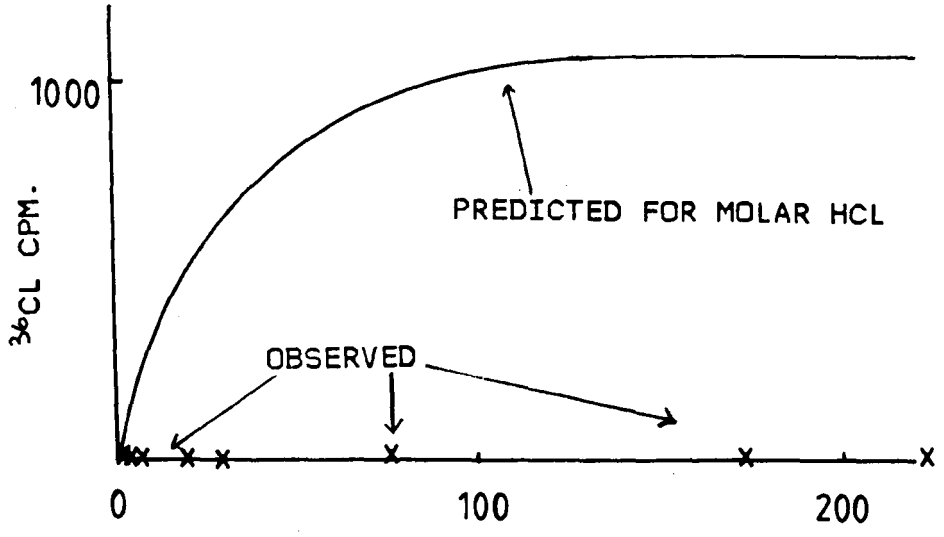

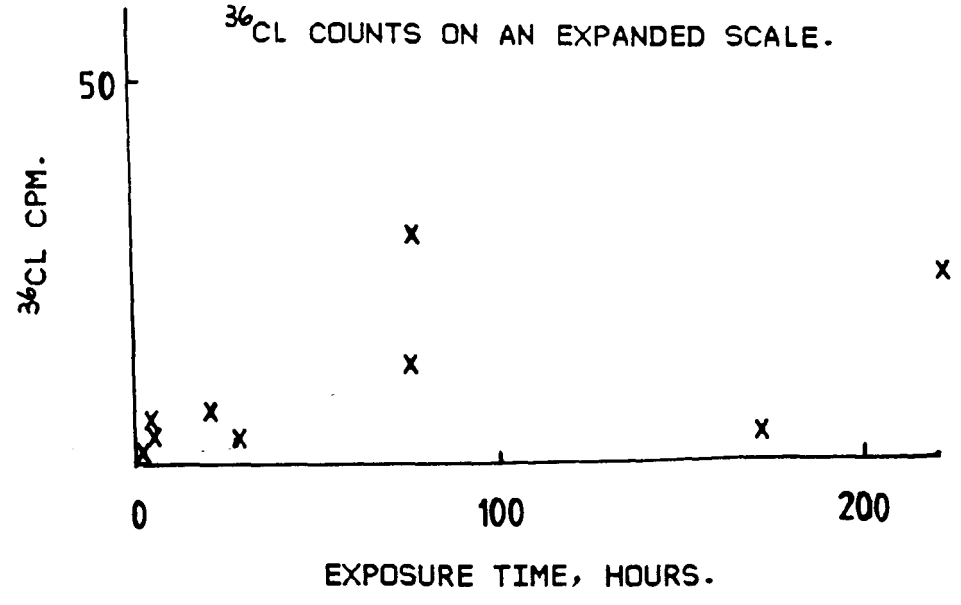

The above results show that the concentration of HCl in the fluid diffusing through unstressed Crystic 272 at 20°C cannot achieve the levels required to weaken E-glass fibres subjected to low stress.

4-13 Measurements on other resins at 20°C.

Complete diffusion profiles for the other polymers of interest were not measured at 20°C. It was considered sufficient to show that, on exposure to molar HCl, water diffused into the material wheras HCl did not. The results in Table 4-3 were obtained using 25mm. polymer rod specimens that had been immersed in the dual-tagged molar acid for two weeks.

TABLE 4-3 UPTAKE OF WATER AND HCL BY POLYMER ROD SPECIMENS AFTER 345-HOUR EXPOSURE TO MOLAR HYDROCHLORIC ACID.

Polymer type	%wt.H_2O in resin	%wt.HCl in resin
Crystic 272	1.87	0.00063
25% Crystic 272 75% Crystic 586	2.41	0.00105
50% Crystic 272 50% Crystic 586	3.21	0.00204
Beetle 870	1.30	0.00050
80% Crystic 272 20% NV 1080	2.07	0.00043

Although these data do show a trend for HCl content to correlate with water content, the measured values are still extremely low in relation to the values that would be obtained by the diffusion of molar HCl. At room temperature it is clear that water will diffuse freely in all the polyester systems examined, but HCl does not appear to be capable of penetrating into the polymer network.

4-14 Effect of temperature.

An important application of E-glass/polyester composites is for the construction of pipes and tanks for handling and storing aqueous liquids at or near room temperature. To ensure that there are no pronounced changes in HCl solubility at slightly higher temperatures, another series of uptake experiments was made. In this case the rod-shaped resin specimens were immersed in the dual-tagged molar HCl, which was maintained at 25 ±0.1 °C in a thermostat bath. Full diffusion profiles were obtained on the Crystic 272 and Beetle 870 resins. The results are shown in Tables 4-4 and 4-5 and are plotted in Figures 4-5 and 4-6.

TABLE 4-4 CRYSTIC 272 DIFFUSION MEASUREMENTS AT 25°C.

Experiment No.	Exposure Time,hr.	%wt.H_2O in resin	%wt.HCl in resin	Measurement method
245	2	0.344	0.00084	combustion
224	5	0.672	0.00011	combustion
240	6.2	0.676	0.00026	combustion
225	6	0.709	0	combustion
246	11	0.867	0.00031	combustion
226	20	1.205	0	combustion
227	43	1.653	0.00063	combustion
228	52	1.660	0.00026	combustion
237	161	1.987	0.00026	combustion
219	362	2.075	0.00021	combustion
244	2	0.391	0.00051	slow extraction
239	6.2	0.670	0.00020	slow extraction
221	6.67	0.786	0	slow extraction
222	6.67	0.663	0	slow extraction
230	49	1.600	0.00079	slow extraction
232	177	1.929	0.00059	slow extraction
230	49	1.600	0.00079	slow extraction
232	177	1.929	0.00059	slow extraction
249	317	1.980	0.00123	slow extraction
250	317	1.981	0.00103	slow extraction
223	367	1.985	0.00036	slow extraction
231	535	1.986	0.00059	slow extraction
352	2	0.362	0.00028	rev. diffusion
354	4	0.497	0.00008	rev. diffusion
355	6	0.630	0	rev. diffusion

353	8	0.690	0	rev. diffusion
351	10	0.754	0.00008	rev. diffusion

TABLE 4-5 BEETLE 870 DIFFUSION MEASUREMENTS AT 25°C.

Experiment No.	Exposure Time,hr.	%wt.H_2O in resin	%wt.HCl in resin	Measurement method
248	2.7	0.257	0.00100	combustion
251	17.2	0.847	0.00211	combustion
257	20	0.903	0.00142	combustion
252	25.7	0.958	0.00074	combustion
258	27.61	0.979	0.00153	combustion
259	46.5	1.072	0.00026	combustion
260	125.6	1.161	0.00116	combustion
256	162.6	1.155	0	combustion
255	168.3	1.208	0.00069	combustion
265	812	1.221	0.00090	combustion
262	2.6	0.345	0.00016	slow extraction
263	4.3	0.450	0.00024	slow extraction
264	6.2	0.547	0.00032	slow extraction
272	10.4	0.675	0.000435	slow extraction
274	18	0.854	0.000837	slow extraction
275	24	0.940	0.000237	slow extraction
279	91	1.175	0.00051	slow extraction
277	122	1.158	0.00063	slow extraction
278	146	1.192	0.00032	slow extraction
270	1007	1.200	0.00071	slow extraction
282	2.6	0.349	0.00016	rev. diffusion
280	4.25	0.440	0.00008	rev. diffusion
281	6.15	0.539	0.00008	rev. diffusion
283	10.35	0.659	0.00024	rev. diffusion
306	18.4	0.846	0.00008	rev. diffusion
310	91	1.147	0.00012	rev. diffusion
284	117.5	1.240	0.00016	rev. diffusion
308	122	1.174	0.00061	rev. diffusion
311	146	1.153	0.00016	rev. diffusion
356	1656	1.172	0.00024	rev. diffusion

The results from the three different radio-assay methods are in good agreement and show that no major difference in behaviour is apparent at this temperature. The measured solubilities and diffusion coefficients for water in the two resins are given in these Figures. It is interesting that the most significant differences between the resins appears to be in the water solubility rather than in the diffusion

FIGURE 4-5. DIFFUSION OF WATER AND HCL INTO CRYSTIC 272 AT 25° C.

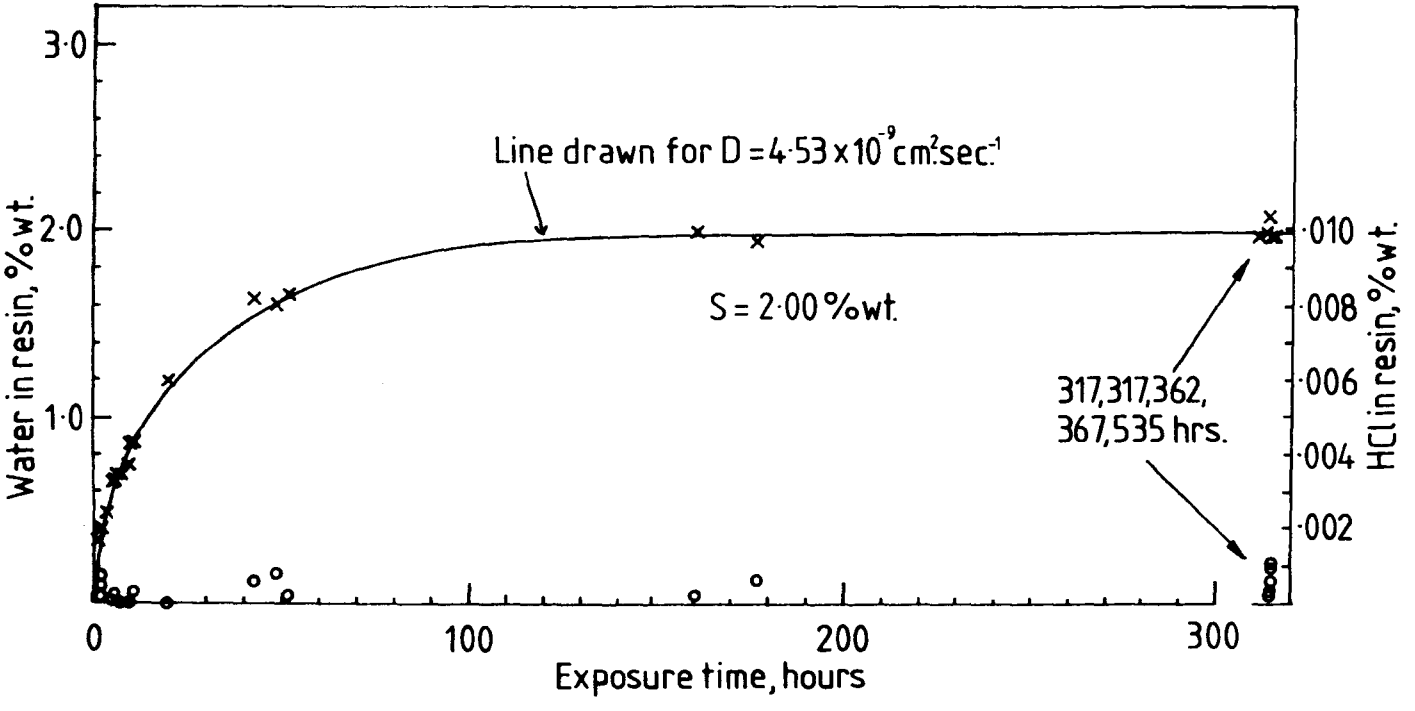

FIGURE 4-6. DIFFUSION OF WATER AND HCL INTO BEETLE 870 AT 25° C.

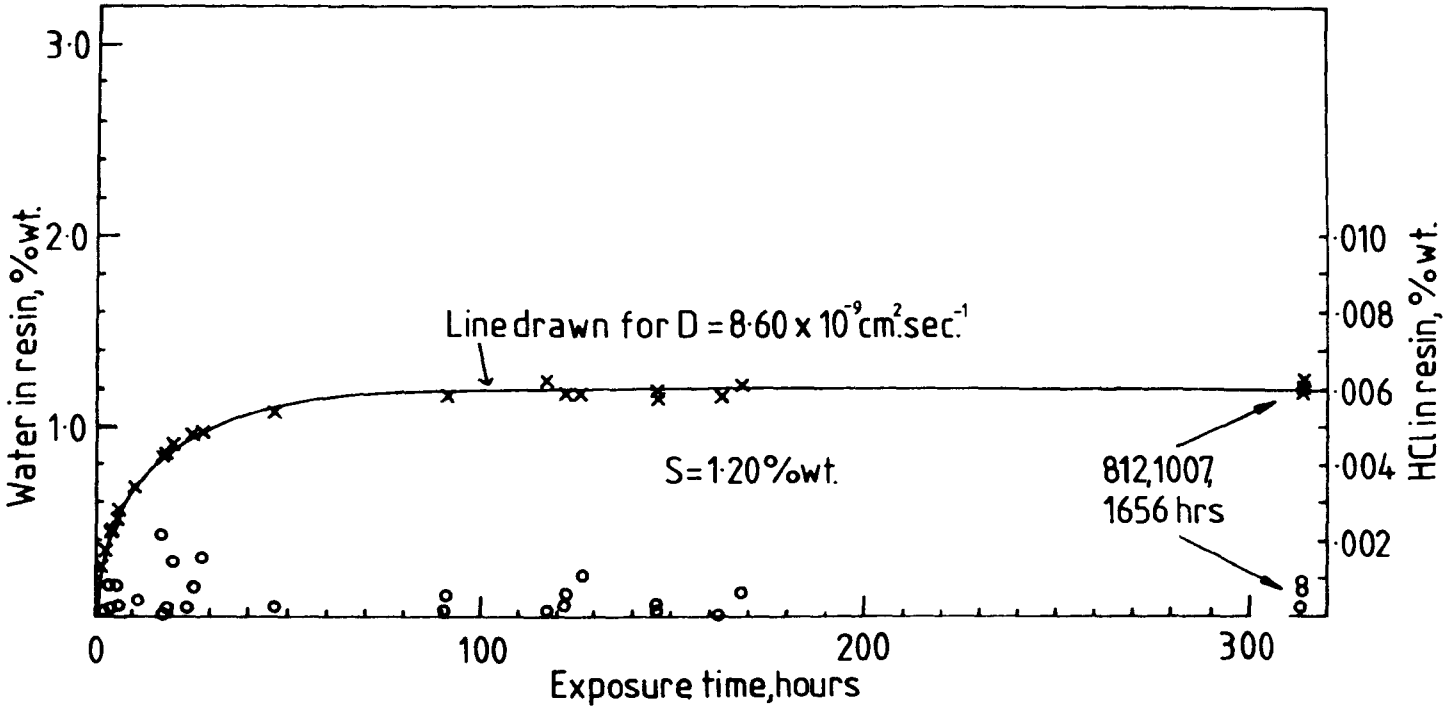

coefficients. The acid still appears to be incapable of diffusing into the polymer.

4-15 Effect of applied stress on polymer solubility and diffusivity.

All the data discussed above was obtained by immersing resin specimens in the liquid diffusant. The specimens were not subjected to an externally applied stress, although there may have been internal stresses in the specimens[103]. These are due to the thermal strains that develop during curing, and the swelling associated with the uptake of the water from the test solutions. In a stress corrosion situation in a composite both internal and externally applied stresses need to be considered. At the tip of a propagating crack, stress intensification results in the development of a complex stress field in the material ahead of the crack[95,104]. Although the majority of the load is carried by the fibres, some is carried by the resin. The stress intensification can generate a high local load in a fibre close to the crack tip[95]. The extent to which the fibres are locally strained also determines the extent to which the adjacent polymer matrix is strained. The existence of a non-uniform stress field at the crack tip and the local strain of the fibres in this region means that the resin barrier at the crack tip may be subject to a significant tensile strain. If this influenced the acid diffusion rate, perhaps by opening up the polymer network, this could be an important factor in the micromechanism of crack propagation*. To assess the size of

---

* It should be noted that in the reinforced composite it is the tensile strain experienced by the polymer, rather than the level of the applied stress, that is most likely to cause the polymer network to become more open. With unreinforced polymer specimens the strain

the effect a method for measuring the effect of stress on acid solubility and diffusivity in the polymer was needed. Various ways of exposing stressed polymer rods to the radioactive diffusant were considered, tried and rejected. It was finally accepted that the practical difficulties involved in providing a low volume, leak-proof enclosure for a weighed 25mm. X 1.2mm.diameter rod that was bearing a tensile load could not be overcome. A major problem was the creep to which these resins were susceptible, which led to serious dimensional changes in the specimens during the relatively long exposures involved in the tests. An alternative approach was eventually adopted in which the stress was applied by bending the specimens. With this arrangement the creep still occurred, but did not lead to the leakage of the diffusant from the system.

4-16 Stress in bent plate specimens.

A specimen subjected to four point bending in the elastic region exhibits a uniform tensile stress between the two inner loading points, given by the formula:

$$\sigma = ED / 2\rho \qquad (4\text{-}4)$$

where: D = sample thickness,

ρ = radius of curvature

E = modulus

ρ = surface stress

It follows that a curved plate, initially without stress, if flattened between e.g. two microscope slides, will develop a tensile stress

---

is directly dependent on the applied stress, and either can be used to quantify the effect.

on its concave surface. This stress will be equivalent to that for an initially flat plate deformed in four point bend, to the same radius of curvature. If, therefore, curved plates of accurately defined curvature and thickness could be made, a stressed flat plate could be made by flattening in a simple rig. With a flat plate an 'O'-ring seal could be used to define a constant area within which the radioactive diffusant could be confined.

4-17 Rotational casting.

Tubes of unreinforced resin can easily be made by centrifuging the liquid during the curing period. A measured amount of catalysed, accelerated resin is introduced into a pipe, which is then spun about its longitudinal axis. The pipe acts as a mould and the resin forms a constant thickness layer on the inside surface of the pipe. When the resin sets, a hollow tube is left and, on release from the mould, can be cut to make the required curved plates. Moulds for making resin tubes were made from lengths of 25mm. and 40mm. diameter aluminum pipe. These pipes were split axially to enable a ground joint to be made between the two halves. After grinding the two halves were clamped together and the outside and inside surfaces were re-machined to restore the circular cross-section of the moulds. A slot was also provided to assist in mould separation and specimen release.

To use the moulds it was neccessary to achieve a high standard of polish on the inside wall. This was then treated with a mould release wax and repolished. To get the moulds to seal the ground joint was coated with silicone rubber sealant. The seal was made by clamping the treated mould together at 50-60°C for 1-2 hours before use. After introducing the measured quantity of resin, the mould ends were sealed

with rubber bungs. The whole assembly was spun in a lathe for four hours and finally the resin was postcured at 80°C for four hours. The method worked well and, by varying the amount of polymer added to the moulds, tubes with wall thicknesses in the range 0.3-2mm. could be produced without difficulty. The curved plates were obtained by cutting the tubes on a mandrel with a jewellers saw, and the cut edges were ground to remove any asperities. The pieces used for the tests were approximately 16mm.wide and 20mm.long.

4-18 Estimation of stress levels in flattened plates.

It was found that the tube sections retained their shape when cut axially, indicating that there were no major residual stresses in the cut plates. A four-point bend attachment was not available for the Instron 1185 test machine, but some tests were made with a three-point bend jig. These were used to see if measured values of flexural strength and modulus line up with the estimates derived from the beam formula given in equation 4-X.

Using specimens cut from cast Crystic 272 sheets, with thicknesses of 2.2mm. and 1.2mm., the standard flexure test method (BS 2782, part 10, Method 1005, 1977) was used to obtain an average value for the flexural failure stress and the flexural modulus. The results based on measurements on four specimens were:

$$\sigma^*_b = 114\text{MPa} \pm 11\text{MPa}$$

$$E_b = 3.58\text{GPa} \pm 0.26\text{Mpa}$$

From the measured deflection at fracture of one of the 2.2mm. plates, it was possible to make a scale sketch of the deformed plate.

From this the radius of curvature could be estimated and from equation 4-4 gave a value of 143MPa.. This compares favourably with the measured value for this specimen of 128MPa.. The beam formula was therefore considered to be an effective measure of the stress applied to the curved plates when they were flattened in the stress rigs.

4-19 Rig for measuring diffusion in stressed plates.

The design of the small stress rigs is shown in Figure 4-7. A number of these rigs were made to enable several tests to be carried out simultaneously.

In use, the curved plate rests on a microscope slide, sited between two Perspex pressure plates. A glass sleeve passes through a central hole in the upper plate and bears on an 'O'-ring, thus forming a small enclosure for the radioactive diffusant. The top Perspex plate serves to compress this 'O'-ring seal by means of the clamping bolts. Assembly was found to be best achieved by initially flattening the curved plate between the lower two pressure plates by hand pressure, since this could be applied fairly uniformly. Great care was needed when tightening up the clamping bolts to avoid specimen fracture. In trying to achieve loads in excess of 0.75 of the fracture strength, uneven loading of the plates led to a failure rate during assembly of about 50%. Assembly was much easier at lower loads.

After assembly, the rigs were easily charged with radioactive diffusant by means of a Pasteur pipette. At the end of each exposure the same pipette was used to remove the excess diffusant. The specimens were recovered by dismantling the rigs, and were cleaned of surface contamination by blotting/rubbing dry the exposed surface with

FIGURE 4-7. RIG FOR EXPOSING STRESSED PLATES TO RADIOACTIVE DIFFUSANT.

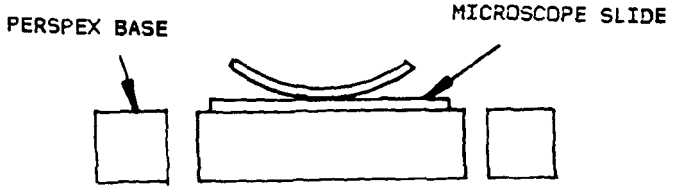

(A) UNSTRESSED CURVED PLATE PRIOR TO ASSEMBLY.

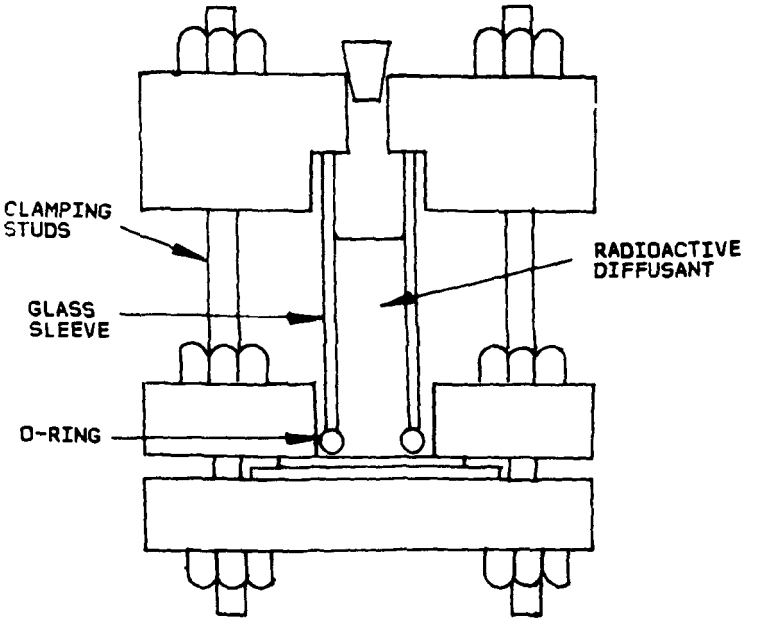

(B) STRESSED PLATE IN ASSEMBLED RIG.

absorbent paper. Counting was carried out by the reverse diffusion method described earlier.

4-20 Effect of stress gradient on solubility and diffusivity.

The method of stressing the specimens described above generates a tensile stress which is at a maximum at the concave surface. This falls progressively as the depth below this surface increases, and reaches zero at the neutral axis of the specimen. At greater depths the stress is compressive, reaching a maximum at the convex surface of the specimen. Quantitative interpretation of the effects of stress on solubility and diffusivity is complicated because of this stress gradient. The current objective, however, was to establish qualitatively whether or not acid solubility and diffusivity were influenced at all by the application of a tensile stress. This was done by making comparative tests, in which the ^{3}H and ^{36}Cl uptake of stressed plates was compared with that found with unstressed plates. To achieve this comparison, curved plate specimens were tested alongside initially flat plates, which are not under stress when installed in the rigs.

The blotting/rubbing method for removing gross contamination of the specimen surface by excess diffusant was checked in a separate experiment. This involved a test in which one of the initially flat plates was exposed to the radioactive diffusant for only a few seconds before the rig was dismantled. It was reasoned that the best chance of observing a stress effect on solubility or diffusivity would be at relatively short exposure times, before creep occurred. It also ensured that the diffusion, if any, would be occurring in that region of the

specimen where the tensile load was highest i.e. near to the concave surface.

4-21 Results for Crystic 272 resin.

In this part of the work attention was concentrated on the Crystic 272 resin. If an applied stress did not open up this resin for diffusion, it was considered unlikely that an effect would be seen with other polyester systems.

In the first experiment with Crystic 272 a curved plate, cut from a 25mm. diameter tube was used. The wall thickness was 0.40mm. The ^{3}H and ^{36}Cl uptakes of this plate was compared with that from two flat plates with thicknesses of 1.2mm.. The surface stress on the curved surface was calculated from the beam formula given earlier.

In presenting the results of this experiment in Table 4-6 below, the actual ^{3}H and ^{36}Cl counts, corrected for the background counting rate, are given, together with other relevant information.

To put these results into perspective, the counter background was 25 ^{3}H counts min^{-1}. and 43 ^{36}Cl counts min^{-1}.. The $^{3}H/^{36}Cl$ ratio in the original diffusant was 32000/7000. The expected ^{36}Cl counting rate in the stressed plate, if the molar acid diffused unchanged, would be 2960 counts min^{-1}.. The results in Table 4-6 do not reveal a large effect on acid uptake as a result of applying the stress. There is a small increase in the amount of ^{36}Cl pickup for the stressed surface, but this could easily be as a consequence of surface cracking.

TABLE 4-6 COMPARISON OF ^{36}CL AND ^{3}H UPTAKE BY STRESSED AND UNSTRESSED CRYSTIC 272 PLATES.SLOW EXTRACTION MEASUREMENTS AFTER 212HR. EXPOSURE TO THE RADIOACTIVE DIFFUSANT.

Specimen	Radius of curvature and thickness		Net counting rate, cpm		Surface stress % of max.
	r,mm.	t,mm.	^{3}H	^{36}Cl	
SR1	flat	1.24	19975	23	0
SR2	12.5	0.40	13534	81	50
SR3	flat	1.28	1485	9	0

In a similar experiment, two more specimens were cut from a slightly thicker tube of Crystic 272. These gave an increased surface stress when the plates were flattened. The water and acid uptakes of these plates were again compared with those from unstressed plates. In these experiments the exposure time was shortened, to maximise any tensile stress effects, and the measurements were made by the reverse diffusion method. The results are given in Table 4-7.

TABLE 4-7 COMPARISON OF ^{36}CL AND ^{3}H UPTAKE BY STRESSED AND UNSTRESSED CRYSTIC 272 PLATES.RESULTS FOR 169 HOUR EXPOSURE.

Specimen	Radius of curvature and thickness		Assay method	Net counting rate, cpm		Surface stress % of max.
	r,mm.	t,mm.		^{3}H	^{36}Cl	
SR8	flat	1.84	rev diff	15979	154	0
SR10	12.5	0.52	rev diff	7640	42	65
SR11	12.5	0.48	rev diff	5625	65	60

Again, the results for the ^{36}Cl uptake are very low in relation to the level expected for the diffusion of the molar acid. Unchanged diffusion of the acid would have given 1671 counts min^{-1}. for SR10 and 1230 counts min^{-1}. for SR11. The flat plate, SR8, gave the highest ^{36}Cl count rate in this group of specimens. The rate corresponding to the uptake if molar acid by this specimen is 3500 ^{36}Cl counts min^{-1}.. It was noticed that the exposed surface of SR8 had been scratched during sample preparation. The increased pickup by the scratched surface emphasises the importance of surface condition in these measurements.

As in the previous test, a general observation was that the stress initially applied to the specimens decayed during the test as a consequence of creep. Significant yielding was evident in the exposed specimens. It was estimated that the stress was reduced by a factor of about 2 after an exposure of 200 hours.

4-22 Results from Crystic 272 at higher stress levels.

The results given above all involved specimens prepared in the 25mm. diameter mould, with wall thicknesses in the region of 0.5mm.. These were compared with flat plates of somewhat greater thickness. Ideally, the flat and curved plates should be of the same thickness for good comparative measurements. In order to obtain thicker,curved specimens, use was made of a 40mm. diameter mould. Crystic 272 tubes with a wall thickness of 1mm. were prepared, and a group of six specimens were cut from these. After grinding the edges carefully with dry emery paper to remove asperities, they were dried in a silica-gel desiccator for a few days before use. Flat, 1mm.thick, specimens were prepared in a similar way. The curvature of the specimens for the stress tests

gave a surface stress, on flattening, of 80% of the flexural strength. The ability to successfully flatten these specimens in the stress rigs was critically dependent on their surface condition. In fact, three of the six specimens fractured during assembly. The remaining three specimens, together with three flat, 1mm. plates, were exposed to the radioactive molar HCl for two weeks, prior to assay. Measurements were made by both the slow extraction and reverse diffusion methods. The results obtained are given in Table 4-8.

TABLE 4-8 ^{36}CL AND ^{3}H UPTAKE BY STRESSED AND UNSTRESSED CRYSTIC 272 PLATES OF THE SAME THICKNESS.RESULTS FOR 336 HOUR EXPOSURE.

Specimen	Radius of curvature and thickness		Assay method	Net counting rate, cpm		Surface stress % of max.
	r,mm.	t,mm.		^{3}H	^{36}Cl	
SR12	20	1	slow ex	13305	40	78.5
SR13	20	1	rev diff	13470	25	78.5
SR14	20	1	rev diff	13079	0	78.5
SR15	flat	1	slow ex	15709	60	0
SR16	flat	1	rev diff	12557	0	0
SR17	flat	1	rev diff	16695	357	0

Specimen SR17 had been deliberately scratched on the exposed surface. The adverse effect of this treatment can clearly be seen in the results. As in the earlier experiments, substantial creep was observed with the curved specimens, when they were removed for counting at the end of the exposure. At this longer exposure time the extent of yielding was considerable.

It is clear from the results obtained that the application of a tensile surface stress in the range of 50%-80% of the fracture stress does not substantially enhance the ability of HCl to penetrate the polymer network for Crystic 272 resin. Neither the stress, nor the

yielding associated with the creep that occurs with these specimens, appears to alter the very low or zero solubility of the acid in the resin. Again, water was seen to diffuse freely into the polymer. Comparing the water uptake for stressed against unstressed plates does not indicate that stress has a large effect on solubility. This is in accord with the work of Marom et al[88]. They have correlated the small increase in water solubility, observed with stressed resins, with an increase in the free volume of the polymer. This free volume increase is a direct consequence of polymer strain. Their measurements showed that the increase in water solubility, even at high stress levels, is only of the order of 2% of the total amount of water present. In the present case this amounts to an increase from 2% water to 2.02% water. This is considered to be far too small an opening effect to significantly affect acid diffusion.

It was not considered necessary to make detailed measurements on all the other resins for which solubility data had been obtained from unstressed specimens. Crystic 272 is a relatively brittle resin. The most extreme flexibilised resin included in the present project is the 1080 material. To complete this phase of the work some further tests were made on stressed plates of this resin, as described below.

4-23 Tests on stressed specimens of Crystic 272 + 20% NV 1080 (resin 1080) at an exposure time of 168 hours.

Rotational casting was again used to prepare tubes of resin 1080 with two different wall thicknesses. Flat plates of this resin were also made by casting between polished glass plates. Specimens suitable for use in the stress rigs were cut from both the tubes and the flat plates. The tests were carried out by the same method as that used

in the Crystic 272 tests. Because of the stress gradient in the stressed plates the results are again qualitative in nature rather than quantitative. The experiment was designed to show whether or not a stressed surface of the material shows an increase in the uptake of the acid, compared with an unstressed surface. For this reason the results are again presented directly as ^{3}H and ^{36}Cl counting rates. This facilitates the comparison of the results from the stressed and unstressed plates. The results are listed in Table 4-9, and include data from curved plates at two different thicknesses. It can be seen that the stress has not significantly changed the uptake of the acid by this resin. The ^{36}Cl counts are again very low in relation to the ^{3}H counts.

These results agree with the results obtained with Crystic 272 resin, in that they do not indicate that an applied stress is capable of altering the inability of bulk polyester specimens to take up hydrochloric acid from aqueous solution. In the 1080 resin experiments, the thicker plates, when flattened in the stress rigs, were clearly close to their fracture stress, as evidenced by the high failure rate of the specimens during assembly in the rigs. Once again it was noted that after exposure to the diffusant under stress for a period of one week, severe creep of the curved plates was apparent. With this resin the effect seemed to be even more severe than with Crystic 272.

4-24 Final comments on results of radioactive tracer measurements.

The results of the work described in this Chapter show that the solubility and diffusivity of HCl in polyester resins, as measured by

TABLE 4-9 ^{36}CL AND ^{3}H UPTAKE BY STRESSED AND UNSTRESSED RESIN 1040 PLATES. REVERSE DIFFUSION RESULTS FOR 168HR. EXPOSURE TO MOLAR HCL.

Specimen	Radius of curvature and thickness		Net counting rate, cpm		Predicted ^{36}Cl counting rate for MHCl diffusion
	r,mm.	t,mm.	^{3}H	^{36}Cl	
SR18	flat	1.40	18370	33	1934
SR19	flat	1.40	7948	30	1837
SR20	12.5	1.00	10171	119	2350
SR21	12.5	1.00	9600	44	2218
SR22	12.5	1.00	8796	24	2032
SR23	12.5	1.00	10338	18	2349
SR24	flat	1.6	9135	19	2085
SR25	flat	1.6	7904	16	1804
SR26	12.5	1.6	11328	47	2586
SR27	12.5	1.6	10784	24	2473
SR28	12.5	1.6	10037	50	2291
SR29	12.5	1.6	9502	66	2169

^{36}Cl uptake, is certainly very low and is possibly zero. The extent of acid penetration detected in the resins is substantially lower than that needed to establish the aqueous acid concentrations that are necessary to weaken E-glass in a composite subjected to a low stress. Matrix cracking is considered to be a more likely source of aqueous acid penetration to the fibres during stress corrosion crack propagation.

CHAPTER 5. DISCUSSION AND CONCLUSIONS.

In the experimental work the combined effects of applied stress and acid concentration on fibre weakening have been measured. A mechanism for the weakening of the glass has been advanced which accounts qualitatively for the synergistic effect of stress and acid concentration. Measurements have been made of the solubility and diffusivity of aqueous hydrochloric acid in a range of polyester resins. The very low levels of acid uptake detected suggest that acid diffusion through the resin is not sufficient to sustain the propagation of stress-corrosion cracks in a composite. To interpret more fully the data from the experimental work, a critical examination of the significance and implications of these results is needed. This is presented below.

5-1 Acid and moisture diffusion through polyester resins.

All the experimental work described in Chapters 2-4 features aqueous hydrochloric acid as the aggressive agent. In stress-corrosion experiments with this substance, diffusion through the resin is often quoted as the way in which the acid reaches the fibres[1,50,84,11,72]. This affords a very plausible explanation for stress-corrosion crack initiation and propagation in regimes of low applied stress. Here, the corrosion proceeds very slowly and it is considered that the applied stress is too low to promote matrix cracking. McCartney[85] has shown that, for a given composite system, there is a minimum applied stress below which matrix cracks will not propagate.

The results in Chapter 4, however, are not consistent with the contention that acid can diffuse through the resin to a significant

extent. The material does appear to be taken up by surface imperfections in the resin, and it was not found possible to prepare specimens without these imperfections. However, the characteristic features of a diffusion process are the gradual build-up of the diffusant in the specimen, culminating in the attainment of a saturation level, representing the solubility of the diffusant in the resin. These features are clearly evident in the results obtained for water diffusion in polyester resins, as exemplified by the data in Figure 4-5. The hydrochloric acid results, in contrast, are not indicative of diffusion. As noted above, there is some uptake of the acid, but this is not in the systematic way required for diffusion. In comparing the data for water with that for the acid the most striking contrast is in the effect of specimen thickness and exposure time, as shown in table 4-1. The samples monitored for water uptake all saturated within the exposure period and gave constant values for the water solubility, irrespective of specimen thickness. The acid uptake was much more erratic and was independent of the sample thickness and the exposure time. The weight of evidence points to occlusion of the acid in the specimen surface as the reason for the measured uptake. The specimen surface inevitably contains microcracks or other imperfections, since it is a brittle material which shrinks after curing, postcuring and cooling. It has also required mechanical release from the glass mould in which it was cast. Further indications of the importance of surface condition in causing this type of uptake are revealed by the increases in acid uptake evident with specimens with large cut edges, or ones that have been scratched.

The surface uptake of the diffusant has restricted the absolute sensitivity of the radioactive tracer method used to measure hydrochloric acid solubility. In all of the diffusion experiments the

acid diffusant was molar hydrochloric acid. It was assumed that the water in this solution entered the polymer network at the molecular level, and permeated through the network by random molecular movement. This accounts for the good conformity with Fick's law (see Figure4-5) and for the known equivalence of moisture uptake from the liquid and vapour phases[77,80]. Diffusion of the hydrochloric acid through the resin would not necessarily be expected to occur at the same rate as water. At saturation, it was also possible that the aqueous fluid in the resin could hold substantially less hydrochloric acid in solution than the original molar diffusant. The radioactive tracer experiments were therefore designed to identify the maximum amount of the acid, in the fluid diffusing through the resin, that could be achieved by molecular diffusion.

The absolute sensivity of the measurements depends on the specific activity of the tagged diffusant, the background counting rate and the stability of the liquid scintillation counter. Taking these factors into account it was estimated that the technique would be capable of detecting the acid at a concentration of 0.001M in the aqueous fluid diffusing through the resin. The surface uptake referred to above, in effect increases the apparent background counting rate, thereby reducing the certainty with which diffusive take-up of the acid can be identified. Because of this it is considered that the method would not detect the acid diffusing to give a concentration of less than 0.005M in the water saturated resin.

In contrast to the dilution associated with acid diffusion, transport of the acid to the fibres by flow through matrix cracks would enable the acid to reach the fibres without change of concentration. The data in Figures 2-7 and 2-8 suggest that this would always be the

dominant cause of fibre weakening at loads high enough to cause matrix cracking. At very high loads, where extensive precracking of the resin occurs through the composite thickness, the resin offers no protection at all to the fibres, and they fracture within the same time as a bare tow of fibres[56]. At more modest loads the matrix cracking proceeds in a progressive manner, opening up the resin only in the vicinity of the crack tip[1]. It follows from this that diffusive transport of the acid to the fibre surface can only be a rate-determining factor in a composite subjected to a low applied stress, below that at which matrix cracking can occur as a consequence of the applied stress. However, the data in Figure 2-8 show that an acid concentration of 0.005M would require a stress equivalent to about 50%-70% of the fracture load of the dry fibres to bring the time to failure within the 10-2000 minute timescale involved in slow crack propagation. This is clearly outside the regime of low stress within which diffusion would be expected to be rate-determining.

This argument assumes, of course, that the small measured uptake of ^{36}Cl detected in the diffusion experiments was due to the occlusion or absorption of diffusant by the specimen surface. An alternative, less likely, explanation is that the diffusion of the acid into the resin is an extremely slow process and that, given sufficient time, the acid concentration would increase and eventually saturate. It is important to evaluate this possibility because the distance between the fibres is extremely small. Diffusive transport might be significant at such small distances, even if the diffusion coefficient is very low. By making some assumptions it is possible to estimate a hypothetical diffusion coefficient for the acid diffusion and to use this to see if diffusion is a feasible mechanism for fibre weakening. Taking the data for Crystic 272 as an example, the uptake at an expo-

sure time of 500 hours in a rod with a radius of 0.062cm. was 0.00075%wt. HCl. At this exposure time the rod was saturated with water at 1.90%wt.. It is evident from Figure 2-8 that the minimum concentration of acid that would be capable of weakening E-glass fibres in a low stress regime would certainly be greater than 0.1M. Suppose that the rod would eventually saturate to give an acid concentration of 0.1M in the aqueous fluid in the resin. Then, in equation (A9)

$$M_{\infty} = 0.1$$

$$M_{500hr.} = (.00075x1000)/(1.9x36.5) = 0.0108M$$

$$M_{500hr.}/M_{\infty} = 0.01081/0.1 = 0.1081$$

From the data in the Appendix this gives $Y = 1.60026x10^{-3}$

from which $D = (1.60026x10^{-3} \times .062 \times 062)/(500 \times 3600)\ cm^2sec^{-1}$

$$= 3.42 \times 10^{-12} cm^2 sec^{-1}$$

This estimate of D is critically dependent on the assumed saturation solubility of the acid in the resin. Table 5-1 below shows values for D corresponding to higher solubilities.

TABLE 5-1 HYPOTHETICAL ACID DIFFUSION COEFFICIENTS FOR CRYSTIC 272 AT 25°C.

Assumed saturation solubility M	Diffusion coefficient cm^2sec^{-1}
0.05	4×10^{-10}
0.10	3×10^{-12}
0.25	3×10^{-13}
0.40	3×10^{-14}
1.00	$<10^{-15}$

These data will be used later in this discussion in relation to the evaluation of the respective merits of the matrix cracking and diffusion mechanisms.

5-2 Veracity of radioactive tracer method for measuring hydrochloric acid diffusion.

It was pointed out in Chapter 4 that tritium could not be used to follow hydrogen ion diffusion in aqueous solutions. This is because of the very rapid dynamic exchange between hydrogen atoms "belonging" to the acid and the water. The preponderance of water in dilute acid solutions means that the traced species would always be the water rather than the acid. Hydrochloric acid has an extremely high affinity for water, in which it is very soluble. In the dilute solutions considered in this work, the acid is ionised and exists as chloride ions and solvated hydrogen ions, i.e.hydroxonium ions H_3O^+. Tagging the acid with ^{36}Cl provides unambiguous evidence of the diffusion of chloride ions. In equating this to hydrochloric acid diffusion it is assumed that equal numbers of hydroxonium and chloride ions must be present in all parts of the system, to preserve electrical neutrality. This is a generally accepted principle, because of the separation of electrical charges that would be associated with unequal ionic diffusion. This would require the input of energy and would not, therefore, be a spontaneous process. Doremus[27], for example , invoked this principle in discussing the diffusion of sodium ions in soda-lime glasses. He noted that the diffusion of sodium ions out of the glass without an associated anion diffusion would set up an electric field opposing the diffusion. Because of this it is considered that the ^{36}Cl tracer provides a valid measure of HCl diffusion in the resin. It is considered very unlikely that the separate diffusion of hydroxonium ions through the resin would occur without the provision of a driving force. Further support for this view follows from a consideration of the mechanism by which the aqueous acid could diffuse through the resin.

If, as is conjectured, water diffuses freely through the resin, whilst the acid does not, there must be a reason for this difference in behaviour. An important feature of the acid is its totally ionic character in aqueous solution. Because the resin is a non-ionising environment, the chloride and hydroxonium ions have a much higher affinity for water than for the resin, and would not be expected to enter the dry resin. Water, on the other hand, is predominantly covalent in character, and is readily able to enter and move through the holes and spaces in the resin network as uncharged molecules. This is clearly what happens when moisture diffuses into the resin from the vapour phase. The implication of this model is that the ionised acid could only enter the polymer after sufficient water had been taken up to establish a continuous liquid network, in which the acid could dissolve. In a sense this is a limiting case of matrix cracking, with very fine interconnected ligaments of liquid extending through the resin. On this hypothesis acid diffusion could not therefore arise if the water diffusion involved the random movement of individual covalent water molecules in a general way through the resin network. If the water molecules did not coalesce to form a continuous phase, the movement of the ions would be prevented. This mechanism accounts for the observed lack of acid diffusion in the polymers. It would also involve the movement of equal numbers of hydroxonium and chloride ions through the water ligaments, thereby justifying the use of ^{36}Cl to trace hydrochloric acid diffusion.

The argument just presented is based on the suggestion that the essentially ionic nature of the acid in aqueous solution inhibits entry into the resin structure unless a suitable aqueous pathway has been created. Another factor that might influence acid diffusion is the size of the diffusing species. The chloride ion is relatively large,

and its inability to enter the resin may be due to this factor alone. This would apply to random entry into the network and to transport through fine liquid ligaments. In Figure 5-1 below the sizes and shapes of some of the molecules and ions of interest are compared. It can be seen that although the chloride ion is the largest one listed, size differences are not necessarily sufficient to account for the inability of this ion to diffuse into the resin.

5-3 Osmosis effects.

The diffusion of water through the resin is very likely to lead to the formation of tiny pockets of liquid at voids in the structure. For example, at places where solid particles of soluble impurities have become embedded in the resin, these can dissolve to form local solution pockets. If these solutions are ionic in character, the ions will not tend to enter the resin, which can then act as a semi-permeable membrane. Ashbee[83] has shown how this results in the osmotic flow of pure water from the resin into the solution. This flow will continue until the pressure developed inside the solution pocket reaches the osmotic pressure of the solution. The resin in the vicinity of such a pocket will be saturated with water. This reduces the modulus and tensile strength of the material[9,81]. Because of this the osmotic pressure is capable of causing matrix cracking in the vicinity of the pocket.

In the classical studies of osmosis the phenomenon is generally associated with solutions containing dissolved material of high molecular weight. If the size of the solute molecule is much greater than that of water, it is easy to see how a material like a resin can be selective in allowing water permeation, but not solute permeation. In the present study the evidence suggests that it may be the ionic

FIGURE 5-1. COMPARISON OF MOLECULAR AND IONIC SIZES.

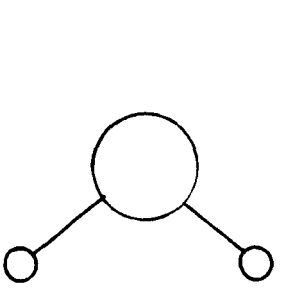

WATER MOLECULE

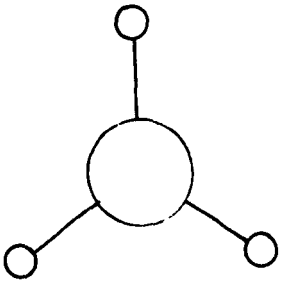

HYDROXONIUM ION

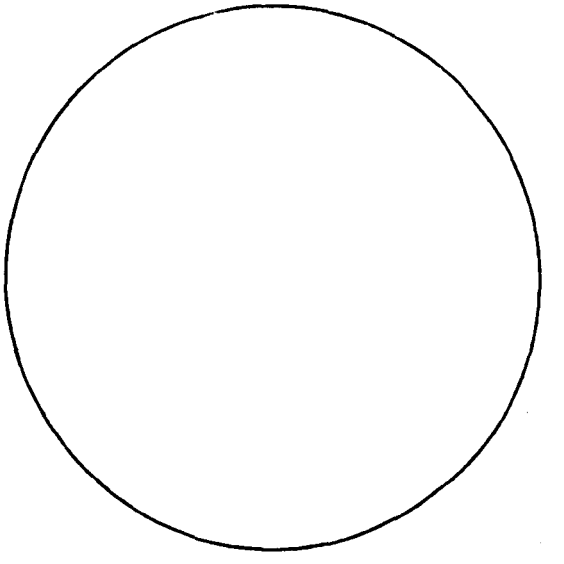

CHLORIDE ION

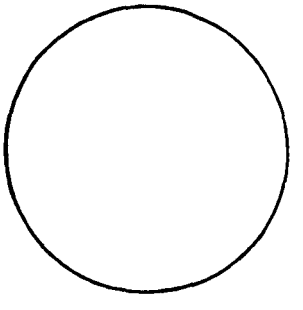

CALCIUM ION

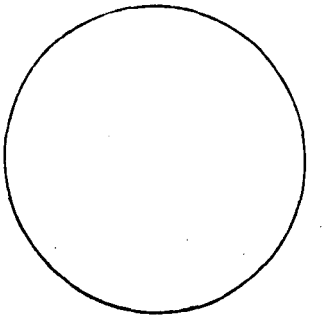

SODIUM ION

character of the inorganic solutes, rather than their size, that would prevent their entry into the resin. The osmotic effect, however, is exactly the same, irrespective of the reason for the impermeability. Ghotra and Pritchard[81] have discussed conventional osmotic pressure development in resins containing water accumulated in resin voids. The leaching of soluble organic material from the resin can lead to the accumulation of large-molecule solutes in the water-filled voids. The resultant semi-permeability is a direct result of the size difference between the water and the leached material.

5-4 Matrix cracking and acid diffusion mechanisms.

The model of slow crack growth in a composite that fits the results of the present work is one in which individual fibres break sequentially as the crack front moves forward. Prior to fibre fracture there is the rate-determining incubation period, the length of which is determined by the acid strength at the freshly exposed fibre surface. The incubation time also depends on the intensity of the local load on the fibre. Clearly, the mode of acid transport across the resin webs separating the fibres has a vital role in influencing the incubation period. Matrix cracking is likely to give instant access of the undiluted acid to the fibres. In the absence of matrix cracking slow diffusion could delay this access to an extent that could dominate the rate of fibre weakening.

An essential difference between the two modes depends on the position at which the crack arrests after each fracture event in the sequence[1]. Matrix cracking features crack arrest at a fibre surface, wheras the diffusion model involves arrest at a matrix surface. This is shown in the diagrams in Figure 5-2 below. It should be noted that

FIGURE 5-2. ALTERNATIVE CRACK PROPAGATION MODELS.

(A) DIFFUSION MODEL.

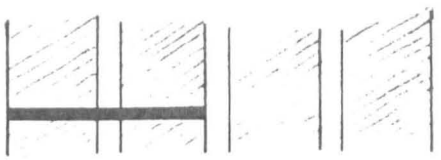

1. CRACK ARRESTED AT MATRIX SURFACE

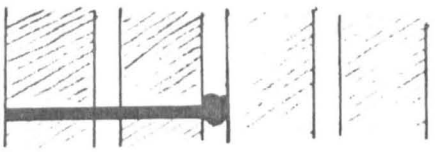

2. ACID DIFFUSES TO FIBRE OPPOSITE CRACK TIP AND WEAKENS IT.

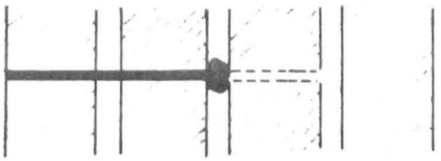

3. WEAKENED FIBRE BREAKS.

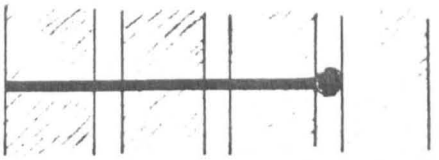

4. MATRIX BEHIND BROKEN FIBRE BREAKS, FORMING CONTINUOUS CRACK. CRACK TIP FILLS WITH ACID. FURTHER DIFFUSION TO NEXT FIBRE IS INITIATED.

(B) MATRIX CRACKING MODEL.

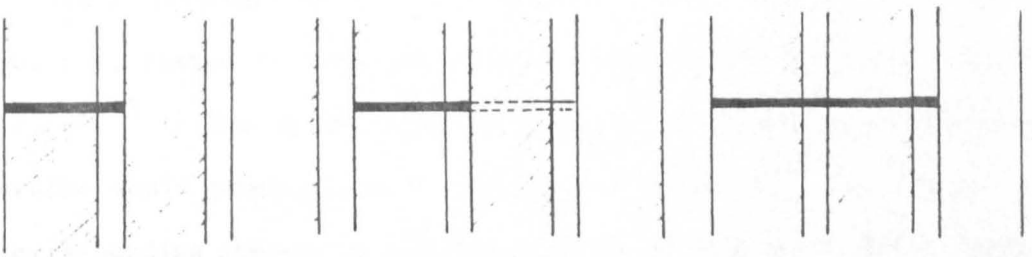

1. CRACK ARRESTED AT FIBRE SURFACE. ACID IN CRACK TIP WEAKENS FIBRE.

2. FIBRE BREAKS AND RELAXES, TRANSFERRING LOAD TO RESIN, WHICH ALSO FRACTURES.

3. NEW CRACK TIP FILLS WITH ACID AND FIBRE WEAKENING PROCESS IS AGAIN INITIATED.

the diffusion mechanism involves fibre fracture ahead of an unbroken matrix, which only breaks after the fibre has fractured and released its load. In both mechanisms the propagation of the crack is delayed by the fibres, which carry the majority of the load, and which must be weakened by the acid before they will break. The discontinuous,stop-start nature of the propagation process has been detected by acoustic emission measurements[2].

5-5 Calculation of incubation periods from measured crack propagation data.

Examination of Figure 5-2 shows that in each fracture event the crack advances by a length equal to the distance separating the fibres, plus the fibre diameter. The time required for this advance is the time required for the acid to reach the fibre, plus the time required for acid of that concentration to weaken the fibre.

Crack propagation data for unidirectional E-glass polyester composites, tested at constant stress intensity, have been obtained by Price[3,15]. For a mean volume fraction of 0.55, it was found that cracks would propagate at rates in the range 10^{-6}-10^{-10}m.sec^{-1}, at corresponding stress intensities of 2.3 - 12.6MPa.m$^{-\frac{1}{2}}$. For a composite with a volume fraction V_f, the distance, S, between fibres of radius r can be calculated from the equations quoted by Hull[95]:

Hexagonal array: $S = 2((\pi/2\sqrt{3}V_f)^{\frac{1}{2}} - 1)r$

Square array: $S = 2((\pi/4V_f)^{\frac{1}{2}} - 1)r$

Substituting the value for the volume fraction (0.55) and the mean fibre radius(8.5×10^{-6}m.) in the above equations gives the mean distance between the fibres as 4×10^{-6}m.. The advance of the crack as-

sociated with each fracture event is thus 21 x 10^{-6}m.. Looking at the extremes of the measured crack propagation rates, this distance can be used to estimate the time delay between successive fracture events:
At 10^{-10}m.sec^{-1}. each fracture event requires 21 x 10^{4}sec. i.e. 3500 mins.
At 10^{-6}m.sec^{-1} each fracture event requires 21sec. These delays represent the time required for the acid to reach the fibres, plus the fibre incubation period.

It should be noted that for the diffusion mechanism these timescales relate to diffusion across a 4x10^{-6}m. polymer web, although the subsequent fracture will extend the crack in the composite by 21x10^{-6}m..

5-6 Diffusion mechanism: estimation of acid concentration needed for fibre weakening at low stress.

At the higher stress intensity the very short incubation period precludes acid diffusion as a viable acid transport mechanism. This is in accord with the generally accepted view that diffusion is more likely to be involved in the failure mechanism at low stress levels. By making certain assumptions it is possible to estimate the acid concentration at the fibre surface that would give the measured incubation period at the lower stress level. It is important to recognise that the diffusion mechanism involves the slow build-up of the acid concentration at the fibre surface. The time interval between fracture events therefore represents the time taken for the acid to achieve a given concentration at the fibre surface, plus the time needed for acid of that concentration to weaken the fibres. For the purpose of the present calculation the weakening period was arbitrarily taken as half of the incubation period i.e. 1750 minutes.

To relate this weakening time to an acid concentration by means of the data in Figure 2-7 it is necessary to know the stress at the fibre surface. For the diffusion model, as shown in Figure 5-1(a), this is separated from the crack tip by a resin bridge 4×10^{-6}m. wide. Despite the availability of the crack tip stress intensity the stress at the surface of a fibre immediately ahead of the crack tip is difficult to estimate. This is because of the highly anisotropic nature of the composite, since simple fracture mechanics formulae are strictly only applicable to isotropic materials. However approximate estimates can be made by assigning "average" properties to the composite, thus making it quasi-isotropic. For such a material the stress ahead of the crack tip is highly non-uniform in the near field region. At a distance r ahead of a planar edge crack in a semi-infinite plate the stress is given by the equation[96,97]:

$$\sigma = K_I(2\pi r)^{\frac{1}{2}} \qquad (5\text{-}2)$$

For very small values of r, the maximum stress developed is taken as the yield stress of the material, and a yield zone exists within which the stress is constant. The size of this zone is given by the equation[96]:

$$r = K_I^2/2\pi\sigma_y^2 \qquad (5\text{-}3)$$

where σ_y is the effective yield stress. The effective yield stress of the resin will be much higher than that of the unreinforced resin, because of the restraining effect of the fibres. The intensified load ahead of this yield zone operates over a very short gauge length of the next fibre. Metcalfe and Schmitz[17] have shown that at short gauge lengths the tensile strength of the fibres, σ^*, is significantly increased. This is because of the lower probability of finding a severe flaw in these short lengths. A value of 3.5GPa., representing the upper bound of industrial E-glass tensile strength, was therefore assigned to σ^*. E-glass does not yield before fracture and the fibres

will constrain the matrix from yielding. If a value of 3.0GPa is assigned as the yield stress of the quasi-isotropic matrix, the size of the yield zone ahead of the crack tip is given by equation 5-3. For a crack tip stress intensity of $2.3MPa.m^{-\frac{1}{2}}$ the value of r is found to be $0.09 \times 10^{-6}m$.. This is well within the $4 \times 10^{-6}m$. distance separating the fibres. It is therefore considered justifiable to use equation 5-2 for predicting the stress at the fibre surface located $4 \times 10^{-6}m$. from the crack tip. For $K_I = 2.3MPa.m^{-\frac{1}{2}}$, the surface tensile stress at a fibre $4 \times 10^{-6}m$. from the crack tip is found to be 460MPa. Hence $\sigma/\sigma_* = 0.13$

Expressing the fibre surface stress in this non-dimensional form enables it to be used for interpolation in Figure 2-8 to find the acid concentration that must be attained to weaken the fibres in the available time. The interpolation gives a value of 0.6M for the critical acid strength for a fibre weakening period of 1750 hours. This is about the concentration of the aqueous hydrochloric acid used by Price in his experiments. The result implies an acid solubility in the resin that is essentially equivalent to the diffusion of the undiluted material. The relevant diffusion coefficient, calculated by the method given in the Appendix, is $8 \times 10^{-11}cm^2.sec^{-1}$.. This is several orders of magnitude higher than the maximum feasible coefficient associated with this solubility, as quoted in Table 5-1.

On this evidence, hydrochloric acid diffusion through the resin, as measured by ^{36}Cl uptake, cannot account for the time-dependent fibre weakening that determines the rate of crack propagation in an E-glass composite.

5-7 Matrix cracking mechanism: correlation of measured crack propagation rates with fibre incubation periods.

The simplest model for the matrix cracking mechanism involves the immediate formation of matrix cracks following the fracture of a fibre at the crack front. If these cracks extend to the next unbroken fibre, undiluted acid can flow to this fibre surface, to initiate the weakening process. If the stress at this fibre surface is known, the length of the incubation period can be obtained by interpolation in Figure 2-8. The fibre breaks at the end of this period, and the crack extends. Stress-corrosion cracking in E-glass composites results from the sequential fracture of fibres in this way. The rate of crack propagation is determined only by the length of the incubation period and by the distance traversed by the crack following each fracture event. Figure 5-1(b) depicts this mechanism, with the crack arresting at a broken fibre, ahead of which microcracks or crazes extend to the next fibre in the system. The prediction of the stress at the surface of this fibre is again difficult, since there is a singularity at the tip of a sharp matrix crack. The stress must clearly be lower than the fracture stress of the fibre, because the crack has arrested. The following strategy was therefore adopted to compare the measured incubation periods in Figure 2-8 with the measured crack propagation rates. At the lower stress intensity level an effective stress, σ_s, is defined as that which gives the correct incubation period for crack propagation at 10^{-10} m.sec^{-1}. The same crack geometry is deemed to apply at the higher stress intensity, such that the effective stress is increased by the ratio 12.6/2.3. This is then compared with that calculated from the measured crack propagation rate. The calculation is as follows:

For K_I = 2.3MPa.$m^{-\frac{1}{2}}$., the crack propagation rate is 10^{-10} m.sec^{-1}. The crack front advances 21 x 10^{-6}m. for each fracture event. the fibre incubation period is therefore: 21 x $10^{-6}/10^{-10}$ = 21 x 10^{4}sec i.e.3500 minutes.

For 0.6M HCl figure 2-7 shows that this corresponds to an effective fibre stress of σ/σ^{*} = 0.125

The effective fibre stress at a stress intensity of 12.6MPa.$m^{-\frac{1}{2}}$.would be 0.125 x 12.6/2.3 =0.684.

For 0.6M HCl this gives an incubation period of less than one minute. The period predicted by the crack propagation rate of 10^{-6}m.sec^{-1} is 21 x $10^{-6}/10^{-6}$ = 21seconds.

It can be seen from this that these data are in excellent agreement. They show how the direct access of the undiluted acid through matrix cracks can account for observed crack propagation rates spanning four time decades.

5-8 Matrix cracking by the direct application of a load.

It has been shown that the diffusion of hydrochloric acid into the resin does not occur to the extent necessary to weaken the fibres. The calculations just presented provide further confirmation that matrix cracking is the route by which the acid reaches the fibres during the stress-corrosion process. There are a number of different ways in which these matrix cracks can be generated in a composite material. The most obvious of these is by the direct action of an applied load. The whole principle of fibre reinforcement is that the fibres, being stronger and stiffer than the polymer matrix, carry the majority of the load. In a uniaxially reinforced composite with a uniform, gradually increasing load applied in the direction of the fibres, matrix

cracking is preceded by fibre breakage and debonding. The debonding is particularly prevalent at the broken fibre ends. This process only occurs at relatively high loads, e.g. 80% of the fracture load. It is characterised by audible evidence of cracking and by the development of a fine network of cracks and crazes. These produce the characteristic whitening of the transluscent composite that occurs prior to tensile failure. This is typical of the type of specimen damage that occurs in a slow strain rate tensile test.

The situation at the tip of a growing stress-corrosion crack differs greatly from this. Firstly, the non-uniform stress field ahead of the crack is highly localised. The fibre-matrix interface immediately ahead of the crack has a vital role in defining the capacity of the material to bear the load. The extension of the stress field into the next fibre ahead of the crack depends on the continuing integrity of the interface linking the fibre to the stress field. If this interface fails, the local stress, intensified by the crack, will cause the matrix to crack, thus linking the crack tip with the fibre surface. This creates the necessary pathway for the environment to reach the fibre. The delay in the propagation of the crack to the next fibre is then principally dependent on the time required to weaken and fracture the fibre. In this mechanism the two critical rate-determining events are the highly localised failure of the interface and the fibre-in-acid incubation period. It is possible that the interface failure could be a time-dependent process, for example if water diffusion to the interface to cause adhesive strength depletion is required. In this case the rate of water diffusion through the resin could be an important resin property, although the time required for the water to bridge 4×10^{-6}m. of resin is only a few minutes.

Aveston[73] and more recently McCartney[8587] have suggested that in many composite systems the fibre strength is large enough to support the load, so that a crack can be formed leaving the fibres intact. This is depicted in Figure 5-3. It is interesting that this is exactly the type of matrix crack envisaged in the model above. Local debonding of the interface must take place before such a crack can form. The crack would be stable under load in the absence of a corrosive environment, but would propagate by stress-corrosion if aqueous acid was present. The McCartney model is concerned with the application of the Griffith fracture criterion to matrix cracking. The aim was to predict the minimum additional load needed to drive the crack right through the specimen. This is not relevant to the stress-corrosion mechanism but it does highlight the importance of the polymer-fibre interface in matrix cracking.

Another important aspect of the mechanism concerns the discontinuous nature of the crack advance, with the fibres breaking in a sequential manner. The stress-corrosion of the fibres, occurring by the demineralisation process described in Chapter 2, reduces the load-bearing cross section of the fibres. This will continue until the reduced section is bearing the fracture load of the fibre, at which point sudden failure will occur. When this happens there is a very rapid release of strain energy to the system, as the fibre relaxes, which will generate tensile stress waves into the surrounding matrix. The rapid loading to which the polymer is subjected during this process creates the most likely conditions for brittle fracture, since the brittle nature of the material is most apparent at high strain rates. The higher the load at the crack tip the more important this factor is likely to be.

FIGURE 5-3. BRIDGED MATRIX CRACK OF THE TYPE DISCUSSED BY Mc CARTNEY[85].

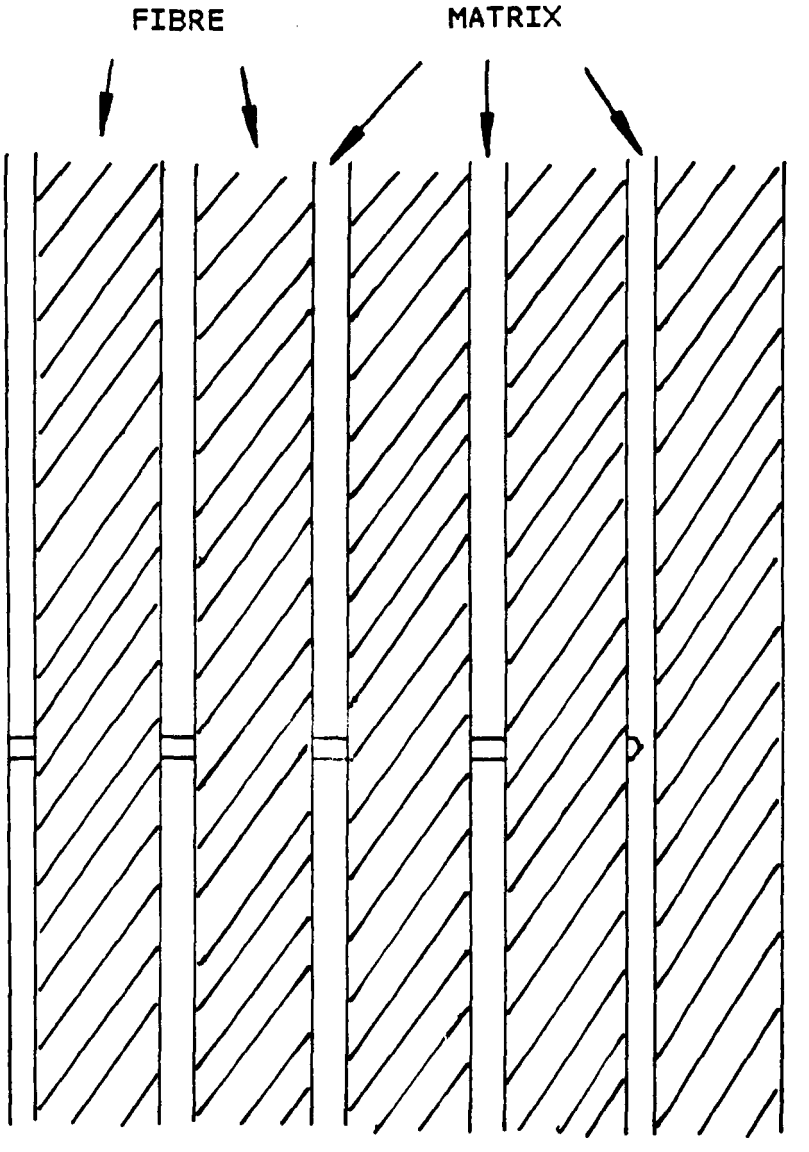

5-9 Matrix cracking: effects of supplementary matrix strains.

There are several mechanisms by which matrix strains can develop in such a way that they are additive with the strains produced by the applied load. These supplementary strains can be important in generating matrix cracking forces when the applied load , even when intensified by a sharp crack, is insufficient to crack the matrix,or break the fibre-matrix interface, in the way just discussed. These strains are internally generated within the polymer matrix and in extreme cases can cause matrix cracking without the application of an external load[56]. An example of this is the residual thermal strain that can develop in multiple ply laminates, as discussed by Bailey et al[45,46,48,71]. This can lead to severe transverse cracking in the centre ply of a freshly prepared, three-ply laminate when the material cools to room temperature after post-curing. The moisture content of the post-cured material appears to have a very important influence on the magnitude of this effect. This type of cracking originates in the basic anisotropy of fibre-reinforced laminae, and a similar effect is associated with the uptake of moisture into a dry composite. A swelling strain occurs as a consequence of this uptake and Menges et al[77] have shown how this can be related to the moisture uptake by the equation:

$$\varepsilon_{sw} = \alpha_{sw}\Delta c$$

where ε_{sw} is the swelling strain, α_{sw} is a swelling strain coefficient and Δc is the moisture uptake.

The strain to failure of a polyester resin is typically 0.02. Values for the transverse swelling strain, ε_{sw}, as quoted by Menges, are of the order of 0.013. For a composite with a high volume fraction, Kies[95,98] has shown how strain magnification occurs in the region

between fibres exposed to a transverse stress. For a volume fraction of 0.5 this amounts to a factor of 4, so that the swelling strain is within the range where transverse cracking could occur in the polyester composites of interest. Localised water diffusion into the matrix ahead of the crack front can therefore provide a transverse cracking mechanism that would eventually bring undiluted acid into contact with the fibre surfaces. Again, this is a situation in which the water diffusion rate into the resin could be a contributory factor in determining the crack propagation rate.

Both the residual thermal strain and the swelling associated with moisture uptake are concerned with the development of transverse cracks in the matrix. There are other mechanisms that will generate strains parallel to the fibre direction that would directly encourage crack propagation, especially when they supplement an external tensile load. One example of this is the osmosis mechanism that has already been discussed above. This requires the formation of pockets of solution ahead of the crack front. As well as the development of osmotic pressure within these pockets, there is another interesting consequence of the inability of ionic species to enter the polymer network. This involves the extension of microcracks created in the composite by one of the other processes described above. On immersion in the corrosive medium the cracks will become filled with the acid and will leach aluminium and calcium from the exposed fibre surfaces. If the resin in the vicinity of these cracks is dry, water will enter the resin in an attempt to saturate it. Since the dissolved ions cannot enter the resin their concentration in the cracks will increase until eventually the solubility limit is reached. Crystallisation of salts in the crack will then occur. The pressure developed by this crystallisation will extend further the resin cracks and the process

can continue. This hypothesis is very similar to that advanced by Jones,Rock and Bailey[56] to account for the stress corrosion that occurs in coupon specimens that have not been exposed to an external load.

There are thus several ways in which matrix cracks can develop in a composite. In the absence of an acid environment the effect would not necessarily be too serious because of the presence of the strong fibres bridging the cracks[85]. These would bear the load and the cracks would not propagate further. In the presence of an environment aggressive to the fibres, however, the propagation of stress-corrosion cracks would be an ever present possibility. The risk of the problem developing would depend critically on the acid concentration and on the local loads to which the fibres were subjected.

5-10 Bundle tests and fibre incubation times.

The bundle tests used in the present work have proved to be very useful. They have enabled a much wider range of test conditions to be explored than would have been possible if the single fibre test technique[13,21,84] had been used. The general shape of the response of the failure times of the fibre bundles to changes in stress and acid concentration conform with those found by Scrimshaw[35] and by Aveston[69]. In this thesis the results from static fatigue tests on bundles have been used to examine correlations with crack propagation rates in composites. It is therefore necessary to consider how closely the measured bundle failure times represent the average fibre incubation periods.

During the tests all the fibres in the bundle are under stress and are simultaneously exposed to the acid environment. Each fibre holds

its share of the load until the weakening effect of the acid causes it to break. Aveston and Sillwood[6] found that 90% of the fibres in the bundle were intact up to the failure time, when quite suddenly most of the fibres fail together. They checked this by monitoring the strand strain, under deadweight loading, as a function of time. This finding was confirmed by cathetometer measurements of strain in the present project. The statistics of bundle failure conform with the Weibull distribution[42] which is known to fit strength distributions from single fibre strength measurements[18,84]. The rationale for using bundle tests to measure mean fibre strength has been discussed by Coleman[99] and by Kelly and McCartney[100]. Because of the distribution of fibre strengths in the bundle the load on the surviving fibres increases as the fibres break. Although reasonably repeatable failure times can be obtained (seeFigure 2-8), the stress on the fibres when the bundle breaks is not the same as when the load was first applied. Kelly and McCartney (loc. cit.) have derived equations which allow the load at failure to be predicted from either the Weibull shape parameter ,m, or from the exponent n in the Paris equation (2-2). Their work suggested that the Paris exponent was the better of these alternatives. In the present work the difference between the fracture load and the mean fibre fracture strength is not large because the distribution of strengths is not particularly wide.

In interpreting the results from the bundle tests it has been assumed that the fibre strength distribution is partly due to the distribution of flaws that are present in the fibres after manufacture. The flaws are the sites from which it is assumed that the stress-corrosion cracks in the fibres grow during the static fatigue tests. The other factor influencing the fibre strength distribution is, of course, the variation in fibre cross-section. Both factors are in-

trinsic properties of the bundles, irrespective of the environment in which they are tested. In Figure 2-8 a non-dimensional scale has been obtained by normalising the data against the dry failure load of the bundles. This enables comparative estimates to be made of the failure times to be determined by interpolation. In using these comparative data, however, it must be recognised that neither the bundle test, nor the single fibre static fatigue test, properly reproduce the conditions under which the fibres in a composite are exposed to the acid. The relatively long gauge lengths used in the laboratory tests contrast with the very short length of fibre exposed to the acid at the tip of a matrix crack. The different severity of the flaws in the fibres at these extremes of gauge length have a marked influence on the absolute magnitude of the load at which fracture is expected to occur. It is therefore considered essential to base any comparisons on normalised, rather than absolute, data.

Additionally, the fibres in the composite are in a highly non-uniform stress field, because of the stress intensification at the crack tip, whilst the bundle and single fibre data involve uniformly stressed fibres. Hence, in trying to relate fracture events in bundle tests to crack tip fracture in a composite a stress averaging process is inevitably introduced. The exact prediction of fibre incubation periods from the results of bundle or single fibre static fatigue tests should not, therefore, be expected. However, it is considered that useful comparative estimates can be obtained by interpolation in the data in Figures 2-7 and 2-8. It has already been shown that these data can be used to account for the variation in observed crack propagation rates with stress intensity in E-glass composites.

5-11 Fibre weakening mechanisms.

It is now clear that there are two mechanisms which can operate to reduce the strength of the fibres. They differ in that one of them can proceed in the absence of an applied stress, whilst the other mechanism requires stress activation. Both mechanisms feature the removal of calcium and aluminium from the glass network by the leaching action of acid solutions. The demineralisation process commences at the glass surface. When the calcium ions are replaced by hydrogen ions in the structure this causes the ionic bonds, which help to hold the structure together, to be broken. The incoming hydrogen ions are able to form covalent links with the non-bridging oxygen atoms in the network. The resulting silanol groups do not contribute to the strength of the glass network. The overall result is the loss of the ionic bonds between the calcium cations and the anionic network sites occupied by the NBO's, which formerly made an important contribution to the network strength. The potential for this weakening in E-glass exists from the time at which the glass is manufactured. The CaO and Al_2O_3 fluxing agents which are added to the glass to improve its physical properties and its workability create the NBO sites which are subject to acid attack. In this sense E-glass is an inherently weak material, but requires exposure to acid to reveal the weakness. It is perhaps ironic that the silanol structure resulting from severe demineralisation, as depicted in Figure 3-1(d), can be dehydrated by firing to restore the fully bridged structure shown in Figure 3-1(a). In composite stress corrosion problems this escape route is not available. It is worth noting, however, that alternative glass formulations are available that are resistant to acid leaching. Provided that these are competitive in cost, and have comparable mechanical

properties, they would provide a complete cure to stress-corrosion problems with reinforced polyester resins.

5-12 Ageing and static fatigue mechanisms.

An important attribute of the surface demineralisation weakening hypothesis is that it provides a credible explanation of the difference between the ageing and static fatigue of the fibres. In the case of static fatigue failure it also accounts for the very marked effects of applied stress and acid concentration on the time required for fibre fracture. Fibre ageing occurs when the fibres are exposed to relatively strong acid solutions, in the range 0.5-1.0M. At this acid strength the demineralisation is able to progress to the subsurface layers of the fibres, leading to the growth of a fully demineralised,very weak sheath surrounding a core of unattacked glass. The strength of the attacked fibre is proportional to the cross-sectional area of the load-bearing core. The development of the sheath is diffusion-controlled and requires the complete demineralisation and hydration of the surface layer of the glass before it can proceed to the subsurface. The sharp boundary between the core and the sheath is a distinctive feature of systems in which a reactant species diffuses into a medium and is subsequently immobilised by reaction at fixed sites within the medium. The mathematical models describing this behaviour that have been formulated by Doremus[27,29] and his associates, by Smets and Tholen[25,26], and by Crank[23] and have been discussed in Chapter 3. The presence of the sharp boundary can be observed with a optical microscope in specimens with a well-developed core-sheath morphology. It has also been detected in specimens that have not developed a visible sheath by the TEM EDX analysis described in Chapter 3. An important contribution of the TEM work was the confirmation that

the sheath is fully demineralised right up to the core boundary, and that the demineralisation of the core is confined to the interface surface. The rate-controlling diffusion processes therefore occur in the sheath and not in the glass core. A diffusion coefficient of 5 x $10^{-13} cm^2.sec^{-1}$ can be fitted to the initial rate of sheath growth but Bledski has found that glass fibres are far from isotropic, and tend to be more dense away from the outer surface. This is probably why the diffusion slows as the centre of the fibre is approached, as shown in Figure 2-20. On protracted exposure of 2-3 weeks fibres subjected to molar hydrochloric acid become fully demineralised. On drying in air these are so weak that they break when attempts are made to lift them with tweezers. This type of corrosive attack is the most severe that arises with the hydrochloric acid/E-glass system. It shows that the successful storage of acid of this strength in tanks made from E-glass/polyester composites would not be possible unless the resin barrier was effective in preventing the acid from reaching the fibres.

The static fatigue of the fibres, featuring the combined effects of stress and surface demineralisation, operates over a much wider range of acid concentrations than the ageing process. The higher the applied stress the less acid is needed to propagate cracks in the fibres. The mechanism can be activated by pure water if the stress is high enough. Subsurface diffusion does not feature in this mechanism. The extent of fibre weakening is controlled only by the extent to which the surface layer of the fibre is demineralised. The hypothesis is that the surface demineralisation caused by the acid is a reaction-limited process which proceeds at a rate governed by the concentration of the residual metal ions in the glass surface. This reaction would be expected to be pseudo-unimolecular, following a simple first-order kinetic equation of the form:

$$N_t = N_0 e^{-kt} \qquad (5\text{-}5)$$

In this equation N_0 is the number of metal ions linked to NBO's in the glass surface at time t = 0 and k is the rate constant. The equation asserts that the maximum rate of exchange of cations for hydrogen ions occurs with a fresh surface, since $dN/dt = -kN$, and N is a maximum at a fresh surface. The rate of surface attack falls off exponentially with time and the loss of strength in the attacked material is directly proportional to $(N_0 - N_t)$. The stress applied to the fibre creates local regions of high surface stress at flaw sites in the fibre surface, because of the stress intensification that occurs at these sites. When the fracture strength at one of these has been lowered sufficiently by the demineralisation a crack will nucleate and will expose fresh surface to the acid. This will be attacked preferentially , in accord with equation (5-5), and once this process has been initiated the crack will grow until the fibre breaks.

Diffusion does not feature in this mechanism because, even at low loads, fracture would be expected to occur before the surface was fully demineralised and hydrated. Subsurface attack by a diffusion-controlled process cannot, therefore, be initiated. In this reaction-controlled mechanism the extent of surface demineralisation clearly determines the stress at which surface fracture , i.e. crack propagation, can occur. This, in turn, is determined by the acid concentration, which controls k in equation (5-5), and by the exposure time, t.

5-13 Comparison of static fatigue mechanism with general stress corrosion mechanisms.

A close examination of the proposed surface demineralisation mechanism shows that this is an archetype of the general stress-corrosion problem with brittle materials. A common feature of all stress-corrosion problems is that the corrosive agent must be capable of causing local weakening or embrittlement at imperfections, flaws, or microcracks, in the material surface. If this surface is under stress, local fracture of the weakened surface at a flaw will nucleate a stress-corrosion crack, exposing fresh surface to the corrosive agent. There is usually very little overall corrosion because the attack is predominantly a surface phenomenon and subsurface attack is diffusion limited. The material fails by the passage of a macroscopically sharp and narrow crack that propagates in a direction normal to the applied load.

The absence of detectable corrosion on glass fibres that had failed by static fatigue in dilute acid was noted in the present work. It has also been noted by Hogg[63] in connection with the EDX analysis of fibres in the fracture surfaces of stress-corroded E-glass pipe specimens. When corrosion effects have been seen in stress-corrosion test specimens these are almost certainly due to post failure attack of the fibres. Examples of this are to be found in the work of Bledski[12], and Noble Harris and Owen[11]. The attack involves post failure exposure of the exposed fibres to acid of sufficient strength to cause core-sheath development or spontaneous cracking. Consideration of the proposed stress-corrosion mechanism suggests that this would only happen to sections of fibre that were not bearing any load. This could be immediately behind the crack front. Alternatively, it could be in a region of the fibre near a break, where local debonding had released the fibre from the matrix, thereby preventing load transfer to that section of the fibre.

Brasses, aluminium alloys and austenitic stainless steels are all particularly sensitive to stress-corrosion[101]. The type of mechanism involved in the nucleation and propagation of cracks in these materials has many similarities with that now proposed for E-glass. It is interesting that cracks will propagate in stressed stainless steel, immersed in hot magnesium chloride solution[102], at a rate of $3 \times 10^{-7} m.sec^{-1}$. This is within the range of crack propagation rates found with E-glass composites.

5-14 Conclusions.

Good progress was made towards achieving all the objectives of the present work, as set out in Chapter 1. The detailed interpretation of the experimental results, as descibed in the preceding text, is considered to justify the following conclusions:

1. A sensitive and effective method for measuring the solubility and diffusivity of aqueous hydrochloric acid in resin specimens has been developed. The method is based on the use of a radioactive tracer technique, using ^{36}Cl to follow the hydrochloric acid diffusion. The simultaneous diffusion of water into the resin from this aqueous solution can also be monitored by using ^{3}H as the tracer isotope.

2. Water was found to diffuse freely in the resin and exhibited a well-defined solubility and diffusion coefficient for each of the polyester resins examined in the programme. The water uptake curves conformed with Fick's law of diffusion, implying that the water diffused into the resin network by random molecular movement. At room temperature the water solubility in the resin was in the range 1%wt.-3%wt.. The diffusion coefficients were of the order of $3 \times 10^{-9} cm^{2}.sec^{-1}$.

3.Hydrochloric acid did not appear to be capable of diffusing from aqueous solution into polyester resin to a significant extent. There was a small uptake of ^{36}Cl by the resin specimens, but this was of an erratic nature. It did not respond to changes in exposure time and specimen thickness in the systematic way required for diffusion. This uptake was attributed to adsorption on the specimen surface or occlusion in surface microcracks.

4.The reason for the difference in behaviour between water and the hydrochloric acid is probably due to the molecular nature of water diffusion in these resins. The water diffusion is favoured by the covalent character of the water molecules. Hydrochloric acid is essentially fully ionised in dilute aqueous solution. The resultant ions would not tend to enter the polymer network unless a continuous pathway through an ionising solvent, in this case water, was available. This would require the coalescence of water molecules in the resin to form continuous ligaments of liquid within the resin. If these were, in fact formed, they would be equivalent to the lower limit of matrix cracking.

5.At the tip of a growing stress-corrosion crack in an E-glass composite the acid reaches the fibres as a consequence of the cracking of the resin matrix. If the resin does not crack in this way stress-corrosion will not occur. This is believed to be the case in the majority of situations in which E-glass composites are used industrially. Stress-corrosion failure in practice is almost certainly initiated by accidental damage or bad design, leading to the development of high stress concentrations in local areas of the structure. The penetration of aqueous acid into sharp matrix cracks in such areas brings with it a high risk of stress corrosion problems.

6. Tensile tests on strands of E-glass filaments have enabled the main features of the two modes of fibre weakening, ageing and static fa-

tigue, to be explored. Static fatigue, in which the fibres are subjected to a constant tensile load during exposure to the acid, is the most severe of the two weakening modes. The strand failure time is critically dependent on the magnitude of the applied load, which synergises the corrosive effect of the acid. Ageing requires a stronger acid concentration. In the range 0.5M-1.0M it results in the formation of a well-defined core-sheath structure.

7.From the results of static fatigue tests on fibre bundles strand failure time versus acid concentration profiles have been mapped for a range of applied loads between 10%-100% of the dry failure load. These provide a measure of the fibre incubation period that is needed before the fibres will fracture.

8.A mechanism that accounts for the weakening of E-glass fibres by aqueous hydrochloric acid has been proposed. The weakening is attributed to the leaching of calcium and aluminium from the glass network by the acid. This is thought to be predominantly a surface reaction, since the acid does not diffuse into the unreacted glass below the surface. The rate of surface attack is determined by the surface concentration of the metal ions and is therefore at a maximum when the acid is in contact with a freshly exposed surface. The effect of the leaching is to eliminate ionic bonding at the sites of non-bridging oxygen atoms in the glass. This is the reason for the loss of cohesive strength in demineralised fibres.

9.Ageing is a process which occurs only with relatively strong acid solutions. With acid of concentrations in excess of 0.5M the surface demineralisation goes virtually to completion, provided that the exposure time is long enough. This leaves a very open and loose demineralised network. This structure is very weak in comparison with the original glass, and is readily saturated with water to form a gel-like structure. Metal ion diffusion can occur through this layer

and enables the corrosive attack to proceed to the subsurface, leading eventually to the appearance of the core-sheath structure. The sheath is very weak and the strength of the corroded fibre resides in the reduced area of the load-bearing core. The reduction of core area as the sheath grows provides a satisfactory explanation of fibre strength loss during ageing.

10.Static fatigue is caused by the same fibre weakening mechanism, i.e. surface demineralisation of the glass network by the acid. Because the fibres are subject to a tensile load the demineralisation does not need to go to completion, as in the ageing process. As soon as the surface strength has fallen to a level equivalent to that of the applied stress, local surface fracture at a site of high stress intensity will nucleate a crack. The freshly exposed surface at the tip of this crack will then suffer preferential demineralisation and the crack will propagate through the fibre. The surface weakening and stress intensification effects responsible for crack growth in the fibres are typical of the stress-corrosion that occurs in a wide range of other materials.

11.The prediction of the rate of stress corrosion crack propagation in a composite is complex because it depends on a number of factors. For a given combination of acid concentration and applied stress these include:

(a)The incubation period required before a stressed fibre exposed to the acid will fracture.

(b)The length and sharpness of the crack that grows in the composite since this determines the stress intensity that drives the crack forward.

(c)The extent of microcracking in the resin matrix that occurs ahead of the crack tip, providing a route for the acid to reach newly exposed fibres.

Clearly, (a) is a property of the fibres and can be characterised by the mapping plot referred to above. Factors (b) and (c), however, are likely to depend on the physical properties of the resin matrix. It is evident that both fibre and matrix properties contribute to the stress-corrosion process. For a given resin system, further confirmation of the veracity of the matrix cracking model was seen in the results from a correlation study. This involved a comparison of measured and predicted crack propagation rates. Data obtained at two different stress intensity levels were compared with estimates of the fibre incubation periods required to sustain the crack propagation rates. The correlation was found to be close over four decades of time.

12. The possible ways in which matrix cracking can occur have been reviewed. The situation holding the most risk for stress corrosion failure is one in which extensive precracking of the composite has occurred. This could be as a result of accidental impact damage, or as a consequence of the application of a high tensile load. Stress corrosion failure is then virtually inevitable if the composite is subsequently subjected to the combined effects of an acid solution and a tensile stress. If the precracking is confined to a local region of the specimen, stress intensification can activate the stress-corrosion mechanism. Progressive resin cracking ahead of the crack tip can occur as a result of the load redistribution that follows fibre fracture. This promotes slow crack growth in the composite that will eventually lead to fracture. Finally, there are a number of ways in which internally generated strains within the resin matrix can supplement the externally applied strain, to promote matrix cracking. These include residual thermal strains, osmotic effects, and the swelling associated with the uptake of moisture by the resin. Stress-corrosion cracking is unlikely to occur if matrix cracking can

be avoided in the manufacture of the composite material, or during its use.

APPENDIX

Solutions to diffusion equations.

Diffusion phenomena feature in several different parts of this Thesis. The basic laws of diffusion have been well authenticated since their first enunciation by A.Fick[86]. The two general equations, which can be used to describe virtually any diffusion situation, are:

$$F = -D\ \partial c/\partial x \qquad (A1)$$

$$\partial c/\partial t = D\ \partial^2 c/\partial x^2 \qquad (A2)$$

In equation A1, F is a flux repesenting the rate of transfer of diffusant through unit area of the material under steady state conditions. D is the diffusion coefficient and $\partial c/\partial x$ is the concentration gradient.

Equation A2 is the one which is relevant to the present work and includes time as an extra variable. A variety of closed solutions to equation A2 are available. The two situations of most interest in the present work concern diffusion into firstly a semi-infinite flat plate, and secondly into a semi-infinite cylinder. For the semi-infinite plate the most widely used solution is the one quoted by Crank[23] :

$$c/c_0 = \text{erfc}\ x/2(Dt)^{\frac{1}{2}} \qquad (A3)$$

where c is the diffusant concentration at time t and depth x below the specimen surface, and c_0 is the saturation concentration at the surface. The erfc function is the error function complement which is readily obtained from a tabulation given in most texts on diffusion or heat transfer (e.g.Crank loc. cit. Table 2-1). This solution forms the basis of a very useful and simple method of measurement for the

diffusion coefficient D. This is the weight gain method, in which the increase in weight of a specimen exposed continuously to the diffusant is determined as a function of time. By measuring the time required for the specimen to achieve half of the saturation concentration, $t_{0.5}$, the diffusion coefficient can be obtained by the very simple expression:

$$D = 0.049(x^2/t_{0.5}) \qquad (A4)$$

The derivation of this equation and its use to measure diffusion coefficients has been discussed by Ellis and Found[92]. A similar treatment has been developed in the present work in relation to diffusion into a semi-infinite cylinder. A solution to the diffusion equation A2 for a cylinder was taken and was used to generate the solution to the whole uptake curve, instead of just the solution for the half-saturation time. This was of great value in the present work because it provided a ready route to the generation of the predicted diffusion curve for any given diffusion coefficient. This could then be compared with the experimentally measured uptake curve and the extent of conformity with the theoretical Fickian diffusion curve could be judged. It is assumed that the diffusion occurs radially in an infinitely long cylinder of radius a and that the initial and boundary conditions are :

$c = c_0$ at $r = a$ and $t \geq 0$

$c = f(r)$, $0<r<a$ at $t = 0$; in this case $f(r) = 0$

The required solution, quoted by Crank, features the use of Bessel's function:

$$M_t/M_\infty = 1 - \sum_{n=1}^{\infty} [4/a^2\alpha_n^2] \exp(-D\alpha_n^2 t) \qquad (A5)$$

where $J_0(a\alpha_n) = 0$ i.e the zero order Bessel function.

Let $a\alpha_n = x_n$ i.e. $J_0(x_n) = 0$

Then $$M_t/M_\infty = 1 - \sum_{n=1}^{\infty} [4/x_n] \exp[-Dx_n^2(t/a^2)] \qquad (A6)$$

At $t_{0.5}$, the time taken to achieve the half-saturation value:

$$0.5 = 1 - \sum_{n=1}^{\infty}[4/x_n^2] \exp[-Dx_n^2(t/a^2)] \qquad (A7)$$

Now the values of x_n at which $J_0(x_n) = 0$ are available as a Table. Given this Table and given a and t it is readily possible to calculate D.

If (A5) is rewritten with $Dt/a^2 = Y$, then:

$$M_t M_\infty = 1 - \sum_{n=1}^{\infty}[4/x_n^2] \exp(-x_n^2 Y) \qquad (A8)$$

For any value of $(1 - M_t/M_\infty)$ this equation can be solved iteratively to find Y. If t is also known it is very straightforward to find D from the simple equation:

$$D = Ya^2/t \qquad (A9)$$

The iterative solution is best carried out by Newton's method, in which:

$$Y_{i+1} = Y_i - f(x)/f'(x)$$

In the present case : $M_t/M_\infty = F$

so that: $f(x) = \sum_{n=1}^{\infty}[(4/x_n^2) \exp(-x_n^2 Y] - F$

and $f'(x) = \sum_{n=1}^{\infty} -4\exp(-x_n^2 Y)$

In practice it was found that a summation over six terms gave excellent convergence. It was found useful to tabulate values of x_n^2 and $4/x_n^2$ for those values of x_n for which $J_0(x_n) = 0$:

BESSEL FUNCTION SOLUTIONS.

x_n	x_n^2	$4/x_n^2$
2.405	5.784025	0.6915599
5.520	30.4704	0.1312749
8.654	74.891716	0.0534104
11.792	139.05126	0.0287663
14.931	222.93476	0.0179424
18.071	326.56104	0.012247

Carrying out the iterations manually on a calculator gave the following results:

CALCULATED VALUES OF PARAMETER Y.

$1 - M_t/M_\infty$	Y	M_t/M_∞
0.1	334.294×10^{-3}	0.9
0.2	214.57×10^{-3}	0.8
0.4	97.6016×10^{-3}	0.6
0.5	63.036×10^{-3}	0.5
0.6	37.882×10^{-3}	0.4
0.8	8.51978×10^{-3}	0.2
0.9	1.60026×10^{-3}	0.1

These values of Y are shown plotted as a function of M_t/M_∞ in Figure A1.

The availability of these Y values means that the very simple equation, (A9), can be used either to determine the diffusion coefficient from the uptake curve, or conversely to predict the uptake curve for any given values of a and D. This latter feature has proved to be particularly useful in comparing measured uptake data with the predicted uptake curves for slightly different D values in a manual curve-fitting process.

Figure A1. Variation of paramater Y with M_t/M_∞.

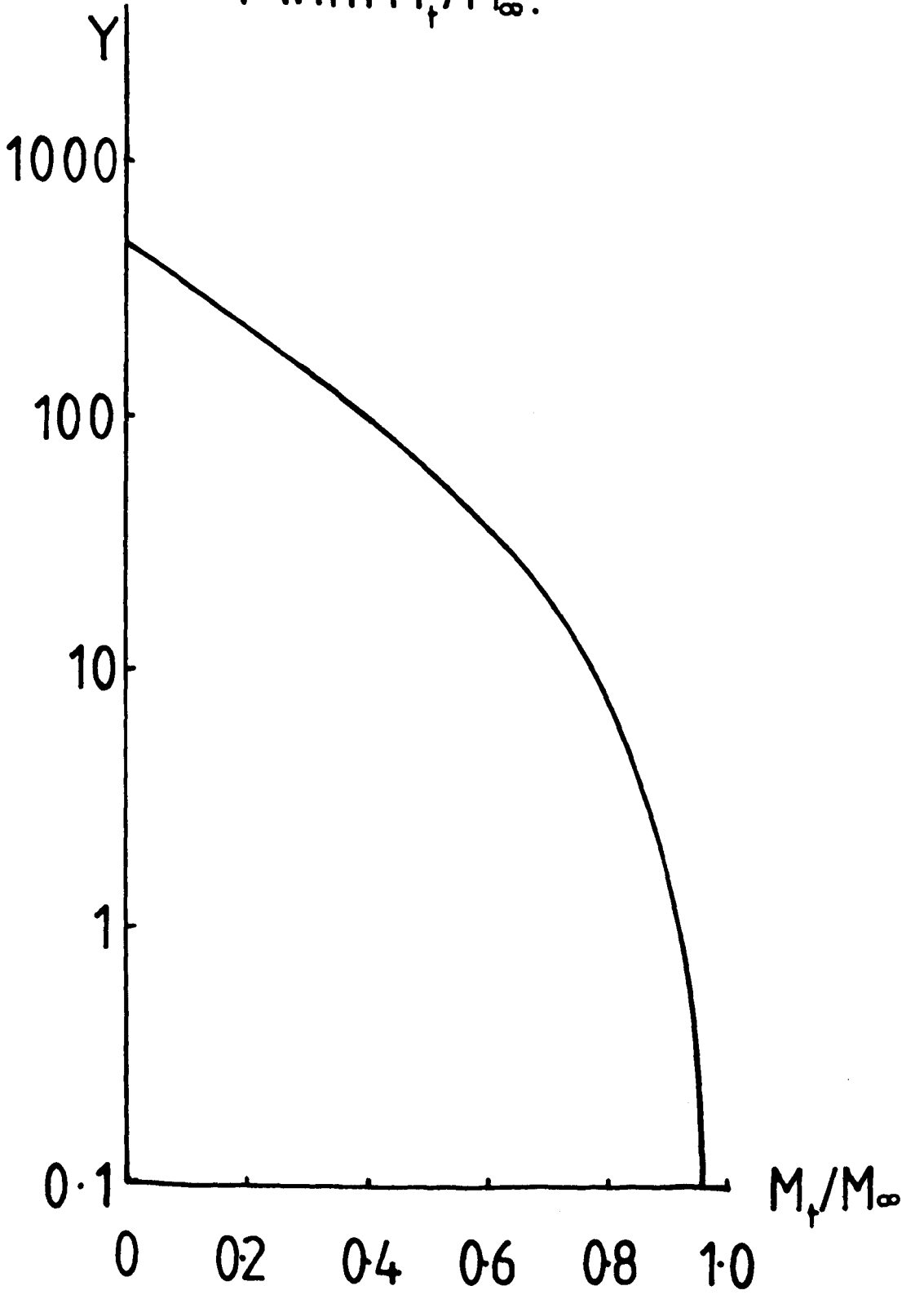

REFERENCES

1. P.J.Hogg, D.Hull, Developments in GRP technology, Vol. 1 (ed B.Harris) Applied Science Publishers, London, 1983 p. 37
2. M.Kumosa, D.Hull, J.N.Price, J. Mater. Sci. 22 1987 331 - 336.
3. J.N.Price, D.Hull, J. Mater. Sci. 18 1983 2798 - 2810
4. P.J.Hogg, Composites 14 (3) 1983 254
5. B.A.Proctor "Glass - Current Issues", Proceedings of NATO Advanced Study Institute Conference, 1984, Dordrecht, Netherlands; Martinus Nijhoff, 1985 524 - 50.
6. J.Aveston, J.M.Sillwood, J. Mater. Sci. 17 1982 3491 - 3498.
7. B.A.Proctor, private communication.
8. S.M.Wiederhorn, J. Non-Cryst. Solids 19 1975 169 - 181.
9. H.A.Barker, I.G.Baird-Smith, F.Jones, paper 12, Symposium on reinforced plastics, N.E.L., Glasgow, 1979.
10. A.G.Metcalfe, M.E.Gulden, G.K.Schmitz, Glass Technology 12 1971 15
11. B.Noble, S.J.Harris, M.J.Owen, J. Mater. Sci. 18 1983 1244
12. A.Bledski, R.Spaude, G.W.Ehrenstein, Composites Science and Technology 23 1985 263-285.
13. J.M.Sillwood, NPL Report DMA(6), 19 January 1982.
14. G.C.Sih, P.C.Paris, G.R.Irwin, Int. J. Fract. Mech. 1 1965 189.
15. J.N.Price, Ph.D. Thesis, Liverpool, 1985.
16. Griffith Proc. Roy. Soc.
17. A.G.Metcalfe, G.K.Schmitz, Proc. ASTM 64 1965 1075.
18. M.J.Pitkethly, M.G.Bader, J.Phys. D. App. Phys. 20 1987 315-322.
19. A.G.Metcalfe, G.K.Schmitz, Glass Technology 13 (1) 1972 5.
20. A.G.Metcalfe, Glass Technology, 13 (1) 1972 5.
21. G.K.Schmitz, A.G.Metcalfe, I. and E.C. Product Research and Development 5 (1) 1966.
22. A,Wikby, Electrochim. Acta 19 1974 329.
23. J.Crank "The mathematics of diffusion", Oxford University Press, 1975.
24. W.J.Zachariasen, J. Am. Chem. Soc. 54 1932 3841
25. B.M.J.Smets, T.P.A.Lommen, Phys. Chem. Glasses 24 (1) 1983 35-36;ibid 23 (3) 1982 83-87.
26. B.M.J.Smets, M.G.W.Tholen, J. Am. Ceram. Soc. 67 (4) 1984 281.
27. R.H.Doremus, J. Non-Cryst. Solids 19 1975 137-144.
28. Z.Boksay, G.Bouquet, S.Dobos, Phys. Chem. Glasses 8 (4) 1967 140-144.
29. W.A.Lanford, K.Davis, P.Lamarche, T.Laursen, R.Groleau, R.H.Doremus, J. Non-Cryst Solids 33 (2) 1979 249-266.
30. T.M.El-Shamy, S.E.Morsi, J. Non-Cryst. Solids 19 1975 241-250.
31. C.Lhymn, J.M.Schultz, J. Mater. Sci. 18 1983 2923-2938.
32. J.M.Marshall, G.P.Marshall, R.F.Pinzelli, Polymer composites 3 (3) 1982 131.
33. D.M.Marsh, Proc. Roy. Soc. A279 1964 420-435; A282 1964 33-43.
34. D.R.Cockram, K.L.Litherland, B.A.Proctor, B.Yale, "Assessing the durability of glass composites", 13&hu.th&hd. International Congress on Glass, Hamburg, 1983.
35. G.Scrimshaw, Peper 6 in PipeCon - Proceedings of conference on large diameter plastic pipes, London, 1980, Published by Fibreglass Ltd., and Amoco Chemicals S.A.
36. R.J.Charles, J. App. Phys. 29 1958 1554-1560.
37. A.G.Evans, Int. J. Fracture 10 (2) 1974 251-259.
38. J.Aveston, A.Kelly, J.Sillwood, Proc. 3&hu.rd&hd. International Conference on Composite Materials, Paris, 1980, 556-568.

39. F.R.Jones, J.W.Rock, A.R.Wheatley, Composites, 14 (3) 1983 262-269.
40. P.J.Hogg, D.Hull, Metals Science, 1980 441-449.
41. W.Weibull, J. Appl. Mech. 18 293-297.
42. Z.Chi, T.W.Chou, G.Shen, J. Mater. Sci. 19 1984 3319
43. B.W.Rosen, Chapter 3 in "Fibre Composite Materials", ASM, Metals Park, Ohio, 1965.
44. R.R.Tummala, J. Non-Cryst. Solids 19 1975 263-272.
45. M.Mulheron, F.R.Jones, J.E.Bailey, Composites Sci. and Tech. 25 1986 119-131.
46. F.R.Jones, M.Mulheron, J.E Bailey, J. Mater. Sci. 18 1983 1522-1532.
47. F.R.Jones, M.Mulheron, Composites 14 1983 281.
48. F.R.Jones, M.Mulheron, J.E.Bailey, J. Mater. Sci. 18 1983 1533.
49. H.T.Hahn, J.Composite Mater. 10 1976 266.
50. J.N.Price, D.Hull, Comp.Sci. and Tech. 28 1987 193.
51. W.S Carswell, R.C.Roberts, Composites, 11 1980 95.
52. P.J.Hogg, D.Hull, BPF Reinforced Plastics Congress, Brighton, 1982 115.
53. P.C.Paris, F.Erdogan, J. Basic Eng. (Trans ASME), 85 1963 528.
54. H.D.Chandler, R.L.Jones, J. Mater. Sci. 19 1984 3849.
55. K.Friedrich, J. Nat. Sci. 16 1981 3292.
56. F.R.Jones, J.W.Rock, J.E.Bailey, J. Mater. Sci. 18 1985 1059.
57. A.C.Garg, Eng. Fracture Mech. 17 1983 575.
58. L.S.Norwood, P.J.Hogg, Composite Structures 2 1984 1
59. B.D.Caddock, K.E.Evans, D.Hull, Fibre reinforced Composites Conference, Liverpool, 1986, Paper C 25/86, published by I.Mech. E., 1986.
60. (a) ASTM D3263-73, Reinforced plastic mortar sewer pipe; (b) ASTM D3681-78, Chemical resistance of reinforced thermosetting resin pipe in a deflected condition.
61. P.J.Hogg, D.Hull, B.Spencer, Composites 12 1981 166.
62. H.H.Collins, Plastics and Rubber: Materials and Applications, 3 1978 6.
63. P.J.Hogg, Ph.D. thesis, Liverpool, 1981.
64. P.J.Hogg, Composites, 14 1983 254.
65. G.K.Schmitz, A.G.Metcalfe, I. and E.C. Product Research and Development 5 (1) 1966.
66. J.N.Price, M.Kumosa, D.Hull, ICCM Meeting, London, 1987.
67. M.J.Owen, R.G.Rose, J. Mater. Sci. 10 1975 1711.
68. J.E.Bailey, T.M.W.Fryer, F.R.Jones, ICCM 3 "Advances in Composite Materials", Vol 1, Eds. A.R.Bunsell et al., Permagon Press, Oxford, 1980, p556.
69. J.Aveston, A.Kelly, L.N.McCartney, J.M.Silwood, "Progress in Science and Engineering of Composites", ed. T.Hayashi, K.Kawata, S.Umekawa, ICCM 5, Tokyo, 1982.
70. J.Aveston, A.Kelly, Phil. Trans. R. Soc. London, A294 1980 519.
71. J.E.Bailey, P.T.Curtis, A.Parvizi, Proc. Roy. Soc. Lond., A366, 1979, 599.
72. C Lhymn, J.M.Schultz, J.Mat. Sci. 18, 1983, 2029-2046.
73. J.Aveston, G.A.Cooper, A.Kelly, "Conference on the properties of fibre composites, NPL", pp 15-26, IPC Science and Technology Press, 1971.
74. R.F.Regester, Corrosion, 25, 1969, p157.
75. M.Kumosa, J. Phys. D: Appl. Phys. 20 1987 69-74.
76. D.Hull, M.Kumosa, J.N.Price, Mater. Sci. Technol., 1987, 1, 177.
77. G.Menges, K.Lutterbeck, "Developments in reinforced plastics - 3", Elsevier, 1984, p97.
78. K.H.G.Ashbee, R.C.Wyatt, Proc. Roy. Soc. London, A312 1969 553-564.

79. T.R.Loader, 14&hu.th&hd. Reinforced Plastics Congress, Brighton, 1984.
80. A.R.Bunsell, "Developments in Reinforced Plastics - 3", Elsevier, 1984, p1.
81. J.S.Ghotra, G.Pritchard, ibid, p63.
82. H.P.Abeysinghe, J.S Ghotra, G.Pritchard, Composites, 14 1983 57.
83. E.Walter, K.H.G.Ashbee, Composites 13 1982 365.
84. F.R.Jones, P.A.Sheard, Fibre Reinforced Composites Conference, Liverpool, 1986, p63, published by I.Mech.E..
85. L.N.McCartney, Proc. Roy. Soc. Lond., A409 329-350 1987.
86. A.Fick, Phil. Mag., (4), 10, 1855, p80.;Annalen Phys., 170, 1855, 59.
87. J.M.Marshall, Ph.D.thesis, CNAA/Manchester Polytechnic, 1981.
88. G.Marom, L.J.Broutman, Polymer Compos., 2,(3),1981, 132-136.
89.S Neumann, G.Marom, J.Mat.Sci., 21, 1986, 26-30.
90. J.M.Marshall, SAMPE Quarterly, 13, (4), July 1982.
91. V.G.Amerikov, T.V.Krivova, G.M.Ronkin, I.F.Yazikov, Z. Fiz. Khim., 55, 1981, 2040-2045.
92. B.Ellis, M.S.Found, Composites 14 (3) 1983 237.
93. R.M.Barrer, "Diffusion in and through solids", Cambridge University Press, 1951.
94. W.Jost, "Diffusion in liquids, solids and gases", Bcademic Press, New York, 1952.
95. D.Hull, "An introduction to composite materials", Cambridge University Press, 1981.
96. J.F.Knott, "Fundamentals of fracture mechanics", Butterworths, London, 1973.
97. B.R.Lawn and T.R.Wilshaw, "Fracture of brittle solids" Cambridge University Press, 1975.
98. J.A.Kies, US Naval Research Laboratory Report NRL 5752, 1962.
99. B.D.Coleman, J.Mech Phys. Solids 7 1958 60-70.
100. A.Kelly, L.N McCartney, Proc. Roy. Soc. Lond., A374, 1981, 475-489.
101. A.J.Sedricks, "Corrosion of stainless steels"
102. A Cottrell, "An introduction to metallurgy", Edward Arnold, London, 1982.
103. J.Kabelka, "Developments in Reinforced Plastics - 3", ed. G Pritchard, Elsevier, London, 1984, p189.
104. J Cook, J.E.Gordon, Proc Roy. Soc. Lond. A282 1964 508.